Analysis of the Molecular Mechanism and Physiological Roles of the GRASP Proteins in the Golgi Apparatus and Autophagy

by

Leibin Wang

A dissertation submitted in partial fulfillment
of the requirements for the degree of
Doctor of Philosophy
(Molecular, Cellular and Developmental Biology)
in The University of Michigan
2018

Doctoral Committee:

Professor Yanzhuang Wang, Co-chair
Professor Lois Weisman, Co-chair
Professor Daniel Klionsky
Professor Haoxing Xu

Leibin Wang

leibinw@umich.edu

ORCID iD: 0000-0002-4213-9655

Dedication

This dissertation is dedicated to my parents, Bao Wang and Guifang Jiang and all of my friends for their love and support.

Acknowledgement

Firstly, I would like to thank my thesis advisor, Dr. Yanzhuang Wang, for his advice and critiques. He is so enthusiastic in science that his ambition and hardworking inspired me to keep moving forward and never backdown. I also would like to thank my committee members, Dr. Lois Weisman, Dr. Haoxing Xu and Dr. Daniel Klionsky for their insightful ideas and suggestions throughout my research.

Secondly, I feel really grateful to conduct my research with all former and current members of the Wang Lab. I have stayed in a really great lab that I can learn everything from. During my PhD study, I further understand the importance of teamwork and how it will affect my everyday work and life. I would like to thank them for all their ideas, suggestions, and sharing materials. Especially, I want to thank Dr. Michael Bekier for collaboration with me on GRASP knockout paper; thank Dr. Danming Tang for teaching me basic techniques in cellular biology, thank Dr. Xiaoyan Zhang for her ideas and continuous support and thank Dr. Shijiao Huang as a lab member to give me technical support, insightful ideas and as a friend to support me.

Thirdly, I would like to thank Dr. Haoxing Xu and Dr. Daniel Klionsky for giving me the chance to rotate in their labs. I really appreciate their guidance and I have spent a wonderful time during the rotations. Moreover, I would like to thank all the staff and faculty members of MCDB

department that they make the department as a home and I never feel lonely with all their support. Especially, I would like to thank Ms. Mary Carr who continuously guide me from the first day of my PhD to the last; and thank Mr. Gregg Sobocinski for his support on confocal microscopy and EM.

Finally, I would like to express my largest gratitude to my parents, Bao Wang and Guifang Jiang. With their love and support, I never give up and always try my best to fulfil my dream.

Chapter II is reprinted from *Molecular Biology of the Cell*, 2017, Volume 28, Michael E. Bekier II*, Leibin Wang*, Jie Li, Haoran Huang, Danming Tang, Xiaoyan Zhang and Yanzhuang Wang (*, These authors contributed equally to this work.): **Knockout of the Golgi stacking proteins GRASP55 and GRASP65 impairs Golgi structure and function**, page 2833-2842, Copyright (2017), with minor modifications. Michael E. Bekier II, Leibin Wang and Yanzhuang Wang designed the project. Michael E. Bekier II, Leibin Wang, Jie Li, Haoran Huang and Xiaoyan Zhang performed the experiments: Michael E. Bekier II performed experiments for Figure 1-5, S1, S6 and S8; Leibin Wang performed experiments for Figure 1A, 5D-H, 6E, S2-5; Jie Li performed experiments for Table 1 and 2; Haoran Huang performed experiments for Figure 6C-D, 6F-H, S7; Xiaoyan Zhang performed the experiments for Figure 6A-B. Leibin Wang, Michael E. Bekier II, Haoran Huang and Jie Li analyzed the data. Leibin Wang, Michael E. Bekier II, Jie Li and Yanzhuang Wang wrote the paper.

Chapter III is a manuscript prepared for *Autophagy*, Leibin Wang, Xiaoyan Zhang, Stephen Ireland and Yanzhuang Wang: **GRASP55 collaborates with the PI3K UVRAG complex to facilitate autophagosome-lysosome fusion**. Leibin Wang, Xiaoyan Zhang and Yanzhuang Wang designed the project; Leibin Wang performed the experiments; Stephen Ireland and Leibin Wang performed EM experiments (Figure 1F and S3); Leibin Wang analyzed the data; Leibin Wang and Yanzhuang Wang wrote the paper.

Table of Contents

List of Tables

Tables:

List of Figures

Figures:

Abstract

The Golgi apparatus resides at the center of the secretory pathway and receives almost the entire output of the endoplasmic reticulum (ER). Within the Golgi, proteins and lipids undergo multiple modifications, including N- or O-linked glycosylation, phosphorylation and proteolytic cleavage. After defined modifications, mature cargo proteins and lipids are sorted into secretory vesicles for transport to the plasma membrane, endosomes and lysosomes, or outside of the cell. In most eukaryotic cells, the Golgi apparatus is composed of stacks of tightly aligned flattened cisternae, which are laterally linked into a ribbon like structure located in the perinuclear region. The Golgi reassembly stacking proteins of 65 kDa and 55 kDa (GRASP65 and GRASP55) were two proteins originally identified as Golgi stacking factors. GRASP65 and GRASP55 localize to the *cis*- and *medial-trans*-cisternae, respectively, where they form homo-dimers and trans-oligomers to hold adjacent cisternae into a stack. Moreover, GRASP55 is also involved in unconventional secretion and autophagy. To further understand GRASPs' functions, my research focused on the following two questions: 1) How do GRASP proteins play a role in Golgi structure and function? 2) How does GRASP55 regulate autophagy?

To answer the first question, in collaboration with others in the lab, I applied the recently developed clustered regularly interspaced short palindromic repeats (CRISPR)/Cas9 technology to knock out GRASP55 and GRASP65, individually or in combination, in HeLa and HEK293 cells. In this study, we showed that double knockout of GRASP proteins disperses the Golgi stacks into single

cisternae and tubulovesicular structures, accelerates protein trafficking, and impairs accurate glycosylation of proteins and lipids. These results demonstrate a critical role for GRASPs in maintaining the stacked structure of the Golgi, and confirmed the hypothesis that a well stacked Golgi is required for accurate post-translational modifications. Additionally, the GRASP knockout cell lines developed in this study will be useful tools for studying the role of GRASP proteins in other important cellular processes.

To answer the second question, I firstly induced autophagy by nutrient deprivation and determined the effects on the Golgi. I found that upon amino acid starvation, *trans*-Golgi derived membrane fragments colocalize with autophagosomes. Depletion of GRASP55, but not GRASP65, increases both LC3-II and p62 levels. Further studies demonstrated that upon amino acid starvation, GRASP55 facilitates autophagosome-lysosome fusion through two mechanisms, one is by physically tethering autophagosomes and lysosomes through the interactions with LC3 on autophagosomes and LAMP2 on late endosomes/lysosomes, and the other is by interacting with Beclin 1, UVRAG, Vps34 and Bif-1 to facilitate the assembly and membrane association of this phosphoinositide 3-kinase (PI3K) complex. These findings indicate that GRASP55 plays an important role in autophagosome maturation during amino acid starvation.

In conclusion, during my PhD research, I generated GRASP55 and GRASP65 knockout cells and confirmed their roles in Golgi structure and function; I also discovered the molecular mechanism of GRASP55's role in autophagy: as a tether between autophagosome and lysosome, and as a regulator of the PI3K-UVRAG complex. My thesis work proposed a novel target for treatment of Golgi and autophagy related diseases.

Chapter I. Introduction

Golgi Apparatus is firstly discovered in 1898 by Camillo Golgi as a partially silver-osmium-blackened fine internal network in Purkinje cells by accident[1]. This later-on found essential organelle is named Golgi to remark his contribution. Golgi Apparatus has been studied for 120 years and its important functions in protein/ lipid modifications, trafficking and sorting have been well understood. Golgi resides at the center of the secretory pathway, which receives almost the entire output of the endoplasmic reticulum (ER), where proteins and lipids undergo multiple modifications including N- or O-linked glycosylation[2, 3], phosphorylation[4] and proteolytic cleavage[5]. After defined modification through the Golgi cisternae, these mature cargo proteins and lipids are sorted and transported to plasma membrane, endosome, lysosomes or secretory granules to maintain cell homeostasis[6, 7]. In most eukaryotic cells, the Golgi apparatus is composed of stacks of tightly aligned flattened cisternae, which are laterally linked into ribbon like structure in the perinuclear region[8], although it is composed of isolated cisternae and tubular network in some yeast and protists[9]. The Golgi reassembly stacking protein of 65 kDa (GRASP65) and Golgi reassembly stacking protein of 55 kDa (GRASP55), are localized to the *cis*- and *medial-trans*-cisternae respectively[10, 11], which play an essential role in Golgi structure formation. They form *trans*-oligomers from adjacent cisternae to hold the flat cisternae together to form a stack and the individual stacks into a ribbons[12-15]. Meanwhile, GRASP proteins have also been shown to be involved in spindle dynamics[16], apoptosis[17], unconventional secretion[18] and autophagy[19]. In my

thesis work, I further categorize GRASPs' role in Golgi structure/function using CRISPR knockout technique and GRASP55's role in autophagosome maturation.

Golgi Architecture

Golgi stack and Golgi ribbon

The Golgi apparatus is composed of isolated cisternae and tubular network in yeast and some protists[9]. However, in most eukaryotic cells, Golgi is composed of stacks of tightly aligned flattened cisternae, which are laterally linked into ribbon like structure in the perinuclear region, surrounded by transport vesicles (Fig. 1.1)[8]. These Golgi cisternae are membrane bound structures in the Golgi cluster with 20-30 nm in width and more than 150 nm in length[20]. And Golgi stack is formed by a set of flattened, disk-shaped cisternae resembling a stack of plates (Fig. 1.2).

Golgi is a polarized organelle, since the Golgi stack mostly consists of three different domains: *cis*-, *medial*-, and *trans*-Golgi cisternae with tubulovesicular structure on each side: *cis*-Golgi network (CGN) and *trans*-Golgi network (TGN)[21]. CGN receives biosynthetic molecules from ER through COPII vesicles[8]; then these proteins and lipids get modified through *cis*-, *medial*-, and *trans*-Golgi cisternae when sorting signals are also added; at last, they get sorted in TGN and transport exclusively through clathrin coated vesicles to reach their final destinations[21]. The polarity across Golgi also exists on several gradients. While fenestration of Golgi reduces from *cis* to *trans*, the thickness of cisternae decreases as well[8]. Glycosylation enzymes are also distributed across Golgi cisternae according to the order of glycan-processing[22]. Moreover, cholesterol level is higher in trans-side of Golgi; while the pH within cisternae is lower and similar to endosomes[23, 24]. This polarity of Golgi stack also indicates that a single cisterna of Golgi doesn't represent a separate Golgi compartment.

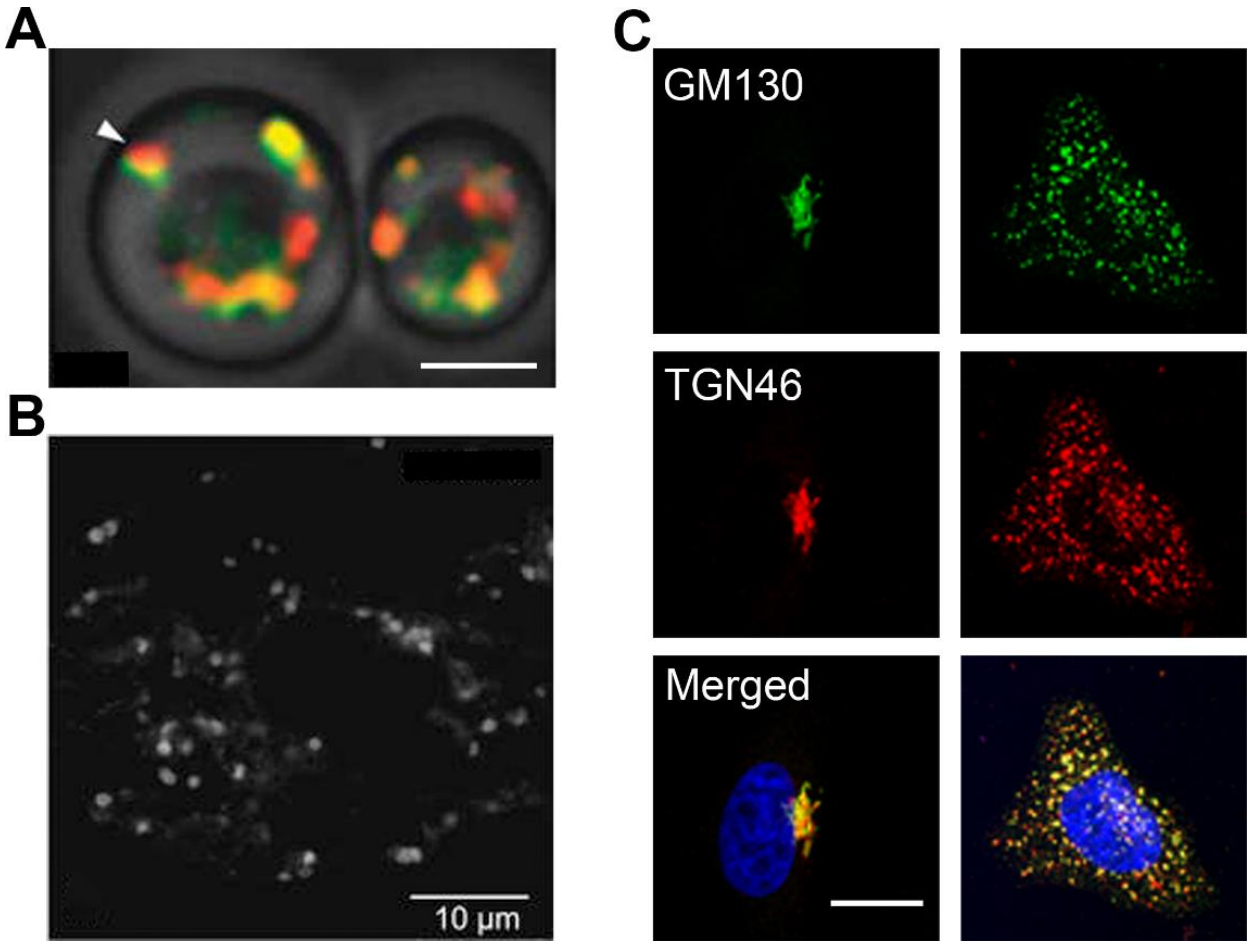

Figure 1.1 The Golgi apparatus in yeast, plants and mammalian cells. (A) In yeast, Golgi is composed of isolated cisternae and tubular network throughout the cytosol. Image shown is cells expressing Sys1–GFP and Sec7–DsRed, arrow shows the apparent partial segregation of Sys1–GFP and Sec7–DsRed within the same cisterna. Scale bar, 2 µm. Image is modified from[25]. **(B)** In plant, Golgi exists as mini-stacks scattering in the cytosol and close to the ER exit sites. Tobacco BY-2 cells Golgi was monitored by ADP-ribosylation factor 1 (Arf1) immunofluorescence. Images presented are from 45-µm optical sections in the confocal laser scanning microscope. Scale bar, 10 µm. Image is modified from[26]. **(C)** In mammalian cells, Golgi is composed of stacks of tightly aligned flattened cisternae, which are laterally linked into ribbon like structure in the perinuclear region. High-resolution AiryScan Confocal immunofluorescence for GM130 and TGN46 in HeLa wild-type cells, untreated (left panel) or 4 hour treatment with Nocodazole (right panel). Noticed that the formation of Golgi ribbon depends on microtubule network. Scale bar, 5 µm. Images are modified from[27].

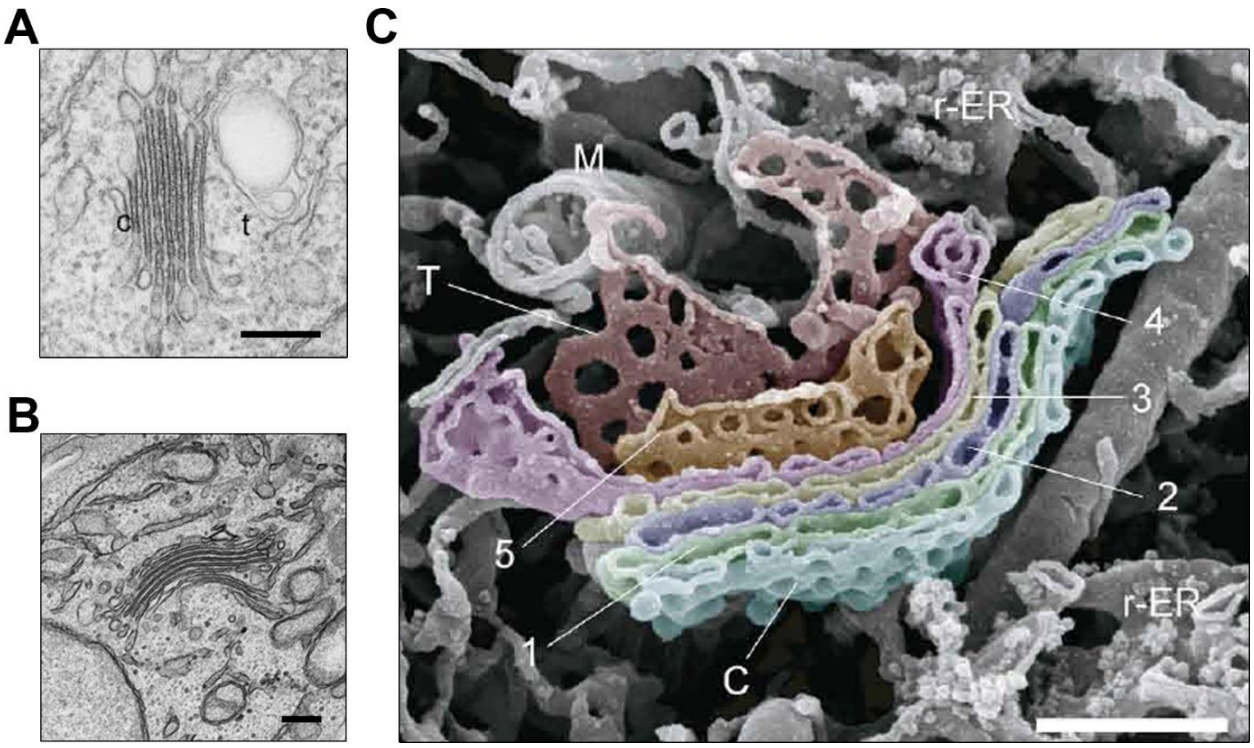

Figure 1.2 The EM picture of Golgi apparatus in plants and mammalian cells. (A) In plant, Golgi exists as mini-stacks scattering in the cytosol. Tobacco BY-2 cells Golgi was monitored by EM. Scale bar, 250 nm. C indicates *cis* side and t indicates *trans* side of Golgi stack. Image is modified from[26]. **(B)** In HeLa cells, Golgi is composed of stacks of tightly aligned flattened cisternae. Scale bar, 200 nm. Image are modified from[27]. **(C)** High magnification of Golgi stack in spinal ganglion cells. This stack has 5 medial cisternae (1-5), with *cis* cisterna (C) and *trans* cisterna (T). r-ER indicates rough ER, M indicates mitochondria. Scale bar, 500 nm. Image is adopted from[28].

GRASP55 and GRASP65 are two homologous peripheral membrane proteins, which have been shown to play an important role in mammalian cells. They localize to the *cis*- and *medial-trans*-cisternae respectively, where they form homo-dimers and trans-oligomers to help adjacent cisternae to form a stack[12, 13]. Mitotic regulated phosphorylation of GRASP55 and GRASP65 are involved in disassembly and reassembly of Golgi stacks during cell cycle. Meanwhile, GRASP proteins are also involved in Golgi ribbon linking[14, 15]. The reason why Golgi forms stacks has been long time a mystery. In Chapter II, we demonstrate that GRASP knockout disperses Golgi stack into single cisternae and tubulovesicular structures, which accelerates protein trafficking

which the cost of inaccurate glycosylation. This finding provides evidence to the hypothesis that Golgi stacking is essential for accurate posttranslational modification[27].

Golgi exists as mini-stacks scattering in the cytosol and close to the ER exit sites in plant and lower animal cells[29], whereas they laterally link together to form Golgi ribbon in mammalian cells[21]. Cytoskeletons, especially microtubules and actins; and Golgi matrix proteins, such as Golgin-84[30], Golgin-160[31] and p115[32] have been shown to play an essential role for Golgi ribbon formation. While microtubule minus-directed motor protein, dynein, enriches Golgi stack at microtubule organizing center (MTOC)[33]; actin helps to maintain characteristic flattened morphology of cisternae directly by providing mechanical stability[34]. Moreover, both GRASP55 and GRASP65 are also involved in Golgi ribbon linking: MEK1/ERK regulation of GRASP55 was shown to regulate Golgi ribbon linking[14], while Mena–GRASP65 interaction collaborates with actin polymerization in Golgi ribbon linking[15].

Golgi Biogenesis

In eukaryotic cells, COPII vesicles generated from transitional ER sites fuse homotypically to form new *cis*-Golgi cisternae or fuse with formerly existed cisternae[35, 36]. During mitosis, Golgi undergoes extensive fragmentation and reassembles in two daughter cells at the exit of mitosis[21]. At G2 phase, Golgi ribbon is broken down by membrane-fission proteins GtBP3/BARS[37] and mitogen-activated protein kinase kinase I (MEKI)[38]. If the mitotic checkpoint is passed, duplicated centrosomes would move to the two poles of the cell and form microtubule spindles. While GRASP55 and GRASP65 form homo-dimers and trans-oligomers to help adjacent cisternae to form a stack in interphase[12, 13]; Cdk1/cdc2 acquires elevated activity during mitosis and phosphorylate the C-terminus of GRASP proteins which interrupts their oligomers' interaction and break up the Golgi stack into single cisternae[12, 13]. Then these separated Golgi cisternae further break down into mitotic Golgi fragments (MGF) via COPI vesicles[39]. During this process, Golgi t-SNARE (soluble N-ethylmaleimide-sensitive factor (NSF) attachment protein receptor) syntaxin 5 (Syn5) is mono-ubiquitinated by Golgi localized E3-ligase, HECT domain and ankyrin repeat containing E3 ubiquitin protein ligase 1 (HACE1)[40] in early mitosis which impairs its interaction with cognate v-SNARE Bet1 and disrupts SNARE complex formation. In late mitosis, ubiquitinated Syn5 recruits valosin-containing protein, p97/p47 to the MGF and is deubiquitinated by VCIP135, which enables SNARE complex assembly to promotes Golgi cisternae reformation[41]. Subsequently, protein phosphatase 2A (PP2A) removes phosphate from GRASP proteins and Golgi stack is reformed (Fig. 1.3)[39, 42].

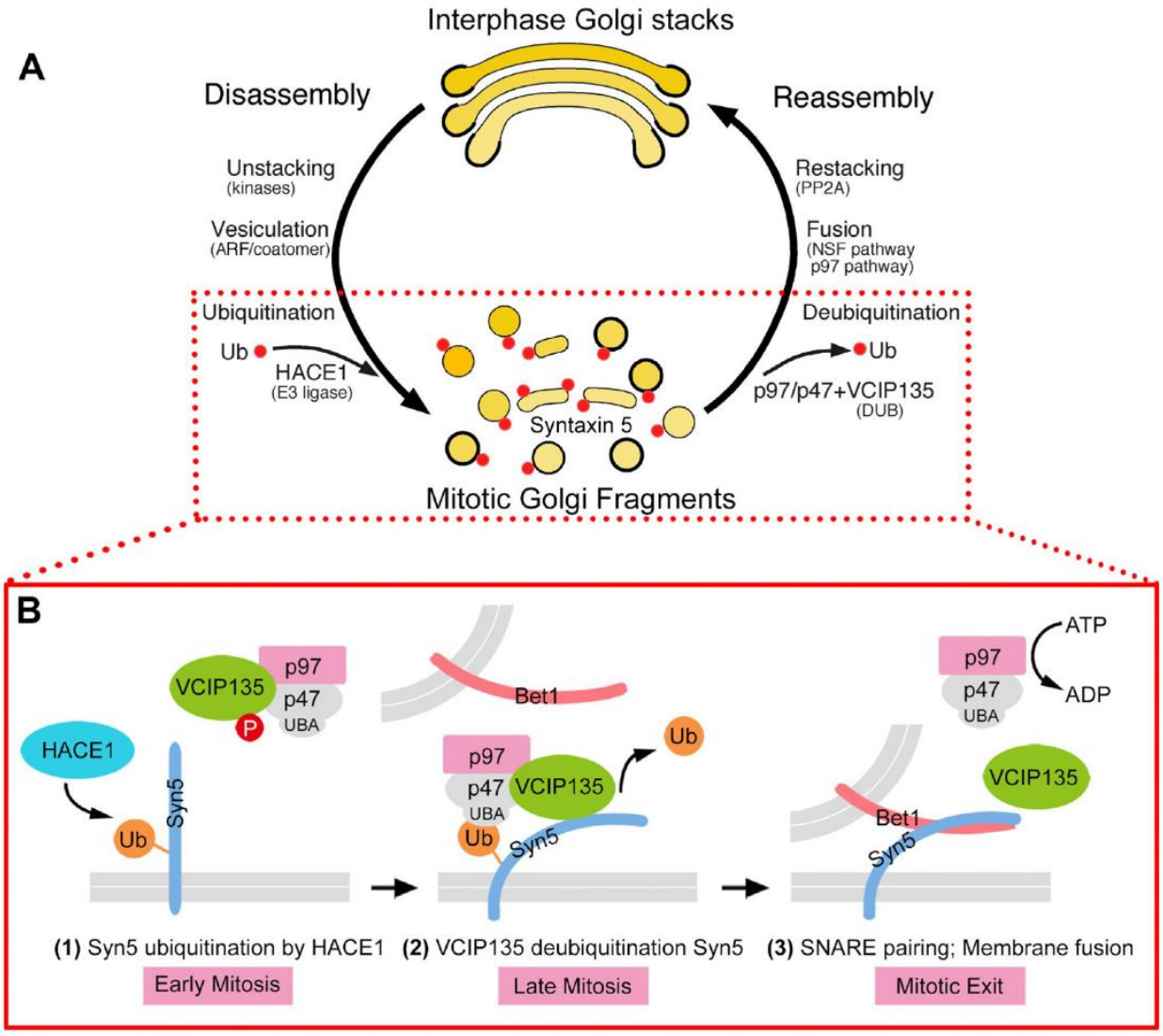

Figure 1.3 Golgi disassembly and reassembly during mitosis[43]. (A) Golgi stacks are disassembled by cisternal unstacking and vesiculation. During mitosis, mitotic kinases with elevated activity, phosphorylate the C-terminus of GRASP proteins which interrupt their oligomers' interaction and break up the Golgi stack into single cisternae. ARF1 and its coatomer vesiculate the cisternae through COPI vesicle budding. At the end of mitosis, Golgi vesicles fuse to generate single cisternae and form stacks, which is mediated by NSF and p97/p47. (B) Monoubiquitination of Syn5 regulates p97-mediated post-mitotic Golgi membrane fusion. Syn5 is monoubiquitinated by HACE1 in early mitosis which impairs its interaction with cognate v-SNARE Bet1 and disrupts SNARE complex formation. In late mitosis, ubiquitinated Syn5 recruits p97/p47 to the MGF and is deubiquitinated by VCIP135, which enables SNARE complex assembly to promote Golgi cisternae formation. Ub, ubiquitin; UBA, ubiquitin-associated domain. This figure is adopted from[43].

Golgi in secretory pathway

ER to Golgi and Golgi to ER transport

As the crossroad of the secretary pathway, Golgi receives almost entire output of ER, where the proteins and lipids undergo multiple modifications. Upon biosynthesis and proper folding, cargo proteins are delivered from ER to Golgi through vesicular coat complex COPII; while retrograde transport from Golgi to ER depends on COPI[24].

ER to Golgi transport is started with generation of COPII vesicles[24]. COPII vesicles consist of five main players: Sar1, Sec23/24 and Sec13/31[44]. Sec12, as the guanine nucleotide exchanging factor (GEF) of Sar1, exchanges GDP to GTP on Sar1[45], which helps Sar1 anchor onto ER membrane[46]. Then the Sar1-GTP recruits Sec23/24 protein complex to ER[46], where the heterodimer binds to and enriches cargo proteins through specific sorting sequence on their cytosolic domains[44]. After the inner layer formed by Sec23/24, another heterodimeric protein complex Sec13/31 is recruited to form the outer layer of COPII vesicle and promote membrane deformation[47]. Upon budding from ER, Sec23 induces hydrolysis of GTP to GDP on Sar1, which disassembles the coat of COPII vesicles, and then the uncoated vesicles fuse with their target membranes[48]. In mammalian cells, uncoated COPII vesicles homotypically fuse into vesicular tubular clusters (VTCs) or structures like ER-Golgi-intermediate-compartments (ERGIC)[49]. Then VTCs follow microtubules to transport to Golgi, with the help of p115 and GM130 as docking tethers, and SNARE protein Syn5 for fusion[50-52].

On the other hand, COPI vesicles are involved in Golgi to ER transport. Similar to COPII vesicles, GEF exchanges GTP to GDP on small GTPase, Arf1, which helps Arf1 membrane association and later on recruit COPI coatomer composed of α, β, β', γ, δ, ε and ζ subunits to form COPI coat[53]. And GTPase activating protein (GAP) hydrolysis GTP to GDP helps deactivate Arf1 and disassemble COPI vesicles[54].

Intra-Golgi transport

As COPI vesicles are well accepted as carriers for intra-Golgi transport, two models have been proposed for intra-Golgi transport: the *vesicular transport* model and *cisternae maturation* model (Fig. 1.4)[55].

In the vesicular transport model, all Golgi cisternae and Golgi enzyme are stationary while cargo proteins are transported across Golgi cisternae through anterograde trafficking by COPI vesicles[55]. This hypothesis could well explain the polarized distribution of Golgi enzymes[55], but have difficulty in demonstrating how large cargos, which is too big for COPI vesicles, like procollagen are transported through Golgi[56] and lack of evidence in COPI dependent anterograde trafficking[55]. On the other hand, in the cisternae maturation model, newly formed Golgi cisternae joins at the *cis* Golgi, while cargo proteins stay in the cisternae, Golgi resident proteins retrograde transport from older cisternae to younger ones through COPI vesicles, which drives the maturation of Golgi cisternae and at last, the *trans* side of Golgi peels off from Golgi stack[55]. This model could better explain how procollagen transport through Golgi cisternae and why this large protein is trafficking at the same rate as small proteins like Vesicular stomatitis Indiana virus (VSVG)[57]. However,

different labs have shown different results on the contents of COPI vesicles, exclusively cargo proteins or glycosylation enzymes, which indicates possibly two or more population of COPI vesicles exist and both two models are partially right[58, 59].

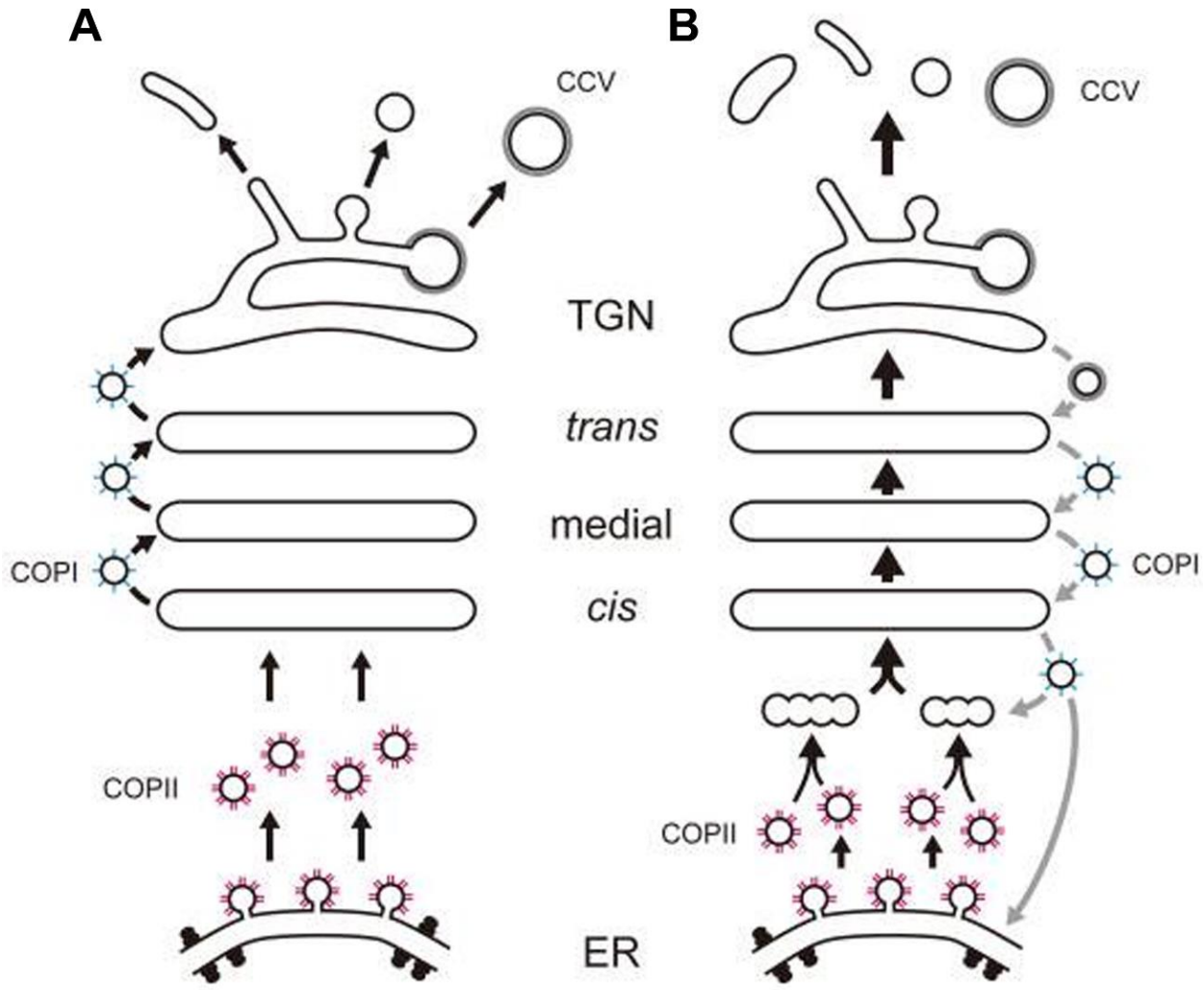

Figure 1.4 Two models of intra-Golgi trafficking: vesicular transport model and cisternae maturation model[55]. (A) Vesicular transport model. All Golgi cisternae and Golgi enzyme are stationary while cargo proteins are transported across Golgi cisternae through anterograde trafficking of COPI vesicles. **(B)** Cisternae maturation model. Cargo proteins stay in the cisternae, while Golgi resident proteins retrograde transport from older cisternae to younger ones through COPI vesicles which drives the maturation of Golgi cisternae. This figure is adopted from[55].

Post-Golgi transport

After defined modification through Golgi cisternae, cargo proteins are transported to TGN where they are sorted and transported to different destinations (Fig. 1.5)[44]. TGN, different from other cisternae in Golgi stack, is a tubular network which is connected to trans-Golgi[60]. Cargo proteins bearing mannose-6-phosphate (M6P) signal binds to M6P receptors (M6PR) which is then recruited to clathrin coated vesicles (CCVs), and transported to late endosome and lysosomes[55]. After M6P bearing cargo is released from M6PR, M6PR and other Golgi resident proteins are recycled back to TGN through retromers[61]. TGN to plasma membrane trafficking could be divided in several classes: pleiomorphic structure for many secretory proteins, recycling endosomes for VSVG and secretory granules for regulated cargo proteins[60]. Meanwhile, TGN is also the interface between Golgi and endocytic system, which could also explain the similarity of pH, cholesterol level and membrane thickness in between[60].

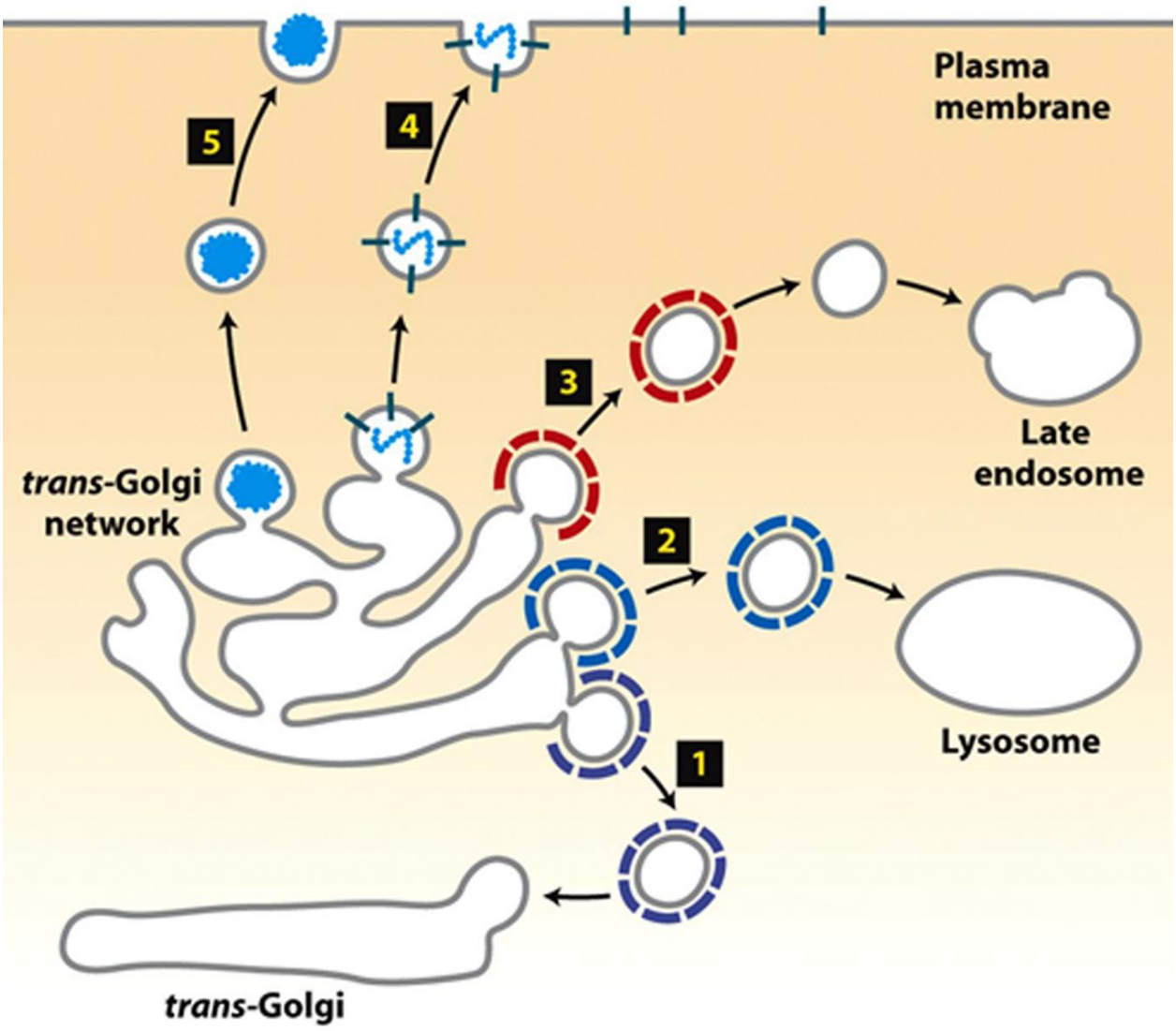

Figure 1.5 Post Golgi transport[44]**.** Trafficking pathway 1 represents retrograde trafficking of resident Golgi proteins via COPI-coated vesicles. Trafficking pathway 2 represents AP-3 complexes mediated vesicles which directly fuse with lysosomes. Trafficking pathway 3 represents CCVs budded from TGN to fuse with late endosomes. Trafficking pathway 4 represents constitutive secretion and trafficking pathway 5 represents regulated secretion. This figure is adopted from[44].

Golgi functions

At the crossroad of secretory pathway, Golgi Apparatus has multiple functions thanks to its unique structure. It connects ER with endosome system, plasma membrane and autophagosomes. Other than its well-known role in protein/lipid glycosylation, Golgi is also involved in cell cycle control, cytoskeleton organization, apoptosis, autophagy, signaling pathway and transcription, etc.

Glycosylation

There are three different kinds of protein glycosylation: N-linked Glycosylation, O-linked Glycosylation and protoglycons[62]. While O-linked glycosylation is added to a subset of Serines or Threonines exclusively in Golgi; N-linked glycosylation initiates in ER, where a 14-residue precursor of oligosaccharides is added to Asparagine residues within Asn-X-Ser/Thr motif of proteins[44]. After three glucose (Glc) and one mannose (Man) are removed from the glycan, the $(Man)_8(GluNAc)_2$ bearing glycoprotein is transported to *cis*-Golgi, where five more mannoses are removed and N-acetylglucosamines, galactose, sialic acids are added to remaining N-glycans by sequentially arranged glycosylation enzymes along *cis-trans* Golgi cisternae[22]. While N-linked glycosylation steps in ER are the same, the number and identity of carbohydrate and even the branches they add to in Golgi is highly diverse and this diversity contributes to different functions of glycoproteins, as known in immune response (Fig. 1.6A)[63]. Delicate Golgi structure maintained by GRASPs ensures proper protein glycosylation by maintaining glycosylation enzymes distributed orderly to process cargo proteins sequentially and slowing down trafficking by restricting vesicles budding and fusion to the rim of cisternae to give sufficient time to glycosylation enzymes for cargo processing (Fig. 1.6B). However, GRASP depletion, which

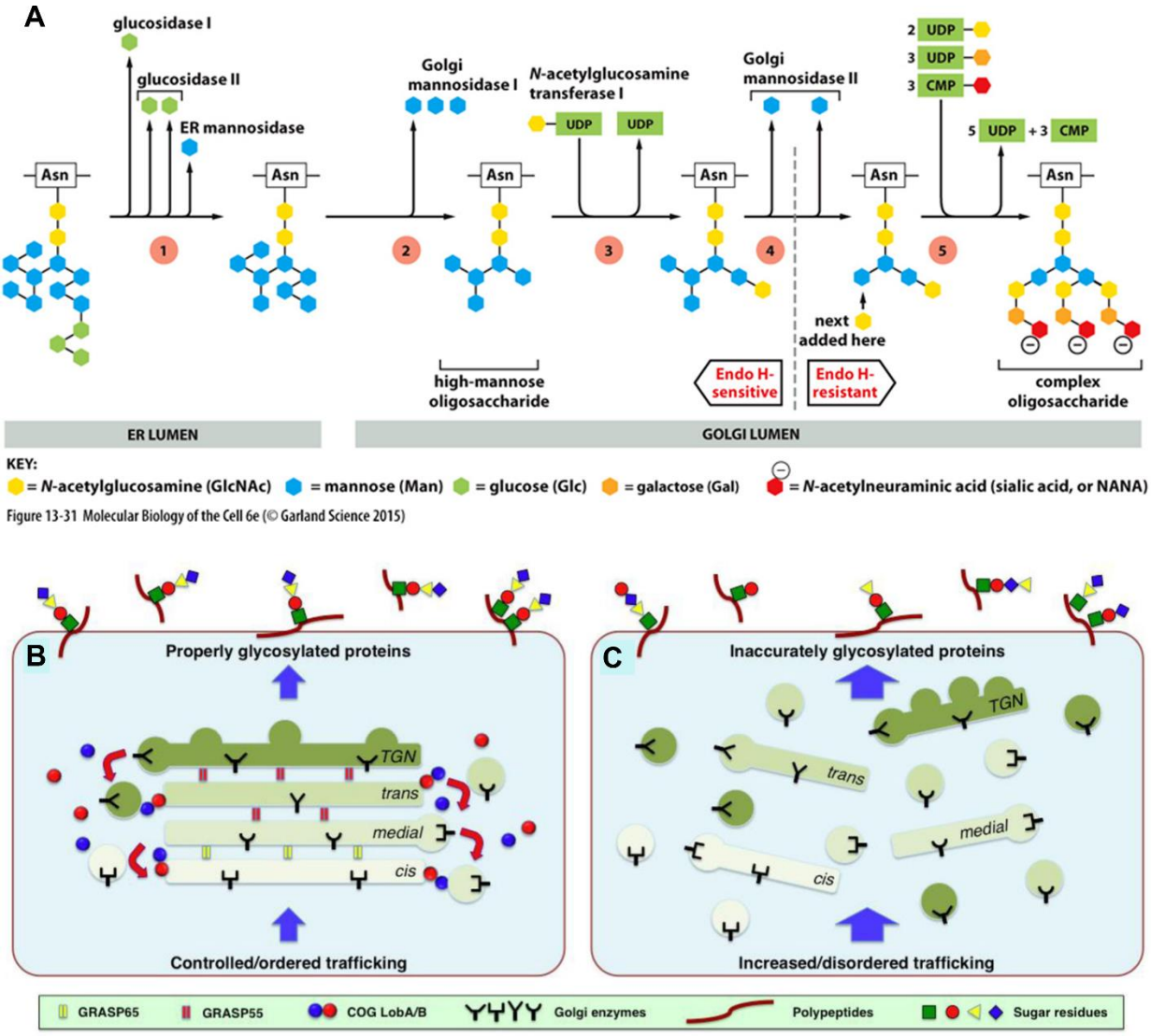

Figure 1.6 Golgi and protein glycosylation. (A) N-linked glycosylation steps in ER and Golgi. N-linked glycosylation initiates in ER, where a 14-residue precursor of oligosaccharides are added to Asn[44], then ER-localized glucosidases I and II remove three glucose and ER-mannosidase' final removal of a mannose allows ER exit. In *cis*-Golgi, mannosidase I and II in the *cis* and *medial* Golgi further remove five more mannoses when the protein remains Endo H sensitive. At last, as N-acetylglucosamines, galactose, sialic acids are added to remaining N-glycans by sequentially arranged glycosylation enzymes in the *medial*- and *trans*-Golgi cisternae these glycan-chains become Endo H resistant. N-Glycosylation model is modified from[44]. **(B-C)** Golgi structure is essential for proper protein glycosylation[3]. **(B)** Normal Golgi structure maintained by GRASPs ensures proper protein glycosylation. The defined Golgi stack mediated by GRASP help to keep Golgi glycosylation enzymes distributed orderly when cargo proteins sequentially processed by different Golgi glycosylation enzymes and slow down trafficking by restricting vesicles budding and fusion to the rim of cisternae to give sufficient time to glycosylation enzymes for cargo processing. **(C)** Golgi structure defect results in glycosylation defects. Golgi structure defect, likely by GRASP depletion, triggers Golgi unstacking, increases vesicles budding and fusion area which accelerates cargo protein transport but lead to protein glycosylation defect. This figure is modified from[3].

triggers Golgi unstacking, increases vesicles budding and fusion area, which accelerates cargo protein transport but leads to protein glycosylation defect (Fig. 1.6C). This effect, we have investigated in GRASP siRNA knockdown cells[64] and also confirmed in GRASP knockout cells[27] as described in Chapter II.

Autophagy

The Golgi apparatus also has a role in autophagosome formation. Atg9, a transmembrane protein, functions as a key regulator of autophagy induction. It helps provide membranes for the formation of the pre-autophagosomal structure (PAS) in yeast[65]. In mammalian cells, Atg9, cycles between the TGN and endosomes, and relocates to autophagosomes upon amino acid starvation or rapamycin treatment, which implicates that Golgi may deliver membranes to autophagosomes[66]. Furthermore, increased secretion of constitutive cargo from TGN to plasma membranes recruits microtubule-associated protein 1 light chain 3 (LC3) to specific domain of TGN and promotes autophagosome formation which requires adaptor protein complex 1 (AP1)-mediated clathrin vesicles delivery of membranes from the TGN to autophagosomes[67]. In addition, Beclin 1 and the PI3K complex are concentrated on the TGN by interaction with GAPR-1, a lipid raft-associated protein on the Golgi[68], which negatively regulate Beclin 1 traslocation to PAS and autophagosomes[69]. Meanwhile, another study has found that Beclin 1-associated autophagy-related key regulator (Barkor) is required for the re-localization of the PI3K complex from the TGN to autophagosomes[70].

In Chapter III, I found that, upon amino acid starvation, the Golgi undergoes partial fragmentation in the order from *trans* to *cis*, and the derived Golgi fragments colocalize with autophagosomes, consistent with the previous publications that Golgi plays a role in autophagosome formation[66, 67]. Moreover, GRASP55 facilitates autophagosome-lysosome fusion through two actions, one is by physically tethering autophagosomes and lysosomes through the interactions with LC3 on autophagosomes and LAMP2 on late endosomes/lysosomes which has also been shown in glucose starvation[230], although glucose starvation does not affect Golgi morphology as seen in amino acid starvation; and the other is by interacting with Beclin 1 to facilitate the assembly and membrane association of the PI3K UVRAG complex. These findings indicate that Golgi may contribute to autophagy as membrane source as well as regulator when GRASP55 plays an important role in autophagosome maturation during amino acid starvation (Wang et al, submitted).

Mitosis

Golgi Apparatus is involved in cell cycle regulation. During mitosis, Golgi undergoes extensive fragmentation and the resulting MGF equally distributes and reassembles in two daughter cells at the exit of mitosis[21]. The breakdown of Golgi ribbon/stacks may work as mitosis checkpoint[33], as microinjection of C-terminus of GRASP55[71] or GRASP65[72], or inhibition of Golgi fission protein, BARS[37], blocks cell cycle in G2 phase, which may work as a similar mechanism as spindle check point, by checking the attachment between microtubules and individual Golgi stacks[33]. Moreover, GRASP65[16] and GM130[73, 74] are required for bi-polar spindle formation; and release of Golgi proteins in mitosis, such as clathrin[75] and Rab6a'[76] are also essential for proper cell division.

Centrosome orientation and microtubule organization

Golgi Apparatus localizes close to centrosome by interaction with microtubules and its motor proteins, which is important for centrosome positioning and directed transport, thereby required for cell polarization and migration[33]. Mitogen-activated protein kinase (MAPK) phosphorylates GRASP65 and reorientate centrosome to promotes cell migration[77]. Moreover, non-centrosomal microtubules, especially Golgi emanating microtubules, are nucleated by GMAP-210, GCC185 and GM130. While GMAP-210[31] and GM130[78] recruit γ-tubulin complex to *cis*-Golgi; GCC185[79] interacts with CLASP at TGN to nucleate non-centrosomal microtubules; which play an important role in Golgi ribbon formation, cell polarity establishment, directed protein transport and migration.

Apoptosis

During apoptosis, Golgi Apparatus undergoes ribbon unlinking and cisternae are broken into tubulovesicular structures which is similar to mitotic Golgi fragments[80]. Multiple Golgi matrix proteins, including GRASP65[81], GM130[82], Golgin-160[83], giantin[84], p115[85] and Syn5[84], are cleaved by caspases, which could contribute to Golgi fragmentation upon apoptosis stimulation. Moreover, Golgi may also function as apoptosis regulator. While non-cleavable Golgin-160 overexpression delays ER stimuli induced apoptosis[86]; p115 is cleaved by caspase 3 and its C-terminal fragment translocates into nucleus as transcription factors, which promotes Golgi fragmentation and apoptosis[85]. Meanwhile, Golgin-160, which is cleaved by Golgi-localized caspase 2 during apoptosis, moves into nucleus and is supposed to have similar function as p115[87].

GRASP55 and GRASP65

GRASPs are peripheral membrane proteins associated to Golgi membrane through their N-terminal myristylation[10]. GRASP65 localizes to *cis*-cisternae of Golgi stack; while GRASP55 localizes at *medial-trans*-Golgi cisternae[11]. GRASP homologous have been found in most eukaryotic cells, from yeast[88], flies[89] to mammalian cells. GRASPs have been implicated in Golgi stack formation and ribbon linking, as well as other cellular processes, including enzyme distribution[90], cargo transport[91], unconventional secretion[18, 92], cell cycle progression[16], apoptosis[17], and cell migration[93].

GRASPs in Golgi architecture

In mammalian cells, Golgi is composed of stacks of tightly aligned flattened cisternae, which are laterally linked into ribbon like structure in the perinuclear region[8], during this process, many Golgi matrix proteins including GRASPs and golgins have been found playing important roles[94]. GRASP proteins were firstly found as Golgi stacking factors through in-vitro Golgi disassembly and reassembly assay[10, 11]. Purified rat liver Golgi fragments into mitotic Golgi fragments after treatment with mitotic cytosol prepared from spinner HeLa cells, which reassemble into Golgi stacks upon further incubation with interphase cytosol. Restacking of newly formed cisternae is blocked by adding GRASP55 or GRASP65 antibodies[10, 11]. Similar results are confirmed through in vivo assay, while micro-injection of GRASP65 antibody[12] or knockdown of GRASP proteins by siRNA[13] blocks Golgi reassembly in post-mitotic daughter cells. These results confirmed that GRASP proteins are essential for Golgi stacking. Moreover, GRASPs are also involved in Golgi ribbon linking. MEK1/ERK regulation of GRASP55 was shown to regulate Golgi ribbon linking

and depletion of GRASP55 blocks G2/M transition[14], while GRASP65 interacts with an actin elongation factor, Mena, which collaborates with actin polymerization in Golgi ribbon linking[15].

GRASP proteins form dimers and phosphorylation regulated trans-oligomers through their highly conserved GRASP domains. The N-terminal GRASP domain contains two PDZ domains, which are common protein-protein interaction modules[12, 13, 95]. C-terminus of GRASP55 and GRASP65 are less conserved, but rich in Serine and Proline, thereby named as Serine/Proline rich (SPR) domains[95]. During mitosis, GRASP65 is phosphorylated by CDK1/cdc2 and polo-like kinase 1 (plk1)[96]; while GRASP55 is phosphorylated by MAPK and ERK2[97], at the C-terminal SPR domain which breaks up *trans*-oligomers and disassembles Golgi stack into single cisternae[12, 13, 95]. The different kinases involved in this process also indicate that GRASP55 and GRASP65 are regulated by different signal pathways (Fig. 1.7).

GRASPs also interact with Golgins to maintain Golgi structure and trafficking homeostasis. GRASP65 forms stable complex with the most well-characterized golgin, GM130[98]. GM130 localizes to the center region of CGN and *cis*-Golgi cisternae[99], where the GM130-GRASP65 complex interacts with p115 and recruits COPII/COPI[51, 100] vesicles to link these vesicles to *cis*-Golgi and directs SNARE complex assembly for membrane fusion[101]. Meanwhile, GRASP55 interacts with another Golgin, Golgin-45, a Rab2 effector; which contribute to maintenance of Golgi structure and protein trafficking[102].

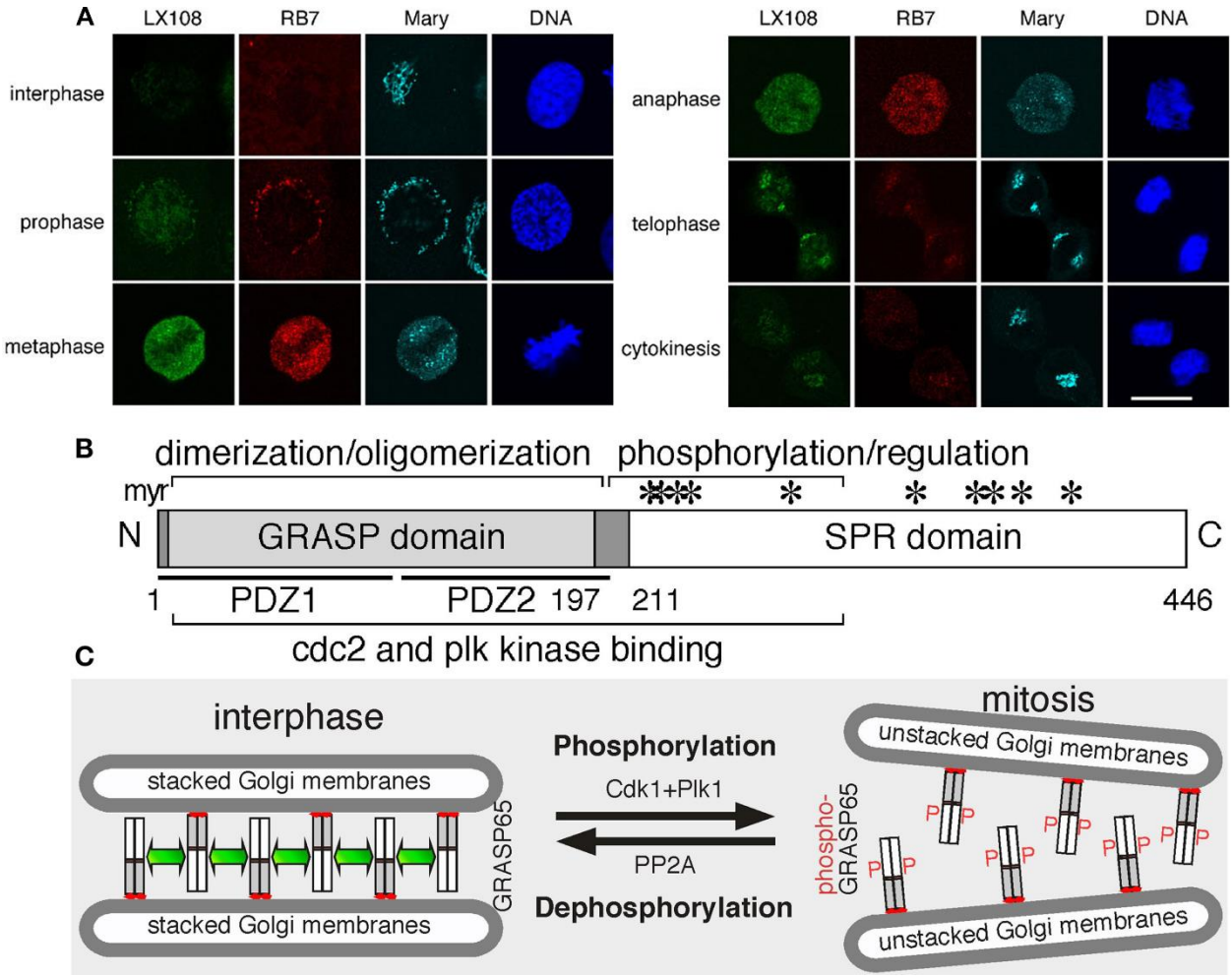

Figure 1.7 Golgi disassembly and reassembly during mitosis depends on GRASP phosphorylation. **(A)** GRASP65 is sequentially phosphorylated and dephosphorylated to promote mitotic Golgi disassembly and post-mitotic reassembly. NRK cells of indicated cell cycle phases are labeled with LX108 (phosphor-specific antibody recognizes T220/T224), RB7 (phosphor-specific antibody recognizes S376) and Mary (total GRASP65). Note that the intensity of LX108 and RB7 signal varies and correlates with the different Golgi status. Scale bar, 10 μm. Images are modified from[103]. **(B)** Schematic domain structure of GRASP65[104]. Myristylation (myr) for membrane association; GRASP domain which contains two PDZ domains underlined, for dimerization and oligomerization; and the SPR domain with known phosphorylation sites (*) indicated. Its homologue, GRASP55, has a similar domain structure. This image is modified from[104]. **(C)** GRASP65 oligomerization and Golgi stack formation[104]. During interphase, GRASP65 dimers oligomerize through their PDZ domain to form a "glue" to hold the membranes together into a stack. During mitosis, GRASP65 is phosphorylated by CDK1 and plk1 at the C-terminal SPR domain which breaks up trans-oligomers and disassemble Golgi stack into single cisterna. On the other hand, GRASP55 is phosphorylated by MAPK ERK2 during mitosis and regulate Golgi stack formation in a similar manner. This image is modified from[104].

Recently a GRASP65 knockout mouse has been reported, with only limited defects in the structure and function of the Golgi[105]. One major concern of this knockout mouse is the potential for only partial deletion of the gene, leaving a possibility that an N-terminal 115 amino acid fragment of GRASP65 may still be translated and this fragment is sufficient for oligomerization[106-108], a key property essential for Golgi stacking[12, 95]. The lack of an obvious phenotype in Golgi stacking in the GRASP65 knockout mouse may also be due to the complementation by GRASP55[11, 109]. Therefore, a complete knockout of both GRASPs is needed to further evaluate their functions. In Chapter II, we have used the CRISPR (Clustered Regularly Interspaced Short Palindromic Repeats)/Cas9 genome editing technique[110, 111] to knock out GRASP55 and GRASP65, single or in combination, to investigate their roles in Golgi structure formation. We designed multiple sgRNAs targeting to exon 1 of GRASP55 and exon 2 of GRASP65, which are directly downstream of the first ATG for translation initiation. Treatment of cells with these sgRNAs resulted in either insertions or deletions that caused a frame shift of the gene with an immediate stop codon, as confirmed by DNA sequencing of individual clones. This ensures that no functional, truncated proteins are generated in the cell lines. Analysis of these cells with light and electron microscopy demonstrated that double-deletion of both GRASPs completely disrupted Golgi stack formation and ribbon linking. Based on these results and previous literature, we conclude that stacking is the primary function of GRASP proteins[27].

GRASPs in unconventional secretion and autophagy

GRASP proteins are firstly found involved in unconventional secretion in *Distyostelium idscoideum*. Acyl-CoA binding protein (AcbA), which lacks signal sequence, is secreted with the help of GRASP proteins[112]. This finding is also confirmed by depletion of yeast homologue of

GRASP, Grh1[113]. Moreover, Drosophila homologue of GRASPs, dGRASP mediates integrin unconventional secretion in Drosophila epithelial remodeling[114]; in mammalian cells and mice model, GRASP55 is required for cystic fibrosis transmembrane conductance regulator (CFTR) mutant (ΔF508) unconventional trafficking to cell surface[18]. Later studies find out that unconventional secretion involves autophagy machinery: Atg5, Atg8 and Atg9; endosomal sorting complex required for transport (ESCRT) protein, vacuolar sorting protein 23 (Vps23) and GRASP55[19, 115]. A novel compartment of unconventional protein secretion (CUPS) is defined as a Grh1-containing membranes which is enriched with Phosphatidylinositol 3 phosphate (PI3P), ESCRT-I, -II, and -III complex, Atg8, Atg9, but lacks components of the Golgi apparatus and the endosomes[115, 116]. Consistent with the role of GRASP55 in unconventional secretion, we propose that GRASP55 plays an important role in autophagy. In Chapter III, we show that, upon amino acid starvation, trans-Golgi derived membrane fragments colocalize with autophagosomes. GRASP55 facilitates autophagosome-lysosome fusion through two mechanisms, one is by physically tethering autophagosomes and lysosomes through the interactions with LC3 on autophagosomes and LAMP2 on late endosomes/lysosomes which has also been shown in glucose starvation[230], and the other is by interacting with Beclin 1 to facilitate the assembly and membrane association of the phosphoinositide 3-kinase (PI3K) UVRAG complex. These findings indicate that GRASP55 plays an important role in autophagosome maturation during amino acid starvation (Wang et al, submitted).

GRASPs' role in other cellular processes

In addition to Golgi stack formation, ribbon linking, unconventional secretion and autophagy GRASPs also have important roles in other cellular processes.

For cargo transport and enzyme distribution, GRASP55 and GRASP65 bind to p24 cargo receptor family proteins, which helps p24's retention in the Golgi[117]; GRASP55 interacts with transforming growth factor-alpha (TGF-α) via its first PDZ domain[118], while both GRASPs interacts with specific class of cargos bearing C-terminal Valine, such as CD8α and Frizzled to efficiently transport them to cell surface[91]. Moreover, the uniform distribution of Golgi enzymes, such as GalNAc-T2, also depends on GRASP65-GM130 complex[90], which may attribute to GRASPs' role in Golgi architecture.

During mitosis, GRASP proteins regulate mitotic entry and progression. Expression of the non-phosphorylatable GRASP domain[13] or the C-terminal SPR domain[72, 119] of the GRASP proteins delays mitosis, likely through inhibition of mitotic Golgi fragments or sequestering mitotic kinases. Moreover, GRASP65 is also involved in spindle dynamics during mitosis, as depletion of GRASP65 causes aberrant spindles and defect in cell division[16]; while phosphorylation of GRASP65 is essential for cell polarizing and migration[77].

During apoptosis, the Golgi is fragmented into tubulovesicular structure when multiple Golgi matrix proteins are cleaved by caspases[80]. GRASP65 is cleaved by caspase-3, and expression of

an uncleavable GRASP65 mutant could partially preserve the Golgi stack and ribbon structure[81, 107].

All these functions of GRASPs indicate that these two GRASP proteins may have gained different roles during evolution in addition to their roles in Golgi structure formation.

CRISPR

CRISPR (clustered regularly interspaced short palindromic repeats) or CRISPR-associated protein 9 (Cas9) system is a well-established RNA-guided editing tool in mediating gene alteration. This adaptive immune defense system, which functions in direct degradation of foreign nucleic acids in bacteria and archaea, is utilized to facilitate RNA-guided site-specific DNA cleavage. By designing guide RNAs (gRNA) with complementary sequences of target gene and transfected by invading viral or plasmid, CRISPR RNAs (crRNAs) and Cas9 proteins direct degradation of endogenous genomic loci (Fig. 1.8). Meanwhile, CRISPR can also be applied in directed mutation when it works as a nicking enzyme to facilitate homology-directed repair with minimal mutagenic[110, 111]. Multiple labs have used this system to knockout their interested proteins and successfully clarify their functions in yeast, plants, animals and mammalian cells[110, 120-122]. In Chapter II, we have used this CRISPR genome editing technique to create loss-of-function alleles (referred to hereafter as "knockout") of GRASP55 and GRASP65, single or in combination in HeLa and HEK cells, to investigate their roles in Golgi structure formation and function.

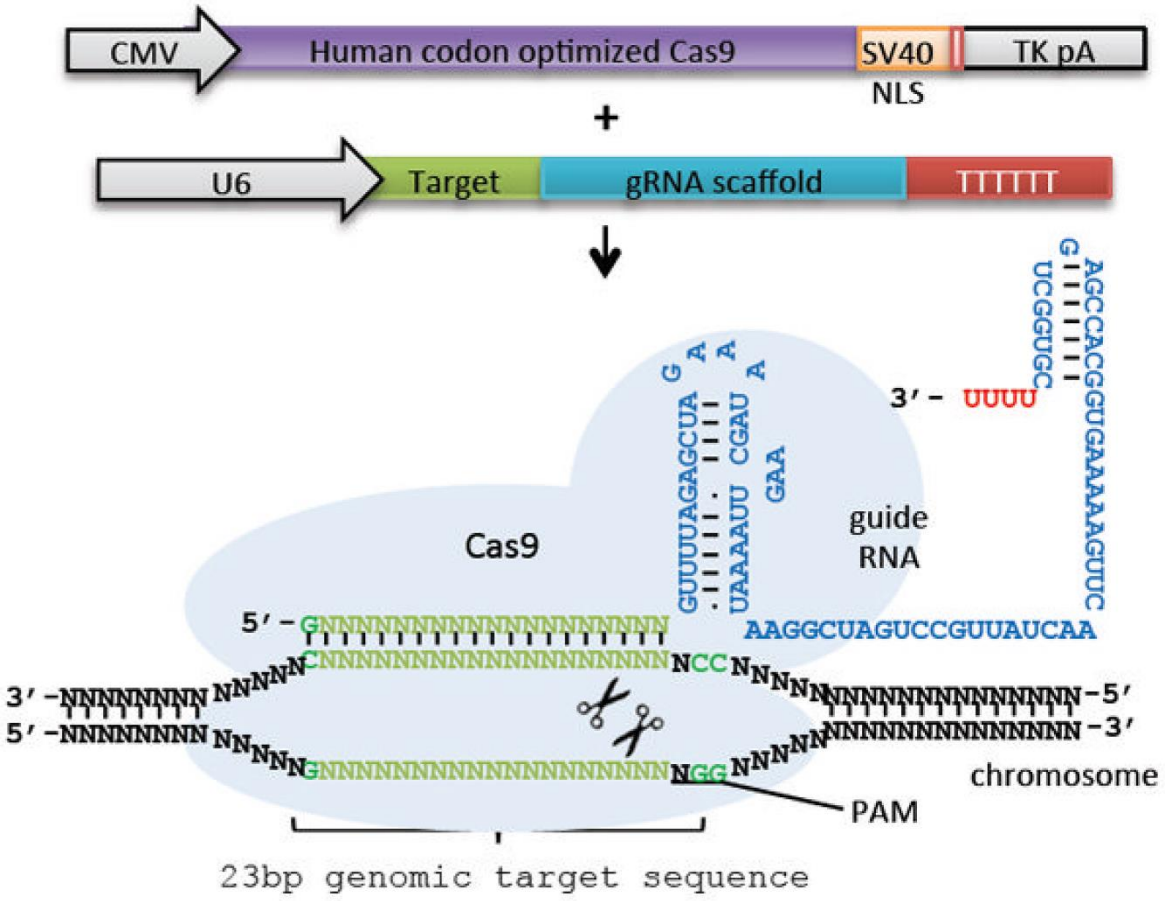

Figure 1.8 Schematic CRISPR system[110]. Co-expression of two constructs: Cas9 protein bearing a C-terminal SV40 nuclear localization signal (NLS) and gRNAs (normally around 23bp) expressed from the human U6 polymerase III promoter. When a target sequence is recognized by the gRNA and the correct PAM is present at the 3′ end, Cas9 unwinds the DNA duplex and cleaves both strands and then the cleaved double strands ligate together randomly which always leads to early stop codon. CMV, cytomegalovirus promoter; TK, thymidine kinase; pA, polyadenylation signal. This figure is modified from[110].

Autophagy

Autophagy is an important cellular process in response to nutrient starvation[123-125]. There are three subtypes of autophagy, depending on how cargos are delivered to lysosomes: microautophagy, chaperone-mediated autophagy (CMA) and macroautophagy (Fig. 1.9)[126]. Both microautophagy and CMA have their cytosolic cargos directly transported to lysosomes: during microautophagy, these cargos are transported into lysosome by invagination of lysosome membranes to form vesicles which subsequently bud into lysosome lumen[127]; however, no vesicle formation nor changes in lysosome membranes take place in CMA mediated selective degradation of cytosolic protein aggreggates[128]. Different from microautophagy or CMA, macroautophagy forms unique double membrane organelle and degrades both protein aggregates and damaged organelles, which is the most universal form of autophagy[129, 130]. Macroautophagy, based on its cargo selectivity, also divides into two subtypes: bulk autophagy and selective autophagy, which is cytoplasm-to-vacuole targeting (Cvt) pathway in yeast[131]. As bulk autophagy degrades cargos non-selectively induced by glucose or nutrient deprivation; in selective autophagy or Cvt, cargos need to be specifically recognized, effectively tethered to, while non-cargo material has to be excluded from the nascent autophagosomes[131]. In my study, I focus on macroautophagy (referred to hereafter as "autophagy").

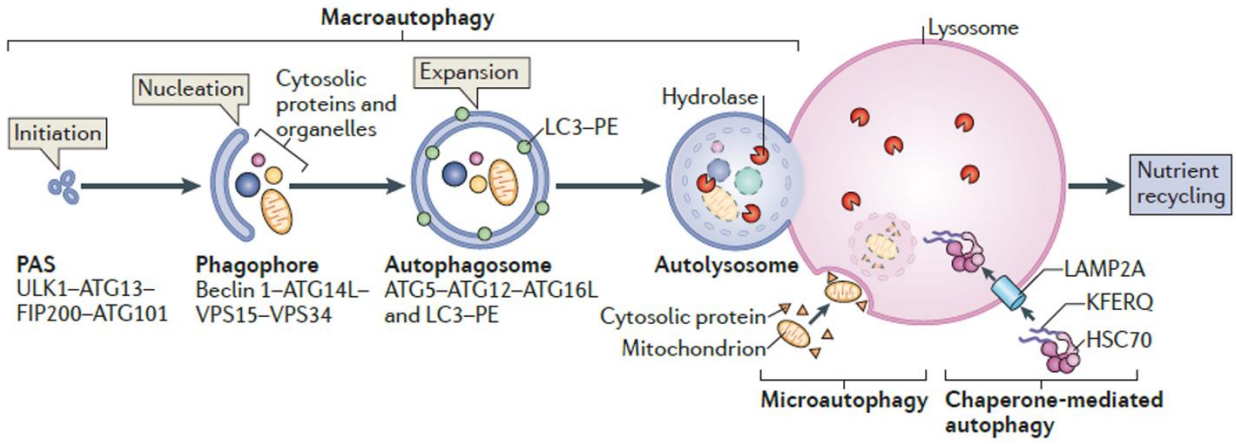

Figure 1.9 Overview of Autophagy[140]. During macroautophagy, upon autophagy induction, ULK1, Atg13, Atg101 and FIP200 (ULK1 complex) get activated and recruit PI3K complex I, which involves Vps34, Beclin 1, Atg14L, p150 and AMBRA1 for further nucleation of PAS. Then Phagophore elongates and forms autophagosome through Atg5-Atg12-Atg16L protein complex and LC3 to initiate two ubiquitin-like reactions. Upon fusion of the double membrane, fully formed autophagosomes fuse with lysosomes to generate autolysosomes for degradation of the sequestrated materials. While in microautophagy, substrates are directly engulfed into lysosome by invagination of lysosome membranes to form vesicles which subsequently bud into lysosome lumen; in CMA, cargos bearing KFERQ motif are recognized by the heat shock cognate 70 kDa protein (HSC70) and transported to lysosomes depends on LAMP2A. In all these three autophagy subtypes, cargos are degraded by lysosome hydrolases and the resulting sugars and amino acids are recycled. This figure is modified from[140].

Autophagy is induced by different signal pathways; amino acid depletion inactivates mammalian target of rapamycin (mTOR), whereas glucose depletion activates AMP kinase (AMPK)[123], both of which subsequently activate Unc-51 like autophagy activating kinase (ULK1/2), Atg13, Atg101 and focal adhesion kinase (FAK)-family interacting protein of 200 kDa (FIP200)[123]. These autophagy regulators activate class III phosphoinositide 3-kinase (PI3K) complex, which involves Vps34, Beclin 1, Atg14L, p150 and AMBRA1[123]. PI3P enriched pre-autophagosomal structure (PAS) then recruits the Atg5-Atg12-Atg16L protein complex and LC3 to initiate two ubiquitin-like reactions that help PAS to elongate and recruit membranes to form autophagosomes[132, 133]. Upon fusion of the double membrane, fully formed autophagosomes fuse with lysosomes to generate autolysosomes for degradation of the sequestrated materials[123]. Rab7 GTPase and its

effectors[134], including the SNARE complex consisting of Syntaxin 17, SNAP29, and VAMP7/8[135], Tectonin beta-propeller repeat-containing protein 1 (TECPR1)[136], the HOPS complex[137], and the PI3K complex formed by Beclin 1, Vps34, Vps15, UVRAG and Bif-1[138, 139], are involved in autophagosome-lysosome fusion.

Autophagy signal pathway in amino acid or glucose deprivation

Different signal pathway intercross in regulation of autophagy, while mTOR is the main regulator in amino acid depletion induced autophagy, AMPK plays essential roles in glucose starvation triggered autophagy.

As main regulator in amino acid depletion induced autophagy, mTOR is involved in two distinct protein complexes: mTOR complex 1 (mTORC1) and mTOR complex 2 (mTORC2). MTORC1 contains mTOR, Regulatory-associated protein of mTOR (Raptor), mammalian LST8/G-protein-β-subunit like protein (mLST8/GβL), and two inhibitory proteins: DEP domain containing-interacting protein (Deptor) and proline-rich Akt substrate of 40 kDa (PRAS40) whereas mTORC2 contains mTOR, rapamycin-insensitive companion of mTOR (Rictor), mLST8, mammalian stress-activated MAP kinase-interacting protein1 (mSin1), protein observed with rictor-1 (Protor-1) and Deptor. Only inhibition of mTORC1, but not mTORC2, is involved in autophagy induction and regulation of protein synthesis reduction; which could be achieved by mTORC1 specific inhibitor, rapamycin[141]. In normal growth condition, MTORC1 phosphorylates ULK1 and ATG13 to inhibit the ULK1 complex activity[142] and prevents translocation of Transcription Factor EB (TFEB) to the nucleus which inhibits the transcription and synthesis of ATG proteins and proteins involved

in the lysosome biogenesis[143]. MTORC1 could be activated by insulin/growth factors or by amino acids through the Rag GTPases. Amino acids in lysosome lumen changes v-ATPase conformation, which recruits Ragulator, GEF of RagA/B[144]; while cytosolic leucine binds to Leucyl-tRNA synthetase (LRS) to reveal its GAP activity toward RagC/D[145], the resulting dimer of $RagA/B^{GTP}$ and $RagC/D^{GDP}$ translocates mTORC1 to lysosome membrane[146] where Ras homologue enriched in brain (Rheb), coactivator of mTORC1, constitutively activates it[147]. Depletion of amino acids changes status of Rags, which releases mTORC1 from lysosomes and the inactivated mTORC1 leads to activation of ULK1 and translocation of TFEB into nucleus, thereby activates autophagy downstream pathways (Fig. 1.10)[148].

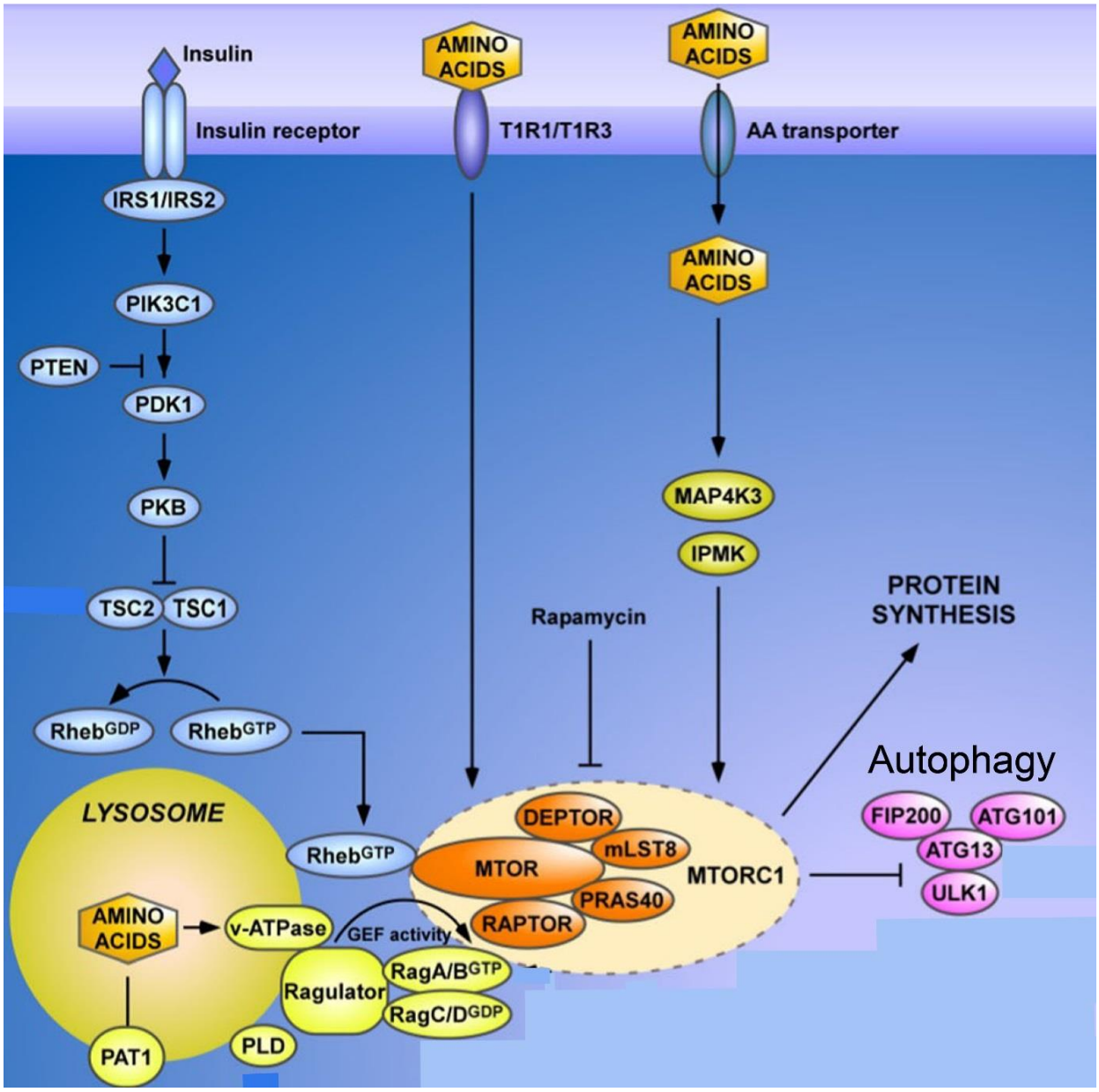

Figure 1.10 Amino acid starvation induced autophagy pathway[148]. In normal growth condition, mTORC1 which contains mTOR, Raptor, mLST8, Deptor and PRAS40, phosphorylates ULK1 and Atg13 to inhibit the ULK1 complex activity[142] and prevents translocation of TFEB to the nucleus[143]. MTORC1 could be activated by insulin/growth factors or by amino acids through the Rag GTPases. Amino acids in lysosome lumen changes v-ATPase conformation, which recruits Ragulator, GEF of RagA/B[144]; while cytosolic leucine binds to LRS to reveal its GAP activity toward RagC/D[145], the resulting dimer of $RagA/B^{GTP}$ and $RagC/D^{GDP}$ translocates mTORC1 to lysosome membrane[146] where Rheb, coactivator of mTORC1 constitutively activates it[147]. Depletion of amino acids changes status of Rags, which releases mTORC1 from lysosomes and the inactivated mTORC1 leads to activation of ULK1 and translocation of TFEB into nucleus, thereby activates autophagy downstream pathways. This model is modified from[148].

AMPK collaborates with mTORC1 in regulation of glucose deprivation induced autophagy. AMP/ATP ratio increase upon glucose starvation which activates AMPK[149]. Activated AMPK directly phosphorylates ULK1 and tuberous sclerosis complex 2 (TSC2). Phosphorylated TSC2 inhibits mTOR, which reduces its inhibitory phosphorylation on ULK1[150]. Removal of inhibitory phosphorylation and addition of accelerated phosphorylation together trigger ULK1 complex formation[149] and later on autophagy progress (Fig. 1.11).

In Chapter III, I found that, upon amino acid starvation, the Golgi undergoes partial fragmentation in the order from *trans* to *cis*, and the derived Golgi fragments colocalize with autophagosomes, consistent with the previous publications that Golgi plays a role in autophagosome formation[66, 67]. However, in a parallel study, we found that glucose starvation does not affect Golgi morphology as seen in amino acid starvation. These opposite effects on Golgi imply two hypotheses. First, the different signal pathways as discussed before might have different downstream effectors on Golgi which modulate it differently. Addition to that, amino acid starvation directs TFEB translocation to nucleus to initiate transcription of a large amount of autophagy and lysosome related proteins[151] and the increased protein synthesis might trigger increased Golgi transport to autophagosomes, which is comparably milder in glucose starvation.

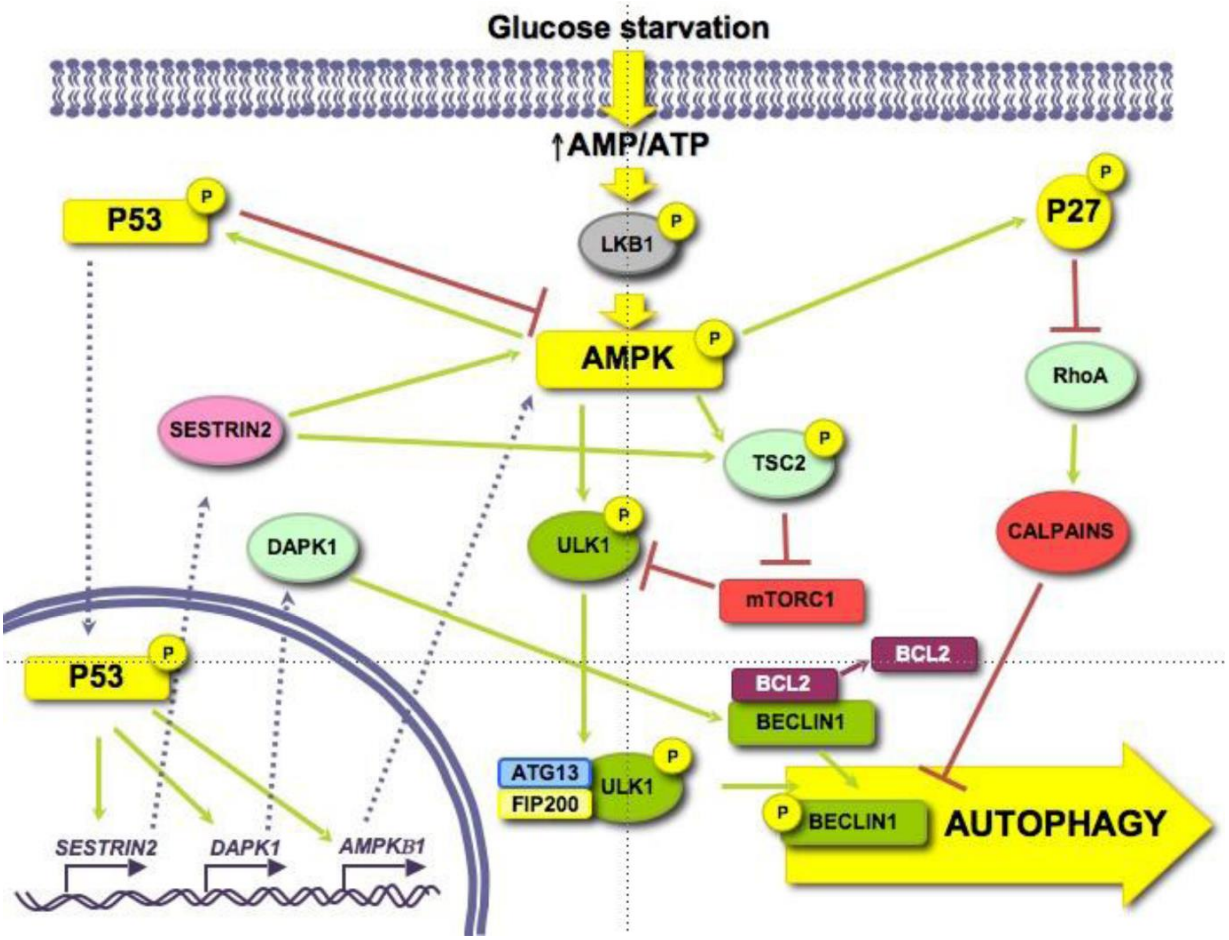

Figure 1.11 Glucose starvation induced autophagy pathway[152]. AMP/ATP ratio increase upon glucose starvation which activates AMPK[149]. Activated AMPK directly phosphorylate ULK1 and TSC2. Then TSC2 inhibits mTOR, which reduces its inhibitory phosphorylation on ULK1[150]. Removal of inhibitory phosphorylation and addition of accelerated phosphorylation together trigger ULK1 complex formation[149] and later on autophagy progress. This figure is modified from[152].

Autophagosome membrane source

Upon autophagy induction, activated ULK1 complex composed of ULK1, Atg13, Atg101 and FIP200[123], triggers PI3K Atg14L complex (Vps34, Beclin 1, Atg14L, p150 and AMBRA1), which enriches PI3P on PAS and then recruits the Atg5-Atg12-Atg16L protein complex and LC3 to initiate two ubiquitin-like reactions that help PAS to elongate and recruit membranes to form autophagosomes[132, 133]. Several membrane organelles have been indicated as the membrane source for autophagosomes. Among these, ER is the mostly well studied organelle. Upon autophagy induction, a main component of PI3K complex, Atg14L localizes at ER and enrich PI3P at specific subdomain of ER, omegasome, a cup/Ω like structure, which is known as the platform for autophagosome formation[153]. Then zinc finger FYVE-type containing 1/double FYVE-containing protein 1 (ZFYVE1/DFCP1), markers of omegasome, translocate to Mitochondria-associated ER membrane (MAM) and recruit Atg5, the ubiquitin-like conjugating system to promote autophagosome formation[154]. Meanwhile, phosphatidylserine (PS) from ER is synthesized into phosphatidylethanolamine (PE), an essential lipid in autophagy, in mitochondria[155]. Other than ER and mitochondria, clathrin heavy chain interacts with Atg16L1, component of Atg5 conjugation system; and clathrin mediated endocytoses promotes autophagosome formation; this finding indicates plasma membrane provides membrane to autophagosomes[156]. Recent studies indicate that Golgi apparatus may also serve as a membrane source in autophagosome formation. In mammalian cells, Atg9, a transmembrane protein cycles between the TGN and endosomes in fed condition, relocates to autophagosomes upon amino acid starvation or rapamycin treatment, which implicates that Golgi may deliver membranes to autophagosomes[66]. Furthermore, increased secretion of constitutive cargo from TGN to plasma membranes recruits LC3 to specific domain of TGN and promotes autophagosome formation which requires AP1-mediated clathrin vesicles

delivery of membranes from the TGN to autophagosomes[67]. In Chapter III, I also find that, upon amino acid starvation, the Golgi undergoes partial fragmentation, and the derived Golgi fragments colocalize with autophagosomes shown by immunofluorescence and EM which supports Golgi's role in serving membranes for autophagosome formation (Fig. 1.12).

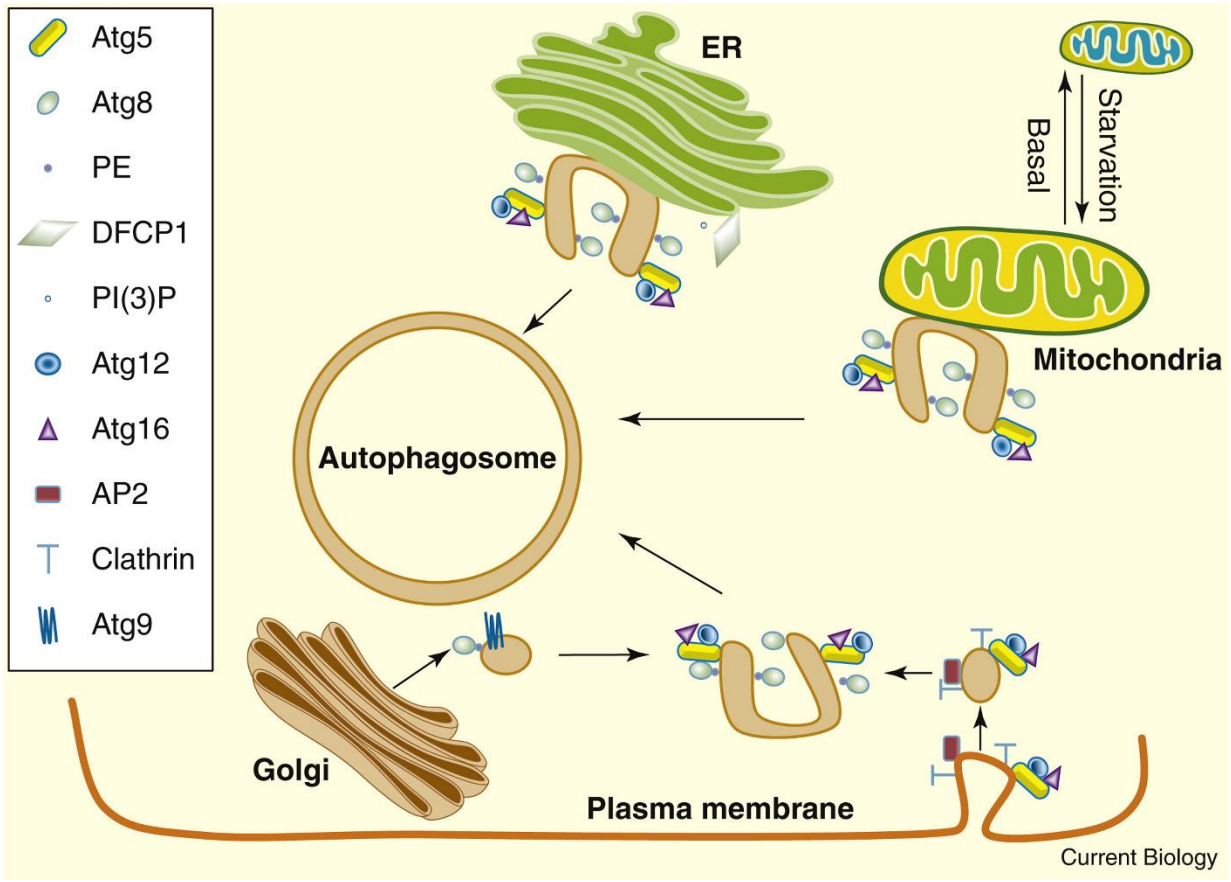

Figure 1.12 Autophagosome membrane sources[157]. Phagophore elongation and autophagosome formation require lipids and proteins from multiple membrane source. Omegasome forms at ER as platform for autophagosome formation, mitochondria supplies lipid to the phagophore. Atg9-containing vesicles delivered from Golgi to the phagophore and endocytosis from plasma membrane also contribute membranes to autophagosomes. This figure is modified from[157].

Autophagosome fusion with lysosomes

Upon fusion of the double membrane, fully formed autophagosomes maturate by removal of PI3P and LC3, which destabilize other autophagy related proteins for recycling[158]. Then these maturated autophagosomes fuse with endosomes and lysosomes to generate amphisomes and autolysosomes for degradation of the sequestrated materials[123].

In both yeast and mammalian cells, Rab7 GTPase is the main player in autophagosome-lysosome fusion[134]. In mammalian cells, Rab7 and its GEF Monensin sensitivity 1/Caffeine, calcium, zinc sensitivity 1 (Mon1/Ccz1) are localized on autophagosomes which is dependent on PI3P[159-161]. Then homotypic vacuole fusion and protein sorting (HOPS) tethering complex interacts indirectly with Rab7 through small GTPase, Arf like GTPase 8 (Arl8) and Rab2[162-165]. Moreover, Pleckstrin homology domain-containing family M member 1 (PLEKHM1) interacts with HOPS[166, 167]; ectopic P-granules autophagy protein 5 (EPG5) interacts with Rab7[168]; TFCPR1, RUN and FYVE domain containing 4 (RUFY4) interact with PI3P[169, 170]; all these proteins are also working as Rab7 effector in mediating autophagosome-lysosome fusion process. Meanwhile, PI3K UVRAG complex formed by Beclin 1, Vps34, Vps15, UVRAG and Bif-1[138, 139] is responsible in generation of PI3P and recruit Rab7 to autophagosome-lysosome interface. After Rab7 and its effector proteins tether autophagosome and lysosome in close proximity, Syntaxin17, recruited by HOPS, together with SNAP29 and VAMP7/8, form SNARE complex to help finish the last fusion step (Fig. 1.13)[171-173].

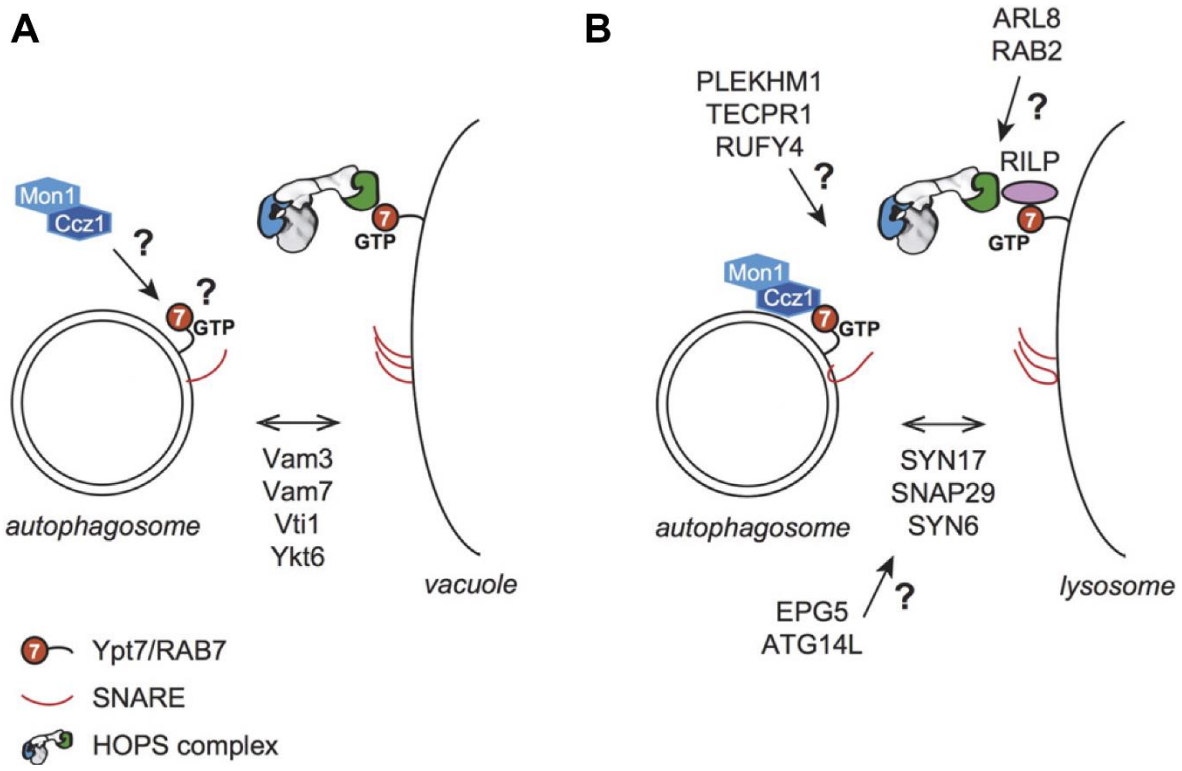

Figure 1.13 Autophagosome-lysosome fusion machinery[158]. (A) Autophagosome-lysosome fusion in yeast. Rab7 and its GEF, Mon1/Ccz1 are localized on autophagosomes, where HOPS interacts with Rab7 to tether autophagosome-lysosome in close proximity. Then SNARE complex composed of Vam3, Vam7, Vti1 and Ykt6 mediates the fusion step. **(B)** Autophagosome-lysosome fusion in mammalian cells. Similar to yeast, Rab7 and its GEF, Mon1/Ccz1 are localized on autophagosomes, where HOPS interacts indirectly with Rab7 through Arl8 and Rab2. PLEKHM1, EPG5, TFCPR1, RUFY4 also work as Rab7 effector in mediating autophagosome-lysosome fusion process. Meanwhile, PI3K complex II formed by Beclin 1, Vps34, Vps15, UVRAG and Bif-1 is responsible in generation of PI3P and recruit Rab7 to autophagosome-lysosome interface (model shown in next figure). After Rab7 and its effector proteins tether autophagosome and lysosome in close proximity, Syn17, SNAP29 and VAMP7/8 form SNARE complex to finish the last fusion step. This figure is modified from[158].

In Chapter III, we have made an unexpected finding that GRASP55 contributes to autophagosome-lysosome fusion upon amino acid starvation by physically tethering autophagosomes and lysosomes by interaction with LC3 and LAMP2; moreover, GRASP55 facilitates the assembly of the class III PI3K complex by interaction with Beclin 1, Vps34, Bif-1 and UVRAG. In my lab colleague's work, the interaction between GRASP55 and Rab7 is also confirmed (unpublished

work), which taken together, establish GRASP55 as an important regulator in autophagosome-lysosome fusion.

PI3K complex in autophagy

Vps34, a class III PI3P kinase, is the core protein in PI3K complex, it interacts with serine/threonine kinase, Vps15 and Atg6 in yeast, or Beclin 1 in mammalian cells[174]. In yeast, there are two distinct complexes, complex I which contains Atg14, localizes to vacuolar membranes and PAS to promote autophagy[175, 176]; while complex II which contains Vps38, localize to vacuolar membranes and endosomes, is involved in vacuolar protein sorting pathway for hydrolase sorting from TGN to vacuole[177].

As the two PI3K complexes are well documented in yeast, the mammalian PI3K complexes are more complicated and still mostly elusive (Fig. 1.14). Atg14L, mammalian homolog of yeast Atg14, forms complex with Beclin 1-Vps34-Vps15 core (thereafter named PI3K Atg14L complex) and localizes to ER, or more specifically to ER-mitochondria contact sites to generate PI3P for autophagosome formation at PAS[154, 178, 179]. Ambra1 is another component of PI3K Atg14L complex, which binds Beclin 1 and associates with ULK1 and the E3 ligase, TNF receptor associated factor 6 (TRAF6), which helps localize the PI3K Atg14L complex to omegasomes[180, 181]. On the other hand, UVRAG, which shares 32% similarity to Vps38, has mutually exclusive binding to the core complex, compared to Atg14L(thereafter named PI3K UVRAG complex)[182]. Bif-1 is another component of PI3K UVRAG complex, which indirectly interact with Beclin 1 through UVRAG[181, 183]. PI3K UVRAG complex stimulates Rab7 GTPase activity thereby

autophagosome-lysosome fusion[184]. Moreover, Rubicon, binds to UVRAG, when UVRAG is phosphorylated by mTORC1, to form PI3K Rubicon complex which inhibits autophagosome-lysosome fusion[185-187]. Other than these main players in PI3K complexes, GAPR1, a Golgi lipid raft associated protein, is shown to tether Beclin 1 on Golgi which inhibits autophagosome formation. Moreover, it is still under debate if PI3K UVRAG complex also works in autophagosome formation[182, 188], if UVRAG/Rubicon complex regulate autophagosome-lysosome fusion independent of Beclin 1[189], and how the balance between these complexes are achieved.

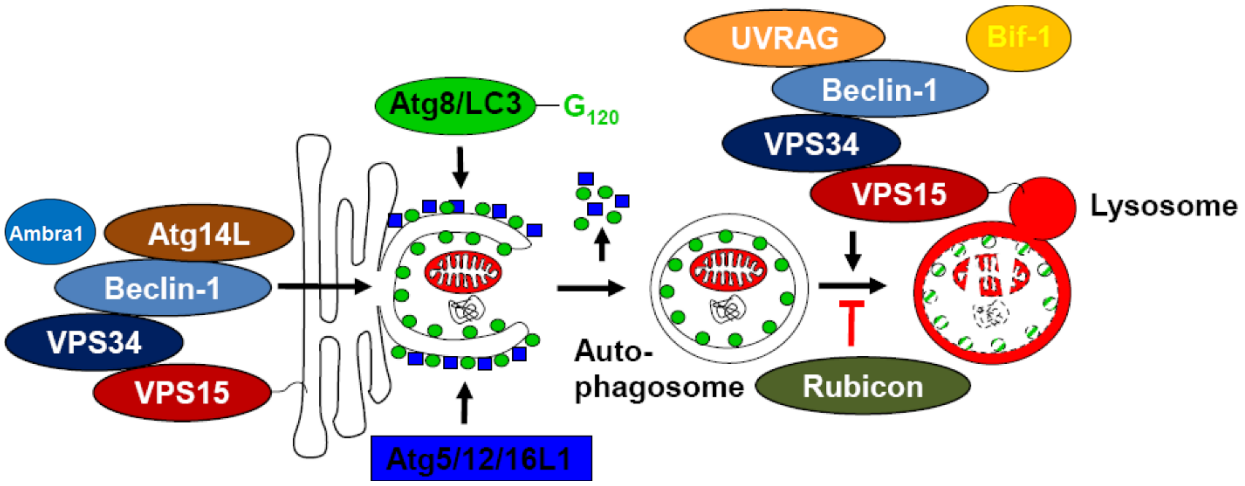

Figure 1.14 PI3K complexes in autophagy[190]. PI3K Atg14L complex which involves Atg14L, Beclin 1, Vps34, Vps15 and Ambra1 localizes to ER, or more specifically to ER-mitochondria contact sites to generate PI3P for autophagosome formation at PAS. PI3K UVRAG complex which involves UVRAG, Beclin 1, Vps34, Vps15 and Bif1 localizes to autophagosome-lysosome interface and mediate autophagosome-lysosome fusion which could be inhibited by Rubicon (PI3K Rubicon complex). This model is modified from[190].

In Chapter III, we identify GRASP55 as a novel regulator of PI3K UVRAG complex which facilitates its assembly by interaction with Beclin 1, Vps34, Bif-1 and UVRAG. GRASP55 depletion results in a reduced level of UVRAG and Bif-1, indicating that GRASP55 may stabilize UVRAG and Bif-1, although the mechanism is unknown so far. Meanwhile, GRASP55 facilitates

Beclin 1's membrane association. Depletion of GRASP55 significantly reduced Beclin 1 membrane association under both control and amino acid starvation conditions, which was rescued by exogenously expressed GRASP55. In addition, the alternative interaction of Beclin 1 with GAPR-1 and GRASP55 is striking, as Beclin 1 almost conclusively interacts with GAPR-1 under growth condition but with GRASP55 upon amino acid starvation, indicating that GRASP55 functions as a positive regulator for Beclin 1 autophagosome localization and plays a necessary role in autophagosome-lysosome fusion.

Chapter II. Knockout of the Golgi stacking proteins GRASP55 and GRASP65 impairs Golgi structure and function

Abstract

Golgi reassembly stacking protein of 65 kDa (GRASP65) and Golgi reassembly stacking protein of 55 kDa (GRASP55) were originally identified as Golgi stacking proteins; however, subsequent GRASP knockdown experiments yielded inconsistent results with respect to the Golgi structure, indicating a limitation of RNAi-based depletion. In this study, we have applied the recently developed clustered regularly interspaced short palindromic repeats (CRISPR)/Cas9 technology to knock out GRASP55 and GRASP65, individually or in combination, in HeLa and HEK293 cells. We show that double knockout of GRASP proteins disperses the Golgi stack into single cisternae and tubulovesicular structures, accelerates protein trafficking, and impairs accurate glycosylation of proteins and lipids. These results demonstrate a critical role for GRASPs in maintaining the stacked structure of the Golgi, which is required for accurate posttranslational modifications in the Golgi. Additionally, the GRASP knockout cell lines developed in this study will be useful tools for studying the role of GRASP proteins in other important cellular processes.

Introduction

The Golgi apparatus is an essential organelle composed of stacks of tightly aligned flattened cisternal membranes, which are often laterally linked into a ribbon-like structure located in the perinuclear region of mammalian cells [8]. The Golgi resides at the center of the secretory pathway, receiving almost the entire output of the endoplasmic reticulum (ER), including proteins and lipids that are modified and processed in the Golgi in a variety of ways, such as N- or O-linked glycosylation[2, 3], phosphorylation[4, 191], lipidation[192], and proteolytic cleavage[5, 191]. Cargo molecules maturing through the Golgi membranes are inevitably sorted and transported to their final destinations, such as the plasma membrane, endosomes, lysosomes, or secretory granules, in a precise manner in order for cells to maintain homeostasis[6, 7].

Formation of the unique, stacked morphology of the Golgi is controlled in part by two homologous peripheral membrane proteins, GRASP65 (Golgi Reassembly Stacking Protein of 65 kDa) and GRASP55 (55 kDa), which are localized to the *cis*- and *medial*-/*trans*- cisternae, respectively. In interphase cells, GRASP proteins form homo-dimers and trans-oligomers from adjacent cisternae to hold Golgi cisternae together to form a stack[12, 13]. GRASP proteins are also implicated in Golgi ribbon formation by linking individual Golgi stacks, likely through bridging proteins[14, 15]. Interestingly, the Golgi apparatus undergoes a unique disassembly and reassembly process during the cell cycle, which is regulated by phosphorylation of the GRASP proteins. Upon mitotic entry, CDK1 and several other kinases are activated and phosphorylate GRASP proteins, which impair GRASP oligomerization, resulting in Golgi cisternal unstacking. As cells exit mitosis, GRASP proteins are dephosphorylated after CDK1 inactivation, enabling GRASPs to oligomerize and

Golgi stacks to reform. GRASP proteins also interact with other Golgi structural proteins to regulate the morphology of the Golgi. For instance, GRASP65 interacts with GM130, while GRASP55 forms a complex with Golgin-45. Both GM130 and Golgin-45 are coiled-coil golgins involved in membrane tethering and Golgi structure formation[102, 193]. Thus, GRASPs and their interacting proteins are essential for Golgi structure formation [194-196].

Further studies in cells using RNA interference (RNAi)-mediated depletion confirmed that knockdown of a single GRASP protein reduced the number of cisternae per stack[13, 16]. This effect was rescued by the expression of exogenous GRASP proteins[107]; while simultaneous depletion of both GRASPs resulted in disorganization of the entire stack[13]. However, GRASP depletion also caused additional effects, and thus GRASPs have been implicated in other cellular processes, including enzyme distribution[90], cargo transport[91], unconventional secretion[18, 92], cell cycle progression[16], apoptosis[17], and cell migration[93]. Thus far, it is not clear whether GRASPs possess all of these functions, or if some of the effects are caused by the disruption of the Golgi stacks when GRASPs are depleted. The exact role for GRASP55 and GRASP65, therefore, remains elusive. In this study, we have used the CRISPR (Clustered Regularly Interspaced Short Palindromic Repeats)/Cas9 genome editing technique[110, 111] to knock out GRASP55 and GRASP65, single or in combination, to investigate their roles in Golgi structure formation and function.

Results

Generation of GRASP55/65 knockout HeLa and HEK293 cells

To establish GRASP55 and GRASP65 single-knockout cell lines, we designed multiple single-guide RNAs (sgRNAs) targeting exon 1 of GRASP55 (55T1, 55T2, 55T3) and exon 2 of GRASP65 (65T1, 65T2) using the target design software developed by Feng Zhang's lab at the Massachusetts Institute of Technology (http://crispr.mit.edu/) (Figure 2.1A). These sgRNAs all target to the coding sequences of the gene immediately downstream of the translation initiation site, and therefore no truncated proteins should be made in the cell. These sgRNAs were cloned into pSpCas9(BB)-2A-GFP(PX458) and pSpCas9(BB)-2A-Puro(PX459) vectors so positive cells could be selected by fluorescence-activated cell sorting (FACS) or by puromycin resistance. This generated a heterogeneous population of cells where ~50% of cells had no detectable levels of the target protein as determined by immunofluorescence microscopy. We then examined the morphology of the Golgi in the mixed populations of cells by immunofluorescence microscopy using GM130 as a Golgi marker. In both HeLa and HEK293 cells, GRASP65- negative cells displayed no significant changes in Golgi morphology compared with cells that expressed GRASP65 (Figure 2.1B and Supplemental Figure 2.S2A). However, GRASP55-negative cells exhibited an increased frequency of mild Golgi fragmentation compared with GRASP55-positive cells (Figure 2.1, B and C, and Supplemental Figures 2.S1 and 2.S2).

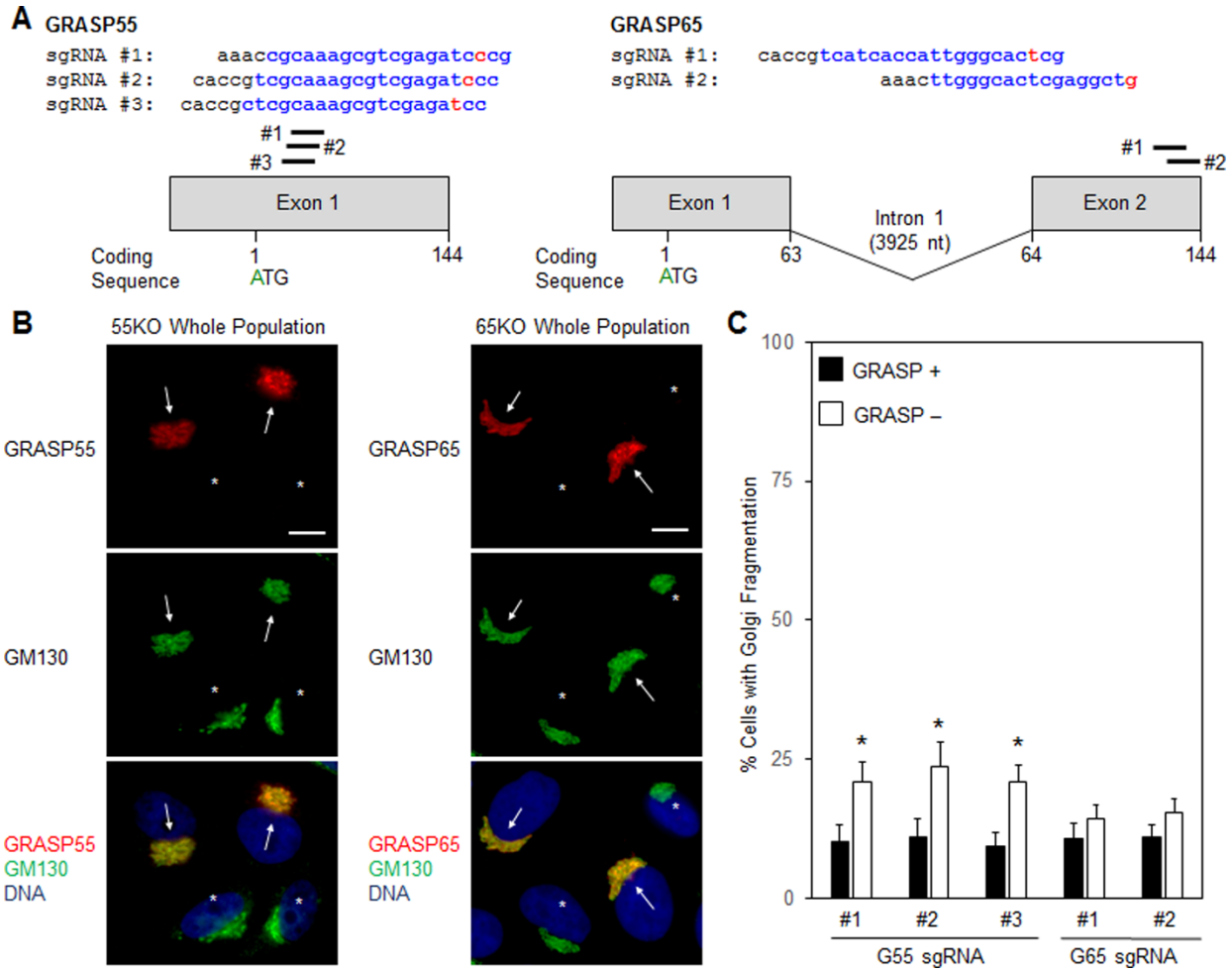

Figure 2.1. Construction of GRASP55 and GRASP65 single knockout cells. (A) sgRNAs designed to target GRASP55 and GRASP65 using CRISPR/Cas9-mediated gene deletion. The translation initiation ATG codon is indicated and referred to as coding sequence 1 (for A); exons are indicated as boxes and introns indicated by a line, with the number of nucleotide at the splicing borders indicated. sgRNAs sequences and relative locations are indicated as lines above the exons of the gene. **(B)** Immunofluorescence images of cell populations transfected with sgRNAs to GRASP55 (left panels) or GRASP65 (right panels). HeLa cells were transfected with GFP-Cas9 plasmids containing sgRNAs against either GRASP55 or GRASP65 and selected for GFP expression by flow cytometry. The Golgi morphology of GRASP knockout cells was assessed by immunofluorescence microscopy for either GRASP55 or GRASP65 co-stained with GM130. **(C)** Quantification of Golgi morphology in GRASP-positive (arrows) and GRASP-negative (asterisks) cells in B. *, $p < 0.05$.

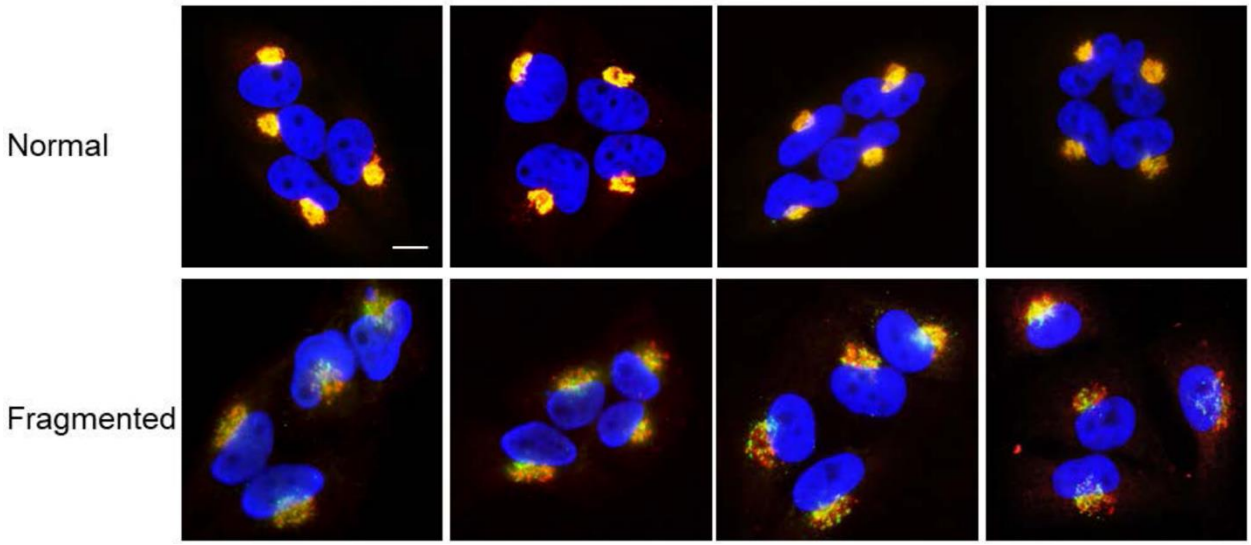

Figure 2.S1. Gallery of cells with normal and fragmented Golgi. HeLa WT (Normal) and DKO (Fragmented) cells were fixed and immunofluorescence was performed using antibodies for TGN46 (red) and GM130 (green). DNA (blue) was stained with Hoechst. Note that a normal Golgi is a compact, single Golgi mass while a fragmented Golgi displays an increase in the number of smaller, dispersed Golgi elements and separation of TGN46 and GM130. Scale bar is 10 μm.

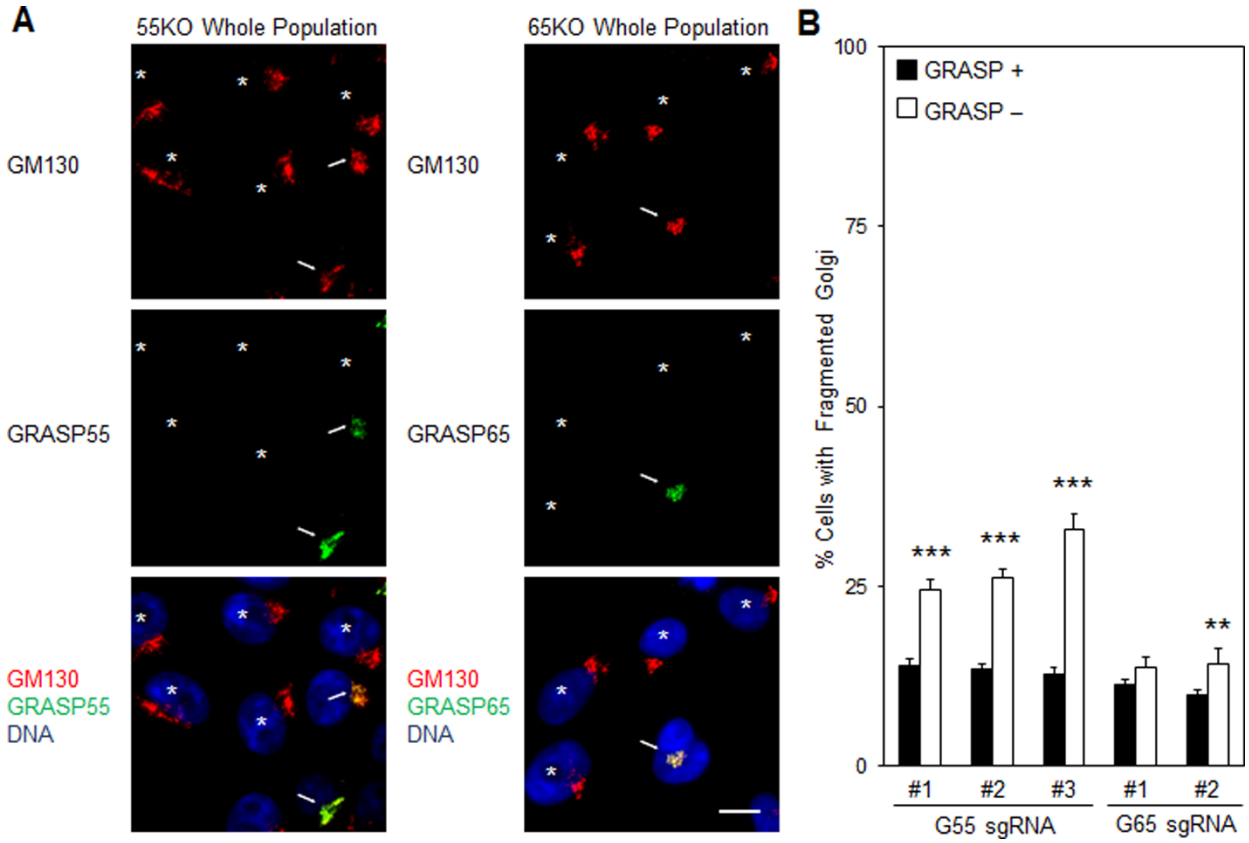

Figure 2.S2. Construction of GRASP55 and GRASP65 knockout HEK293 cells. (A) Immunofluorescence images of cell populations transfected with sgRNAs to GRASP55 (left panels) or GRASP65 (right panels). HEK293 cells were transfected with Puro-Cas9 plasmids containing sgRNAs against either GRASP55 or GRASP65 and selected for puromycin resistance. The Golgi morphology of GRASP knockout cells was assessed by immunofluorescence microscopy for either GRASP55 or GRASP65 co-stained with GM130. **(B)** Quantification of Golgi morphology in GRASP-positive (arrows) and GRASP-negative (asterisks) cells in A. **, $p < 0.01$, ***, $p < 0.001$.

Knockout of a single GRASP protein has minor effects on the Golgi morphology

We then generated stable clones of GRASP single-knockout cells using three targets of GRASP55 (55T1, 55T2, 55T3) and two targets of GRASP65 (65T1, 65T2) in HeLa and HEK293 cells by plating selected whole populations at low density followed by clonal expansion. Multiple clones for each target were generated; consistent results were obtained in different clones generated by different sgRNAs targeting to the same gene (Table 2.1). Genetic deletion of GRASP55 and GRASP65 was confirmed by genomic sequencing (Table 2.2). Representative clones for each targeting sgRNA were further characterized.

Western blot analysis of GRASP55 knockout clones demonstrated that GRASP55 depletion was effective; as no GRASP55 signal was detected (Figure 2.2A and Supplemental Figure 2.S3A). Knockout of GRASP55 significantly increased the level of GRASP65 in HEK293 cells (Supplemental Figure 2.S3, A and B), although this effect was not as obvious in HeLa cells (Figure 2.2, A and B). GRASP55 deletion also resulted in a significant reduction of Golgin-45 in HeLa cells, while GM130 protein levels remained unchanged in both cell lines (Figure 2.2, A and B, and Supplemental Figure 2.S3, A and B). Deletion of GRASP55 resulted in a minor, but significant, increase in the level of Golgi fragmentation in both HeLa and HEK293 cells, as assessed by immunofluorescence microscopy for GM130 and TGN46 (Figure 2.2, C–E, and Supplemental Figure 2.S3, C–E). However, colocalization of GM130 and TGN46, as measured by Pearson's correlation coefficient, remained unchanged in HeLa cells.

Table 2.1. Multiple GRASP knockout clones were generated in this study.

Cell Line	Gene Target	sgRNA	Number of Clones	Golgi Morphology
HeLa	GRASP55	55T1	4	Mild increase in fragmentation
HeLa	GRASP55	55T2	4	Mild increase in fragmentation
HeLa	GRASP55	55T3	4	Mild increase in fragmentation
HeLa	GRASP65	65T1	6	Normal
HeLa	GRASP65	65T2	6	Normal
HeLa	GRASP55 + GRASP65	55T1 & 65T1	9	Abnormal, dispersed Golgi
HEK	GRASP55	55T1	5	Mild increase in fragmentation
HEK	GRASP55	55T2	5	Mild increase in fragmentation
HEK	GRASP55	55T3	2	Mild increase in fragmentation
HEK	GRASP65	65T1	10	Normal
HEK	GRASP65	65T2	5	Normal
HEK	GRASP55 + GRASP65	55T2 & 65T1	20	Abnormal, dispersed Golgi

Multiple GRASP single-knockout clones for each target sgRNA and multiple double-knockout clones from 55T2 and 65T1 were isolated and characterized for use in this study. Note that the morphology of the Golgi, as assessed by immunofluorescence, was similar in individual clones across target sgRNAs for single knockout clones and the abnormal, fragmented morphology of the Golgi was consistent between double-knockout clones.

Table 2.2A. Genomic sequence analysis of HeLa GRASP knockout clones.

Cell Line	Clone	Gene Sequence	In/del	Frequency	Predicted Protein Sequence
HeLa	WT	GRASP55	N/A	2/2	M G S S Q S V E I P G G G T E G Y H V L R V V Q E N S P G H R A G L E P F F D F I V S I N G S R L
HeLa	WT	GRASP65	N/A	2/2	V Q E N S P A Q Q A G L E P Y F D F I I T I G H S R L
HeLa	55T1	GRASP55	1 nt insertion	12/12	M G S S Q K R R D P G R G H R G L P R S A G S T R K F P R T Q S W F G A F L*
HeLa	65T1	GRASP65	1 nt deletion	4/9	V Q E N S P A Q Q A G L E P Y F D F I I T I G H F E A E Q G E *
		GRASP65	2 nt deletion	3/9	V Q E N S P A Q Q A G L E P Y F D F I I T I G H E A E Q G E *
		GRASP65	13 nt deletion	2/9	V Q E N S P A Q Q A G L E P Y F D F I I T I G H F P N L P L L C L L M C V C V S S S V P Q G A P V Y P S L P F F L K G V P A L S P L L P G L Y S E P D W G P A Q C S A S E L C G V D R G H M A S W R W Q Q G P R G L P P G A *
HeLa	DKOC1	GRASP55	166 nt deletion	13/18	M V Q D *
		GRASP55	25 nt deletion	5/18	M G S S H R G L P R S A G S T R K F P R T Q S W F G A F L *
		GRASP65	1 nt insertion	10/13	V Q E N S P A Q Q A G L E P Y F D F I I T I G H F E A E Q G E *
		GRASP65	16 nt insertion	3/13	V Q E N S P A Q Q A G L E P Y F D F I E A E Q G E *

The genetic loci corresponding to GRASP55 or GRASP65 was amplified by PCR from genomic DNA preparations in HeLa GRASP single- and double-knockout clones. The majority of GRASP knockout clones exhibited multiple mutated alleles. The predicted protein sequence from the mutated loci indicates that indels generated by CRISPR/Cas-9 lead to a frameshift that results in the production of a short, non-GRASP protein with an early stop codon. Novel protein sequences and stop codons (asterisks) that are generated by indels are in red text.

Table 2.2B. Genomic sequence analysis of HEK293 GRASP knockout clones.

Cell Line	Clone	Sequence Target	In/del	Frequency	Predicted Protein Sequence
HEK	WT	GRASP55	N/A	2/2	M G S S Q S V E I P G G G T E G Y H V L R V V Q E N S P G H R A G L E P F F D F I V S I N G S R L
HEK	WT	GRASP65	N/A	2/2	V Q E N S P A Q Q A G L E P Y F D F I I T I G H S R L
HEK	55T2	GRASP55	28 nt deletion	6/14	M G S S Q G L P R S A G S T R K F P R T Q S W F G A F L *
		GRASP55	1 nt insertion	4/14	M G S S Q S V E I P G R G H R G L P R S A G S T R K F P R T Q S W F G A F L *
		GRASP55	7 nt deletion	3/14	M G S S Q S V G R G H R G L P R S A G S T R K F P R T Q S W F G A F L *
		GRASP55	22 nt deletion	1/14	M G W A P R A T T F C G *
HEK	65T1	GRASP65	20 nt deletion	16/24	V Q E N S P A Q Q A G L E P Y F D F I I T I G P T C L C F A C L C V F V C L H L S H R G P Q S T L P S L F F *
		GRASP65	***	8/24	V Q E N S P A Q Q A G L E P Y F D F I I T I G P M V G T R R M T P *
HEK	DKOC1	GRASP55	1 nt insertion	6/10	M G S S Q S V E I P G R G H R G L P R S A G S T R K F P R T Q S W F G A F L *
		GRASP55	7 nt deletion	2/10	M G S S Q S V G R G H R G L P R S A G S T R K F P R T Q S W F G A F L *
		GRASP55	28 nt deletion	1/10	M G S S Q G L P R S A G S T R K F P R T Q S W F G A F L *
		GRASP55	22 nt deletion	1/10	M G W A P R A T T F C G *
		GRASP65	20 nt deletion	9/16	V Q E N S P A Q Q A G L E P Y F D F I I T I G P T C L C F A C L C V F V C L H L S H R G P Q S T L P S L F F *
		GRASP65	***	7/16	V Q E N S P A Q Q A G L E P Y F D F I I T I G P M V G *

The genetic loci corresponding to GRASP55 or GRASP65 was amplified by PCR from genomic DNA preparations in HEK293 GRASP single- and double-knockout clones. The majority of GRASP knockout clones exhibited multiple mutated alleles. The predicted protein sequence from the mutated loci indicates that indels generated by CRISPR/Cas-9 lead to a frameshift that results in the production of a short, non-GRASP protein with an early stop codon. Novel protein sequences and stop codons (asterisks) that are generated by indels are in red text. (***, 1 + 2 nt insertion, denotes a triple insertion that includes a single insertion upstream of a double insertion that still results in a frameshift and early stop codon)

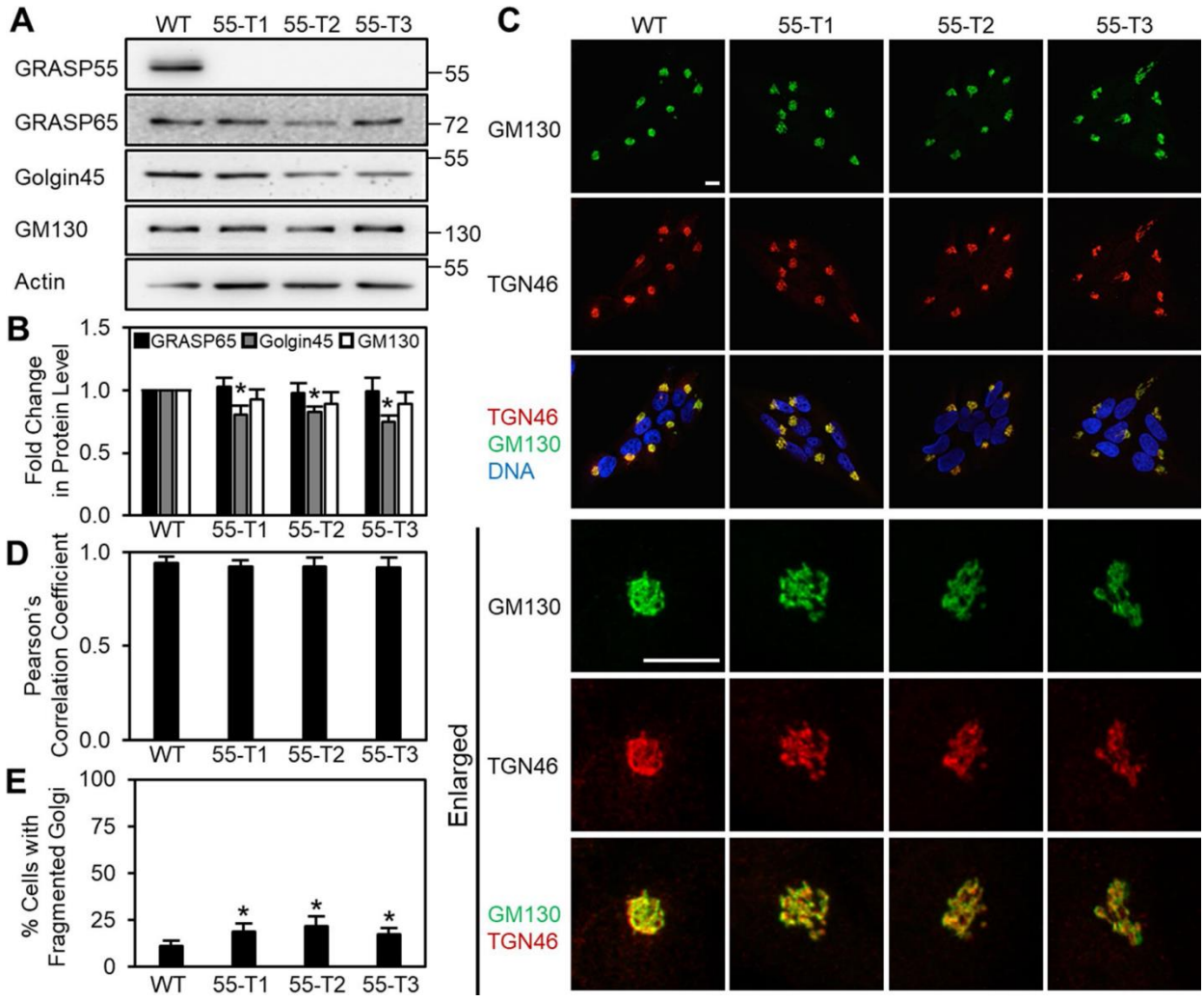

Figure 2.2. GRASP55 deletion has minor effects on the Golgi structure. (A) Western blots of Golgi proteins in GRASP55 knockout HeLa cells. Wild-type and representative GRASP55 knockout clones from 3 separate sgRNAs (T1, T2, and T3) were lysed and blotted for GRASP55/65, Golgin-45 and GM130. **(B)** Quantification of A for the relative levels of GRASP65, Golgin-45, and GM130 in GRASP55 knockout cells. **(C)** Immunofluorescence of GRASP55 knockout clones stained for GM130 and TGN46. The lower three rows are increased magnifications of the Golgi in a single cell. **(D)** Co-localization of GM130 and TGN46 quantified by the Pearson's Correlation Coefficient in GRASP55 knockout clones from C. **(E)** Quantification of Golgi fragmentation in GRASP55 knockout clones in C. *, $p < 0.05$.

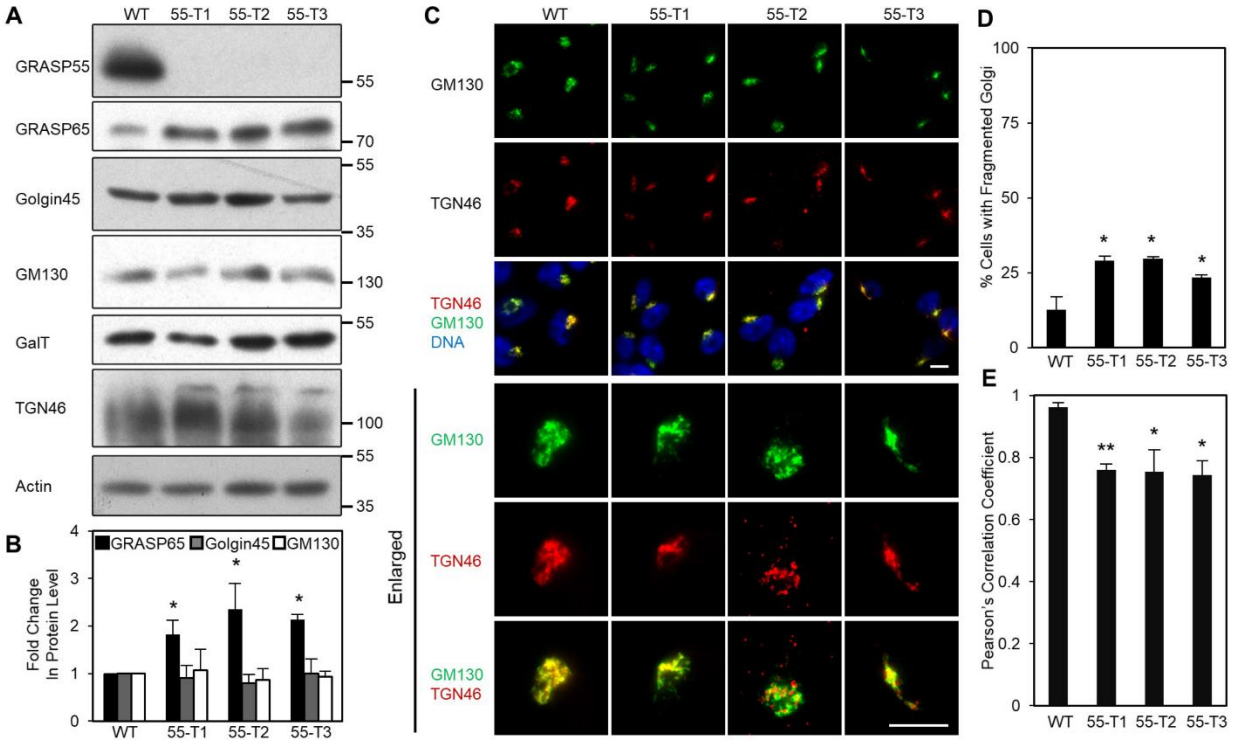

Figure 2.S3. The effect of GRASP55 knockout on Golgi morphology and Golgi protein abundance in HEK293 cells. (A) Western blots of Golgi proteins in GRASP55 knockout HEK293 cells. Wild-type and representative GRASP55 knockout clones from 3 separate sgRNAs (T1, T2, and T3) were lysed and blotted for GRASP55/65, Golgin-45 and GM130. (B) Quantification of A for the relative levels of GRASP65, Golgin-45, and GM130 in GRASP55 knockout cells. Scale bars are 10 μm. (C) Immunofluorescence of GRASP55 knockout clones stained for GM130 and TGN46. The lower three rows are increased magnifications of the Golgi in a single cell. (D) Quantification of Golgi fragmentation in GRASP55 knockout clones in C. (E) Co-localization of GM130 and TGN46 quantified by the Pearson's Correlation Coefficient from z-stacks in GRASP55 knockout clones from C. Blinded determination of the Golgi morphology of 300 cells from each sample was quantified across three biological replicates. Error bars represent SEM. A Student's t-test was performed to determine statistical significance. *, $p < 0.05$, **, $p < 0.01$.

Knockout of GRASP65 was also confirmed by Western blotting (Figure 2.3A, 2.S4A). Interestingly, GRASP65 deletion significantly increased the protein level of GRASP55 in both HeLa and HEK293 cells (Figure 2.3A, 2.S4A), indicating that a mechanism of compensation might exist between GRASP proteins. GRASP65 deletion also reduced the level of GM130, in particular in HEK293 cells (Figure 2.3A-B and 2.S4A-B), consistent with previous reports [13]. GRASP65 knockout had no significant effects on Golgi morphology when assessed by immunofluorescence microscopy (Figure 2.3C-E and 2.S4C-E).

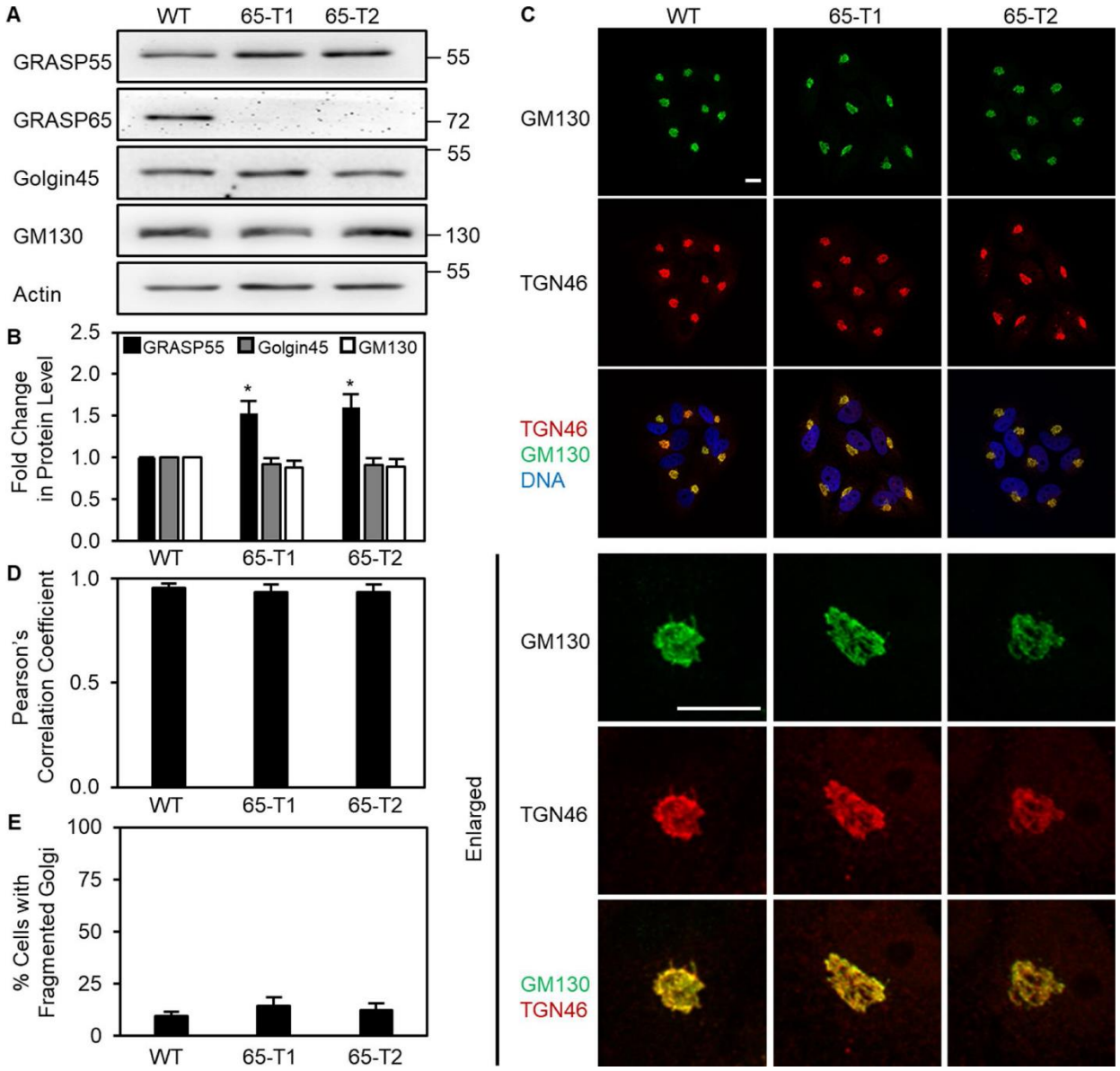

Figure 2.3. GRASP65 deletion does not cause Golgi ribbon unlinking. (A) Western blots of Golgi proteins in GRASP65 knockout HeLa cells. Wild-type and representative GRASP65 knockout clones from two separate sgRNAs (T1 and T2) were analyzed by Western blot for GRASP55/65, Golgin-45, and GM130. **(B)** Quantification of A for the relative levels of GRASP55, Golgin-45, and GM130 in GRASP65 knockout cells. Error bars represent SEM. **(C)** Immunofluorescence microscopy of GRASP65 knockout clones stained for GM130 and TGN46. The lower three rows are increased magnifications of a single cell's Golgi. Scale bars are 10 μm. **(D)** Colocalization of GM130 and TGN46 quantified by the Pearson's correlation coefficient of z-stacks from GRASP65 knockout clones from C. Error bars represent SEM. **(E)** Quantification of Golgi fragmentation in GRASP65 knockout clones in C. Blinded determination of the Golgi morphology of 300 cells from each sample were quantified across three biological replicates. Error bars represent SEM. A Student's *t* test was performed to determine statistical significance. $*p < 0.05$.

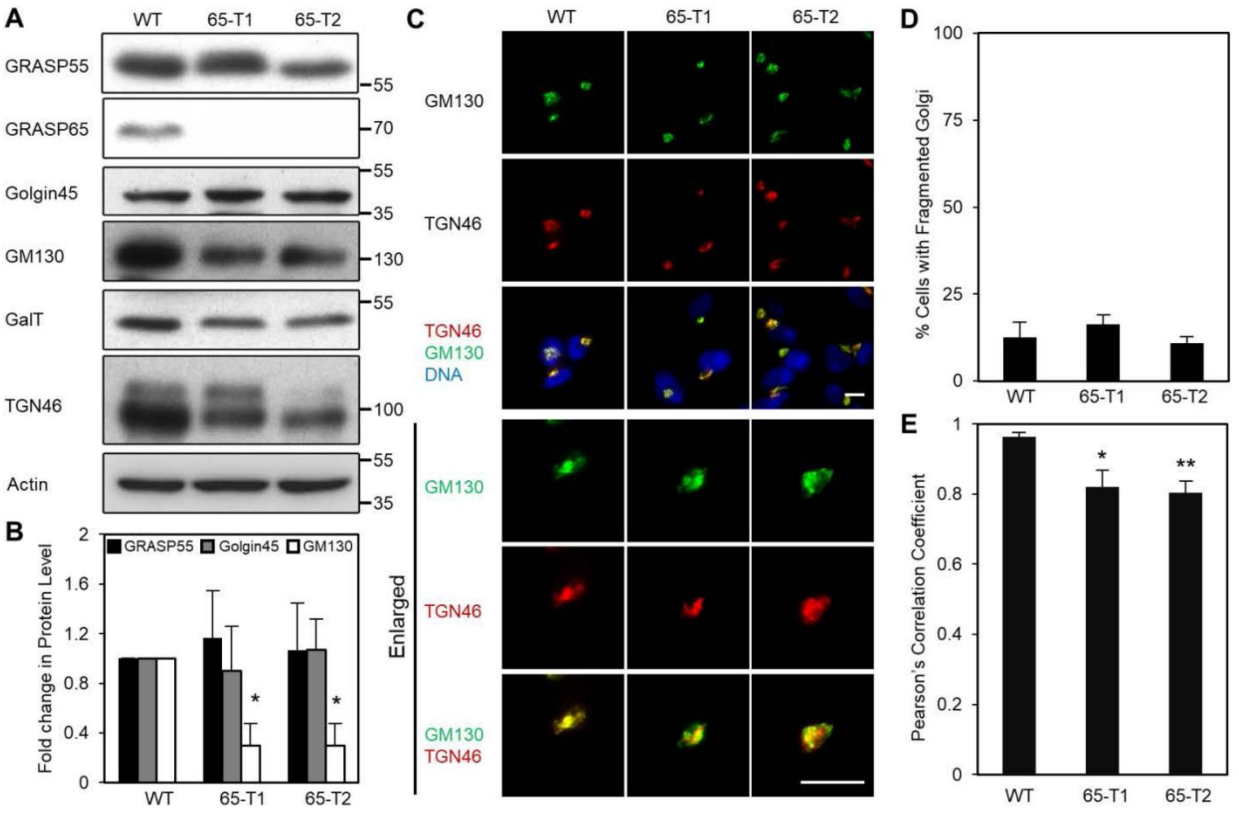

Figure 2.S4. The effect of GRASP65 knockout on Golgi morphology and Golgi protein abundance in HEK293 cells. (A) Western blots of Golgi proteins in GRASP65 knockout HEK293 cells. Wild-type and representative GRASP65 knockout clones from two separate sgRNAs (T1 & T2) were analyzed by Western blot for GRASP55/65, Golgin-45 and GM130. **(B)** Quantification of A for the relative levels of GRASP55, Golgin-45, and GM130 in GRASP65 knockout cells. Error bars represent SEM. **(C)** Immunofluorescence microscopy of GRASP65 knockout clones stained for GM130 and TGN46. The lower three rows are increased magnifications of a single cell's Golgi. Scale bars are 10 μm. **(D)** Colocalization of GM130 and TGN46 quantified by the Pearson's Correlation Coefficient from z-stacks in GRASP65 knockout clones from C. Error bars represent SEM. **(E)** Quantification of Golgi fragmentation in GRASP65 knockout clones in C. Blinded determination of the Golgi morphology of 300 cells from each sample was quantified across three biological replicates. Error bars represent SEM. A Student's t-test was performed to determine statistical significance. *, $p < 0.05$, **, $p < 0.01$.

Double deletion of both GRASP55 and GRASP65 results in severe Golgi fragmentation

Deletion of GRASP55 or GRASP65 individually had only a mild impact, if at all, on the Golgi morphology when assessed by immunofluorescence microscopy. This can be explained by three reasons: 1) GRASP55 and GRASP65 play complementary roles in Golgi structure formation; the second GRASP protein can largely maintain the Golgi structure intact when the first one is deleted[13]; 2) the increased level of the other GRASP protein when its homolog is deleted may provide compensatory effect on Golgi structure formation; and 3) light microscopy does not reach the appropriate resolution to assess Golgi stack formation, therefore the effect must be assessed by electron microscopy (EM). To address the first two possibilities, we simultaneously deleted both GRASP proteins in HeLa and HEK293 cells. Similar to the generation of GRASP55/65 single knockout cells, 65T1 HeLa and HEK293 cells, instead of wild type cells, were transfected with GRASP55 sgRNA target #2 to generate a double-knockout population and multiple, individual clones were selected (Table 2.1). Deletion of both GRASP55 and GRASP65 was confirmed by Western blotting and DNA sequencing of the genomic DNA (Figure 2.4A and Table 2.2). Further characterization of two representative clones demonstrated that GRASP double-knockout resulted in a significant reduction in the protein levels of both GM130 and Golgin-45 in both HeLa (Figure 2.4A-B) and HEK293 cells (Figure 2.S5A-B). We then assessed the Golgi morphology by immunofluorescence for GM130 and TGN46. Double knockout of GRASP proteins resulted in a dramatic dispersal of the Golgi in 95.3% of the HeLa cells (~65% in HEK293 cells) and significant decrease in the co-localization between GM130 and TGN46, indicating a disruption of Golgi stack formation (Figure 2.4C-E and 2.S5C-E). Furthermore, adding back of a single GRASP protein in GRASP double-knockout cells was sufficient to rescue the Golgi ribbon-linking defect observed

by microscopy (Supplemental Figure 2.S6). Overall this indicates that GRASP proteins play complementary roles in Golgi ribbon linking.

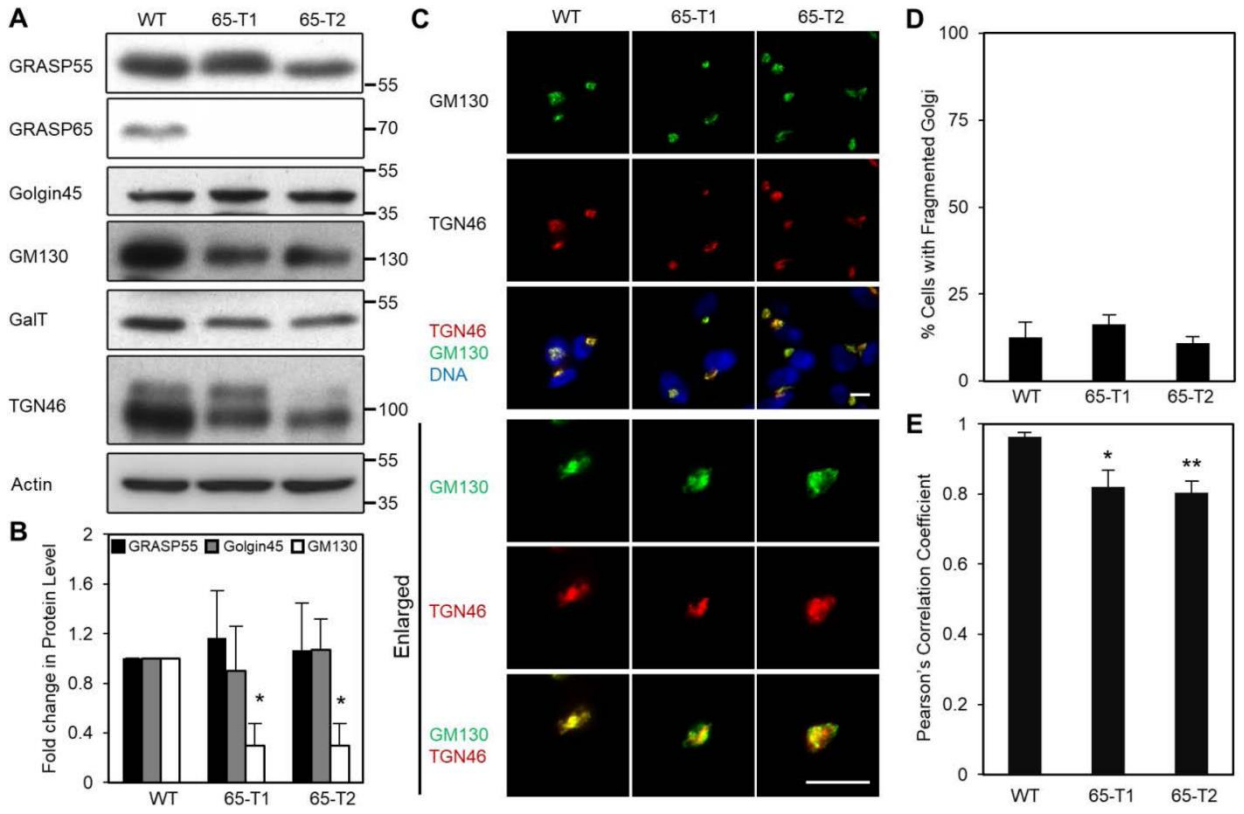

Figure 2.4. Double deletion of GRASP55 and GRASP65 results in Golgi fragmentation. (A) Western blots of Golgi proteins in GRASP55 and GRASP65 double-knockout cells. Wild-type and two representative GRASP55 and GRASP65 double-knockout clones (DKO-C1 and DKO-C2) were analyzed by Western blot for GRASP55/65, Golgin-45, and GM130. **(B)** Quantification of the relative levels of Golgin-45, and GM130 in GRASP double-knockout cells in A. Error bars represent SEM. **(C)** Immunofluorescence microscopy of GRASP55/65 double-knockout cells stained for GM130 and TGN46. The lower three rows are increased magnifications of a single cell's Golgi. Scale bars are 10 μm. **(D)** Colocalization of GM130 and TGN46 quantified by the Pearson's correlation coefficient of z-stacks from GRASP double-knockout clones from C. Error bars represent SEM. **(E)** Quantification of cells with fragmented Golgi from GRASP double-knockout clones in C. Blinded determination of the Golgi morphology of 300 cells from each sample were quantified across three biological replicates. Error bars represent SEM. A Student's *t* test was performed to determine statistical significance. *$p < 0.05$; **$p < 0.01$; ***$p < 0.001$.

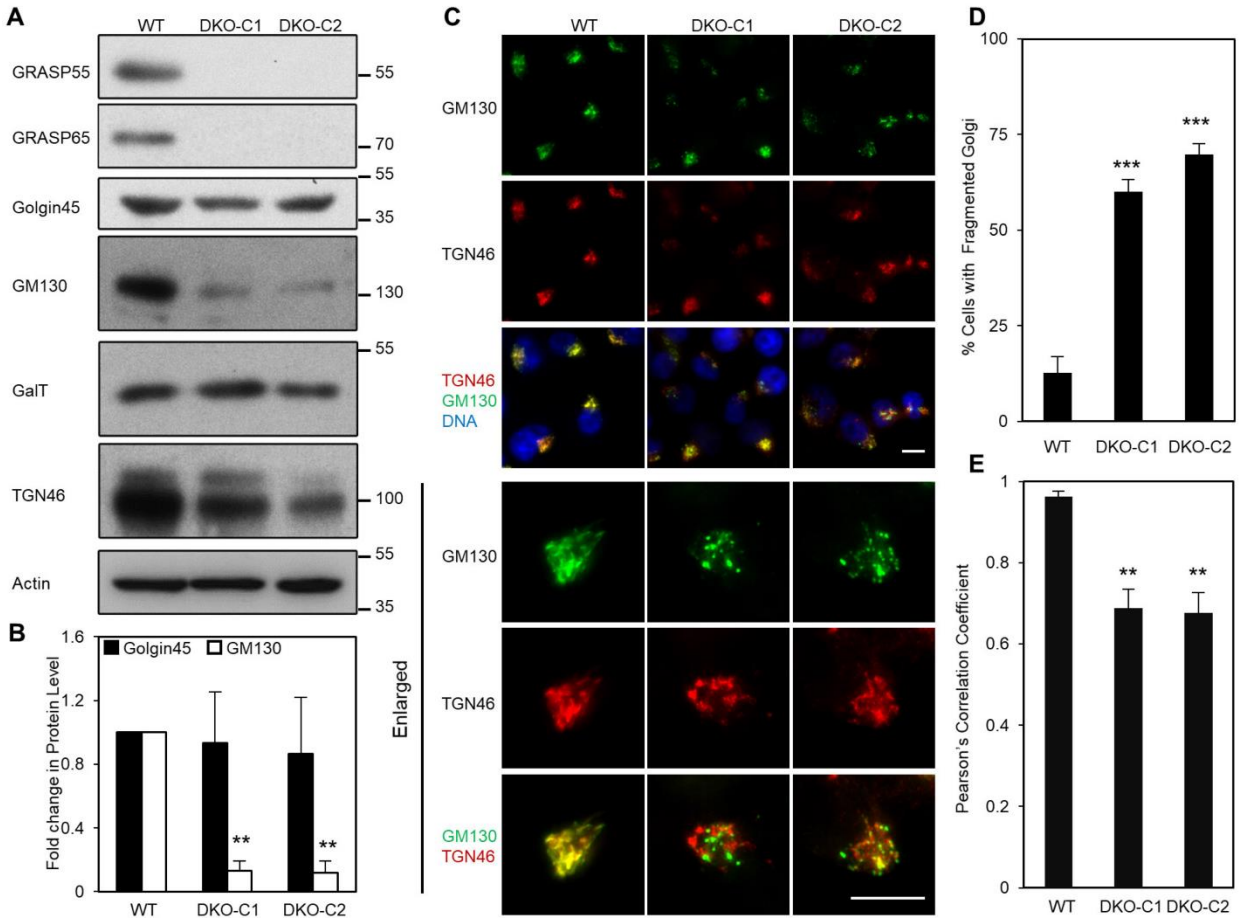

Figure 2.S5. The effect of GRASP55 and GRASP65 double knockout on Golgi morphology and Golgi protein abundance in HEK293 cells. (A) Western blots of Golgi proteins in GRASP55 and GRASP65 double knockout cells. Wild-type and two representative GRASP55 and GRASP65 double-knockout clones (DKO-C1 and DKO-C2) were analyzed by Western blot for GRASP55/65, Golgin-45 and GM130. **(B)** Quantification of the relative levels of Golgin-45, and GM130 in GRASP knockout cells in A. Error bars represent SEM. **(C)** Immunofluorescence microscopy of GRASP55/65 double knockout cells stained for GM130 and TGN46. The lower three rows are increased magnifications of a single cell's Golgi. Scale bars are 10 µm. **(D)** Co-localization of GM130 and TGN46 quantified by the Pearson's Correlation Coefficient from z-stacks in GRASP double knockout clones from C. Error bars represent SEM. **(E)** Quantification of cells with fragmented Golgi from GRASP65 knockout clones in C. Blinded determination of the Golgi morphology of 300 cells from each sample was quantified across three biological replicates. Error bars represent SEM. A Student's t-test was performed to determine statistical significance. **, $p < 0.01$, ***, $p < 0.001$.

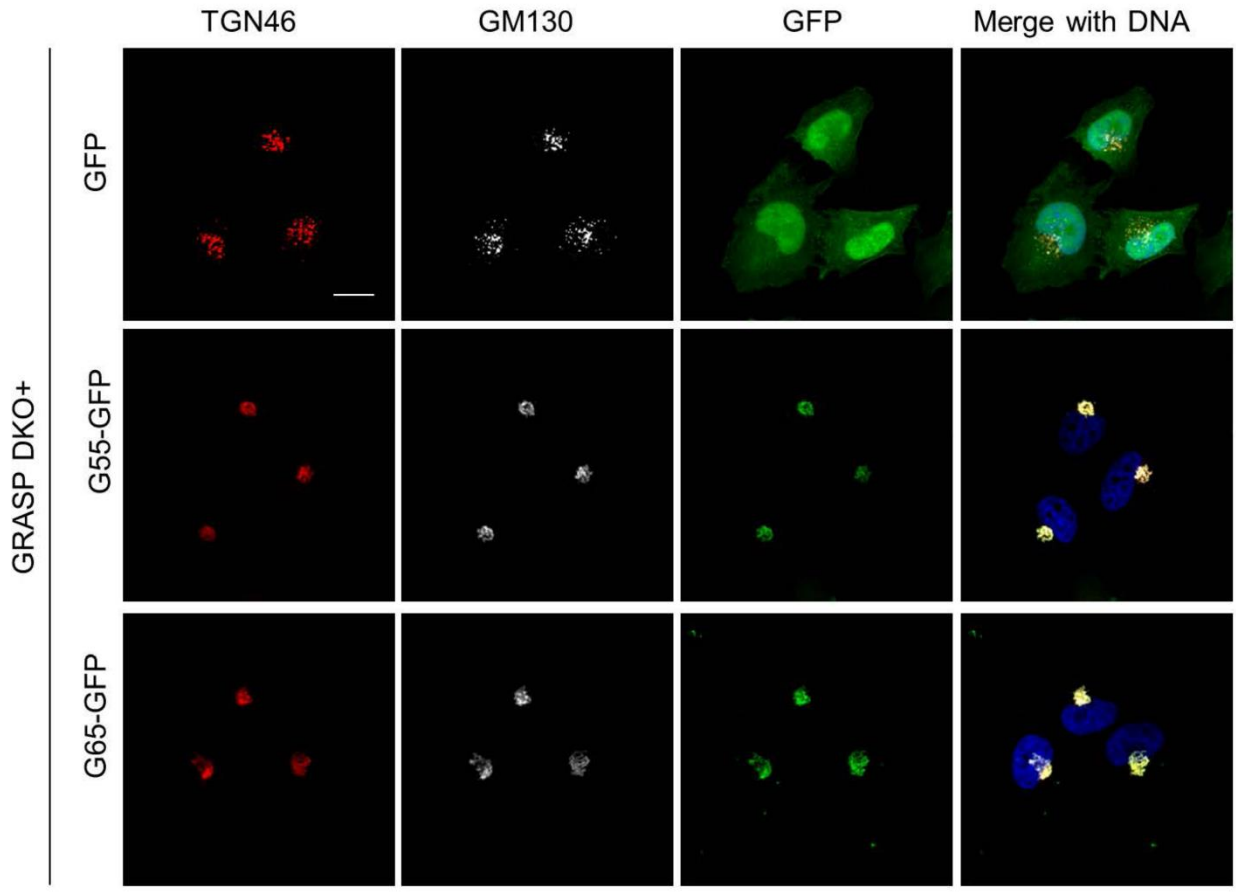

Figure 2.S6. Adding back a single GRASP protein rescues the Golgi ribbon in GRASP double knockout cells. GRASP double knockout cells were transfected with plasmids encoding GFP, GRASP55-GFP, or GRASP65-GFP. Transfected cells were fixed and immunofluorescence was performed using antibodies against GM130 and TGN46 to assess the morphology of the Golgi. Note that addback of a single GRASP protein is sufficient to rescue the ribbon-linking defect in double knockout cells. Scale bar is 10 μm.

GRASP deletion impairs Golgi stacking

To more closely examine the morphology of the Golgi in GRASP single- and double-knockout cells, we performed AiryScan confocal microscopy, which significantly improves resolution compared to standard confocal microscopy[197]. Similar to conventional confocal microscopy, the morphology of the Golgi in GRASP55 and GRASP65 single-knockout clones exhibited a compact Golgi ribbon and significant colocalization between GM130 and TGN46, similar to the morphological characteristics of the Golgi in parental cells. However, the Golgi in GRASP double-

knockout cells was extremely fragmented and disorganized, with a significant decrease in co-localization between GM130 and TGN46 (Figure 2.5A). To specify the effects of GRASP deletion on Golgi stacking, we treated WT and GRASP knockout cells with nocodazole, which is known to disassociate the Golgi ribbon into distinct Golgi stacks, but does not significantly disrupt Golgi stack formation in interphase cells. Upon nocodazole treatment, GM130 and TGN46 colocalized in wild-type control cells, as assessed by AiryScan confocal microscopy. Deletion of a single GRASP did not significantly affect colocalization between GM130 and TGN46; however, double deletion of both GRASPs resulted in severe separation between GM130 and TGN46 (Figure 2.5B-C), indicating that GRASP double knockout impairs stack formation.

To determine the ultrastructural details of the Golgi in GRASP knockout cells, we performed electron microscopy. As shown in Figure 2.5D-E (galleries of images are shown in Figure 2.S7A-D), depletion of a single or both GRASP proteins resulted in a higher frequency of disorganized membranes, such as short and unaligned cisternae, reduced number of cisternae in the stack, and vesicle accumulation; the effects were more dramatic in GRASP double knockout cells. Quantitation of the EM images showed that the ratio of disorganized membrane clusters versus distinguishable Golgi stacks in the perinuclear region of the cell was significantly increased in GRASP knockout cells compared to wild type HeLa cells (3.5 ± 2.7% in wild type, 43.0 ± 4.4% and 27.0 ± 2.8% in GRASP55 or GRASP65 knockout cells, respectively, and 73.2 ± 10.0% in double knockout cells) (Figure 2.5D-E). Moreover, even the distinguishable Golgi stacks in both single- and double-knockout cells did not seem to be normal, as they often contained swollen and shorter Golgi cisternae that were not properly aligned, and reduced number of cisternae per stack (Figure 2.5G-H). If only well-organized Golgi stacks in the cells were quantified, the number of

organized Golgi stacks per cell was significantly reduced in GRASP55 and GRASP65 single knockout cells (0.41 ± 0.06 and 0.55 ± 0.02, respectively) compared to control cells (2.06 ± 0.11); while almost no well-organized Golgi stacks were visible in GRASP double knockout cells (Figure 2.5F). These results provide strong evidence that GRASP55/65 are required for Golgi stack formation.

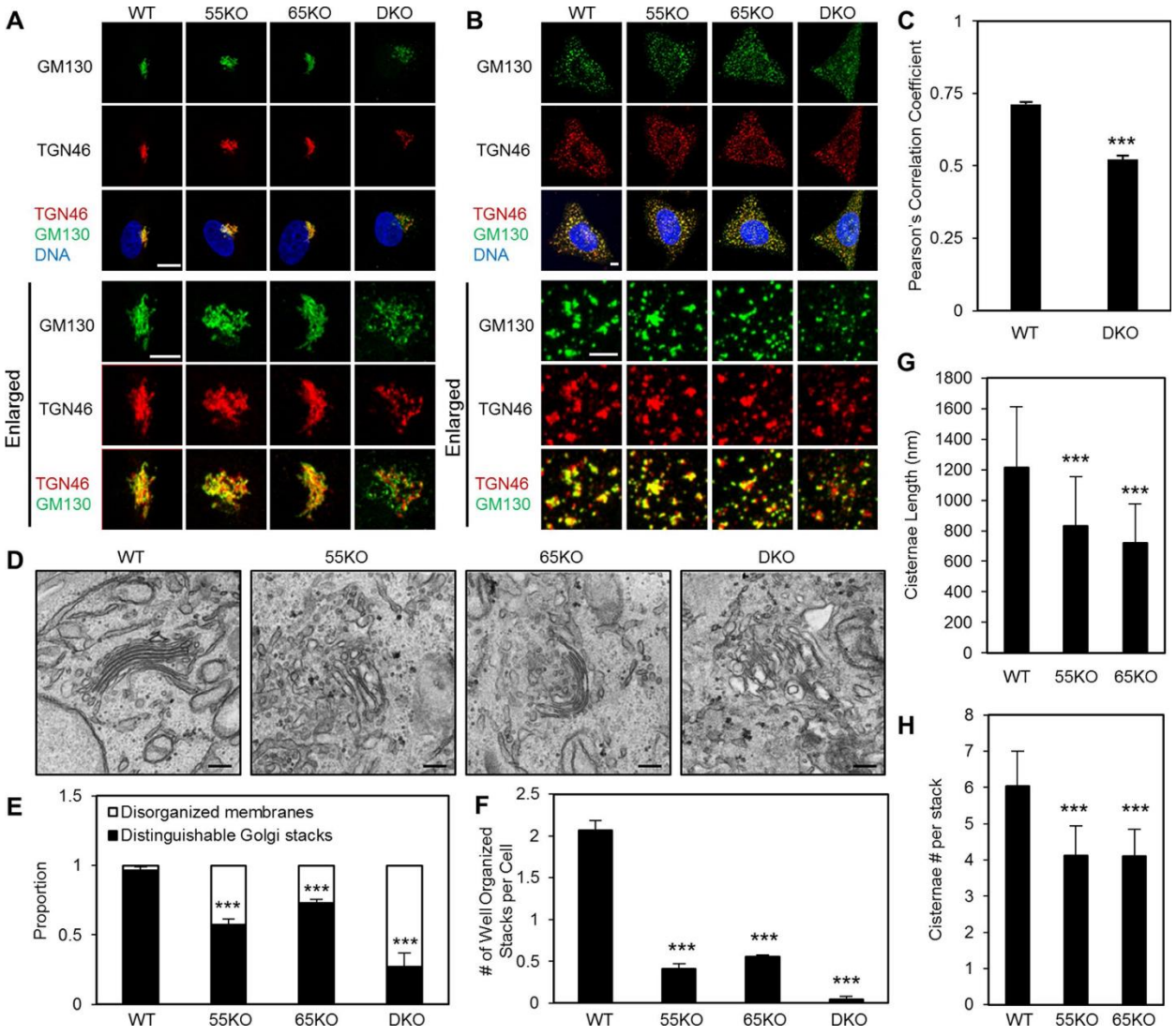

Figure 2.5. Double deletion of GRASP55 and GRASP65 proteins impairs Golgi stack formation. (A) High-resolution AiryScan confocal immunofluorescence images of GM130 and TGN46 in HeLa wild-type

and GRASP single- and double-knockout clones. The lower three rows are increased magnifications of a single cell's Golgi. Scale bar is 10 μm. **(B)** High-resolution AiryScan confocal immunofluorescence images for GM130 and TGN46 in HeLa wild-type and GRASP single- and double-knockout clones after 4 h treatment with 100 ng/ml nocodazole. The lower three rows are increased magnifications of a single cell's Golgi. Scale bar is 5 μm. **(C)** Quantification of GM130 and TGN46 colocalization in B. Pearson's correlation coefficient in wild-type and GRASP55 and GRASP65 double-knockout cells from 20 cells across three biological replicates and quantified using the ImageJ2 coloc2 plug-in with z-stacks. Error bars represent SEM. A Student's *t* test was performed to determine statistical significance. **(D)** Electron micrographs from wild-type and GRASP single- and double-knockout HeLa clones. Note the reduced number of cisternae in GRASP single-knockout cells and the disorganized Golgi membranes in double-knockout cells. Scale bar is 200 nm. **(E)** Quantification of the proportion of cells exhibiting distinguishable Golgi stacks vs. disorganized membranes in D. **(F)** Quantification of well-organized Golgi stacks per cell in wild-type and GRASP single- and double-knockout clones from D. **(G)** Quantification of the length of well-organized Golgi stacks in wild-type and GRASP single-knockout clones from D. Double-knockout cells were not quantified due to the lack of well-organized stacks. **(H)** Quantification of the number of cisternae per stack in wild-type and GRASP single-knockout clones from D. Double-knockout cells were not quantified due to the lack of well-organized stacks. In all EM pictures, E–H, at least 20 cells across three biological replicates were quantified. Error bars represent SEM. A Student's *t* test was performed to determine statistical significance. ***$p < 0.001$.

Figure 2.S7A. HeLa WT

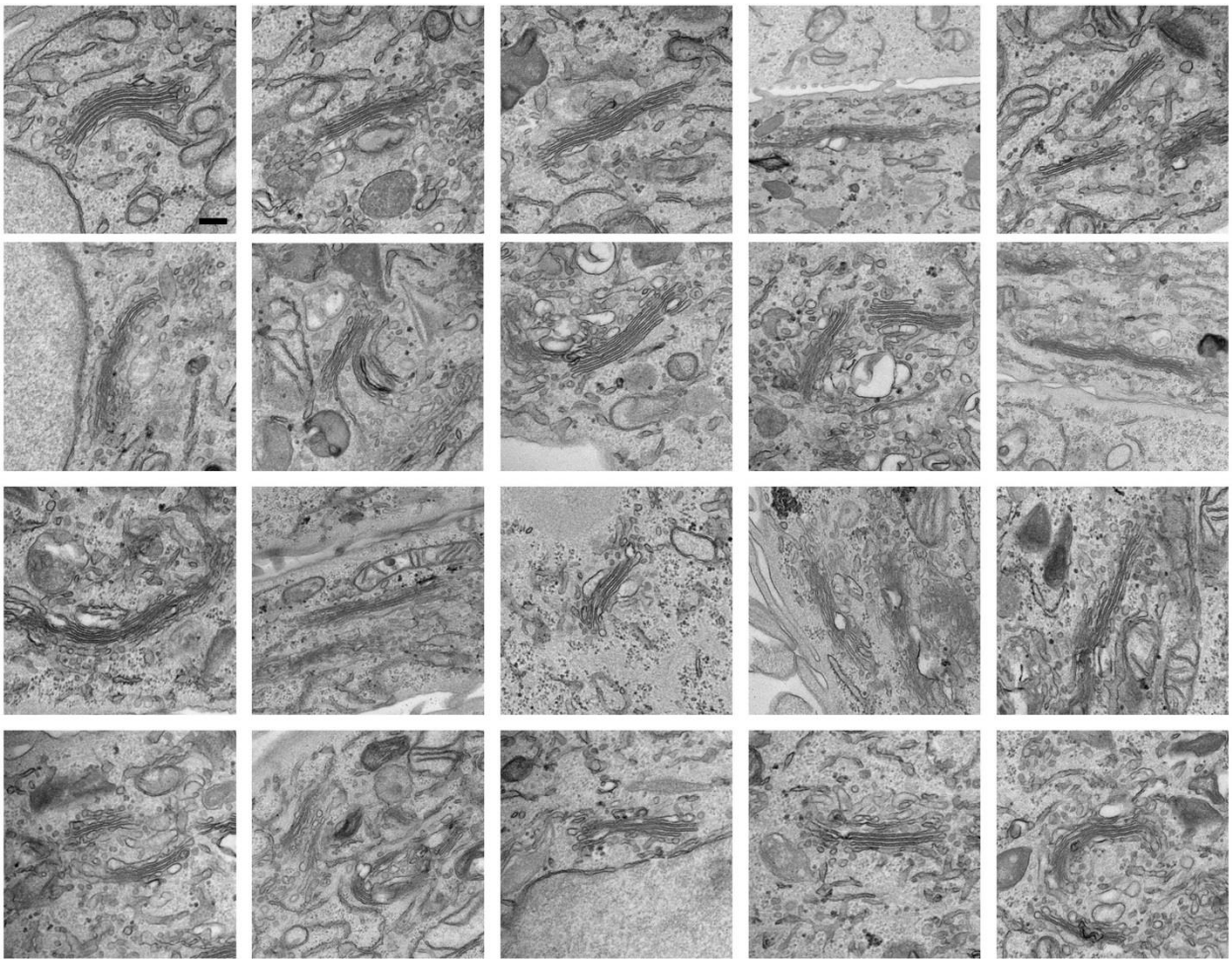

Figure 2.S7B. HeLa 55KO

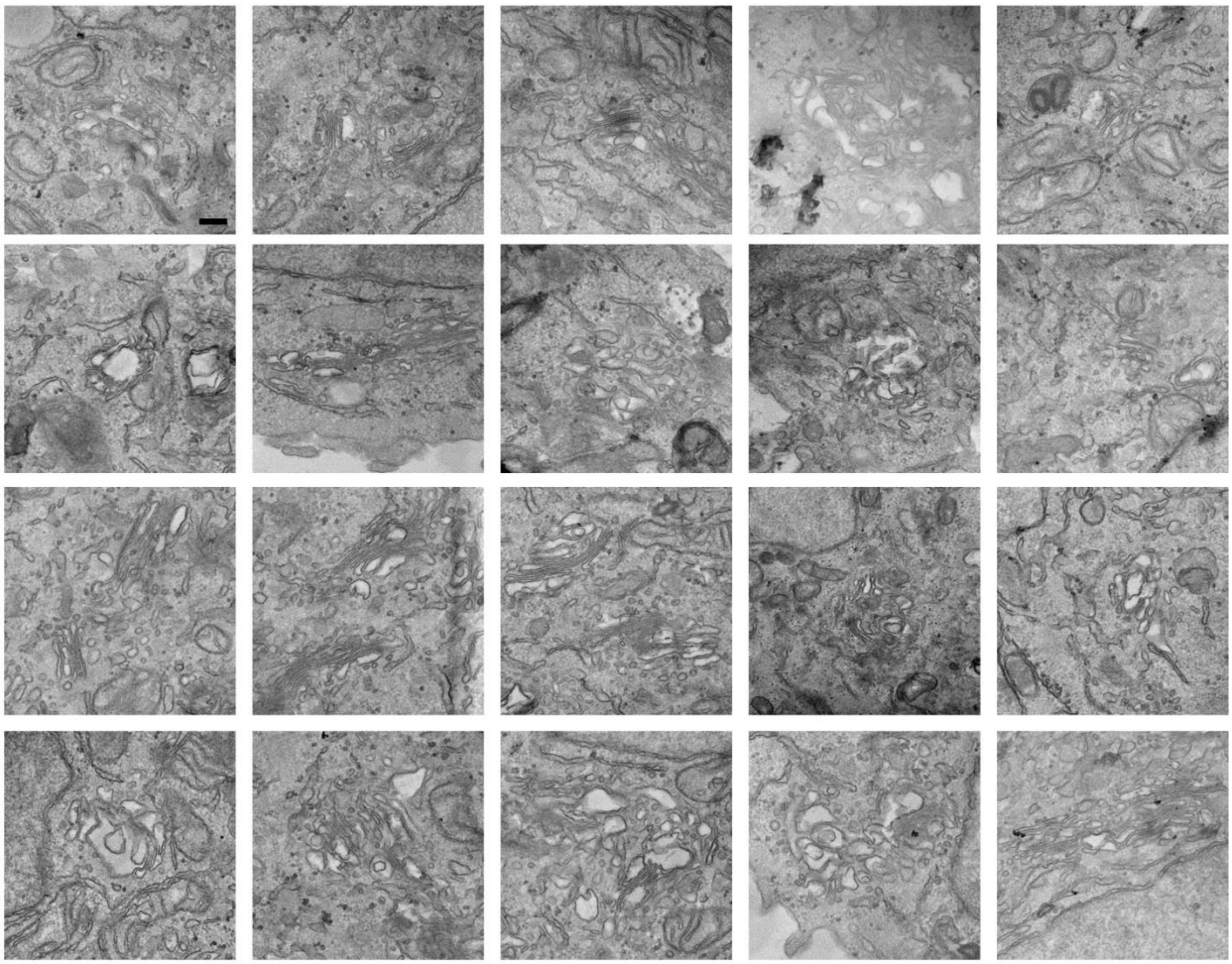

Figure 2.S7C. HeLa 65KO

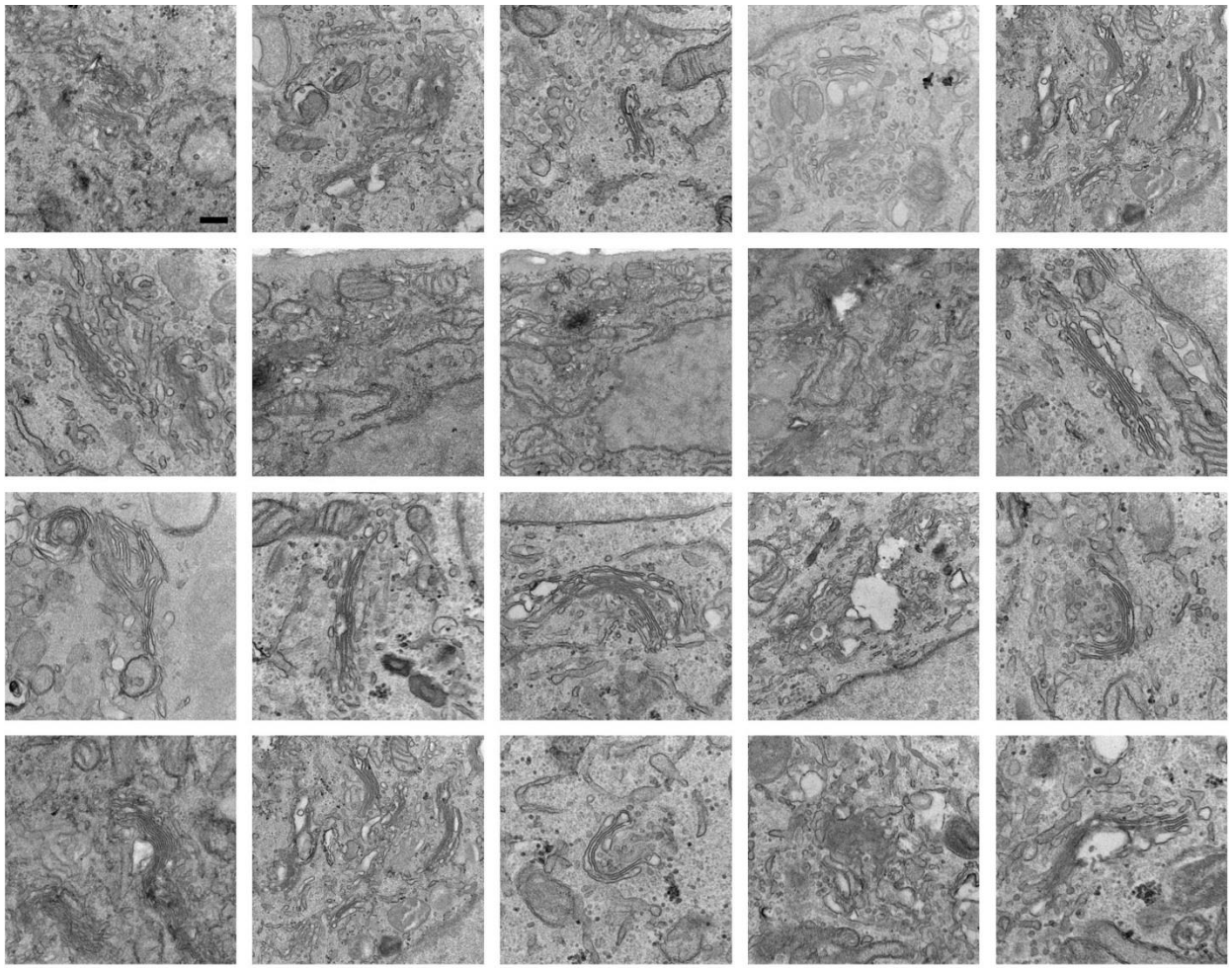

Figure 2.S7D. HeLa DKO

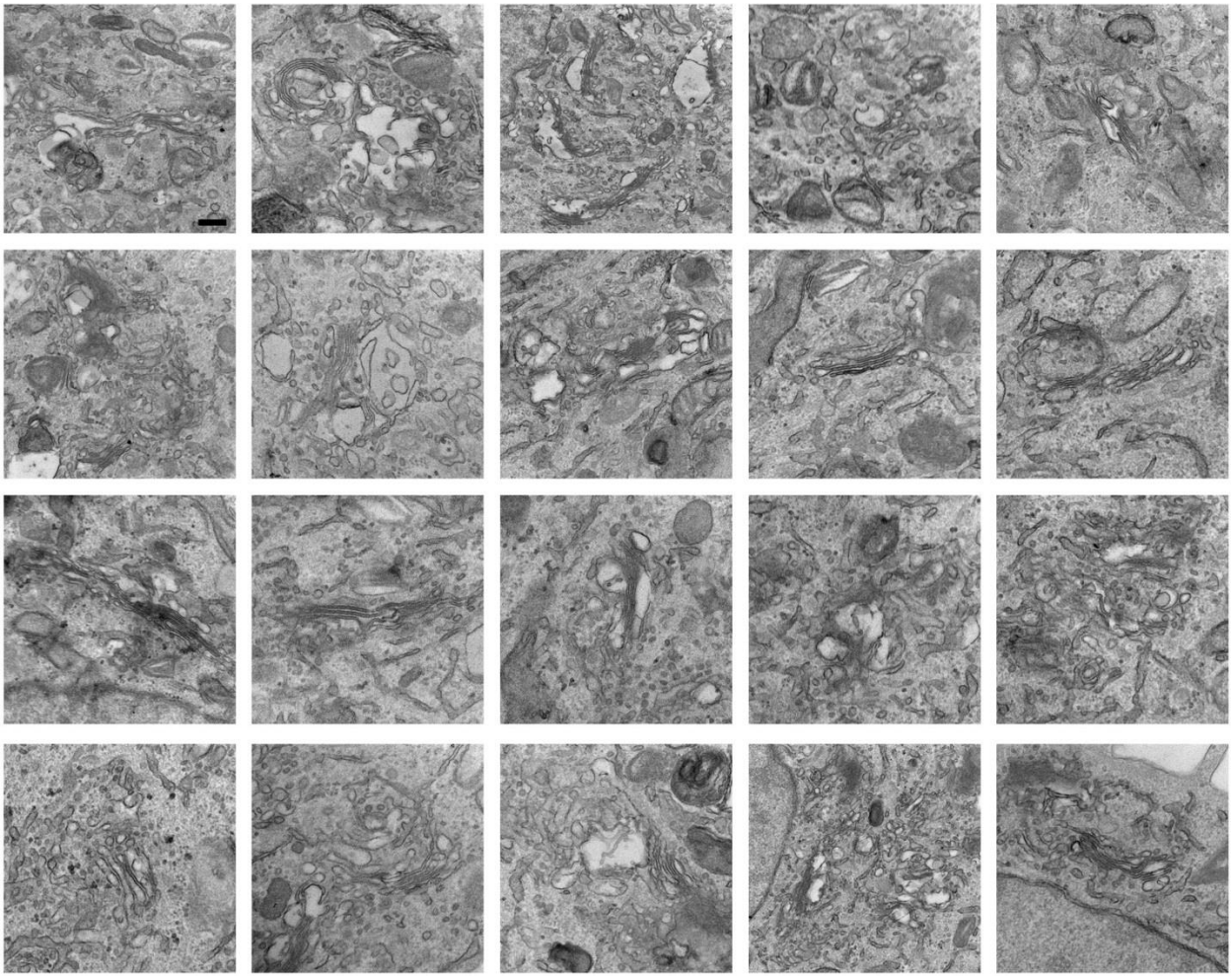

Figure 2.S7. EM Gallery from WT and GRASP knockout HeLa cells. Representative EM micrographs of the Golgi region in WT **(A)**, GRASP55 knockout **(B)**, GRASP65 knockout **(C)**, and GRASP55/65 double knockout **(D)** cells. EM images of Golgi membranes were taken in the perinuclear region. Scale bars are 200 nm.

GRASP knockout accelerates protein trafficking but impairs accurate glycosylation of proteins and lipids

Previous studies showed that GRASP depletion by RNAi disrupts Golgi stack formation, which subsequently impairs accurate protein glycosylation and sorting[64]. To test the effect of GRASP knockout on protein trafficking, we expressed the temperature-sensitive mutant of vesicular stomatitis virus G protein (VSV-G) in cells by viral infection[64]. As shown in Figure 2.6A-B, single

or double deletion of GRASP proteins accelerated VSV-G trafficking indicated by the increased amount of VSV-G protein that is resistant to EndoH treatment at 30 min after the temperature shift.

To test the effect of GRASP deletion on glycosylation of plasma membrane proteins, we performed cell surface staining with fluorescently labeled Wheat Germ Agglutinin (WGA) and Maackia amurensis lectin (MAA), which binds sialic acid, N-acetylglucosamine (GlcNAc); and α(2,3) sialic acid of glycans, respectively. GRASP single-knockout cells displayed a reduction in the intensity of both lectins on the cell surface; while double deletion of both GRASPs resulted in a similar effect (Figure 2.6C-D). We also assessed the glycosylation pattern of two glycoproteins, Lamp1 and Lamp2, using a mobility shift assay[64]. The mobility of Lamp1 and Lamp2 on SDS-PAGE was largely increased in GRASP single- and double-knockout HeLa and HEK293 cells, indicating a reduction in glycosylation of both Lamp1 and Lamp2 (Figure 2.6E). These results indicate that GRASP knockout disrupts accurate protein glycosylation for proteins both inside the cell and on the cell surface.

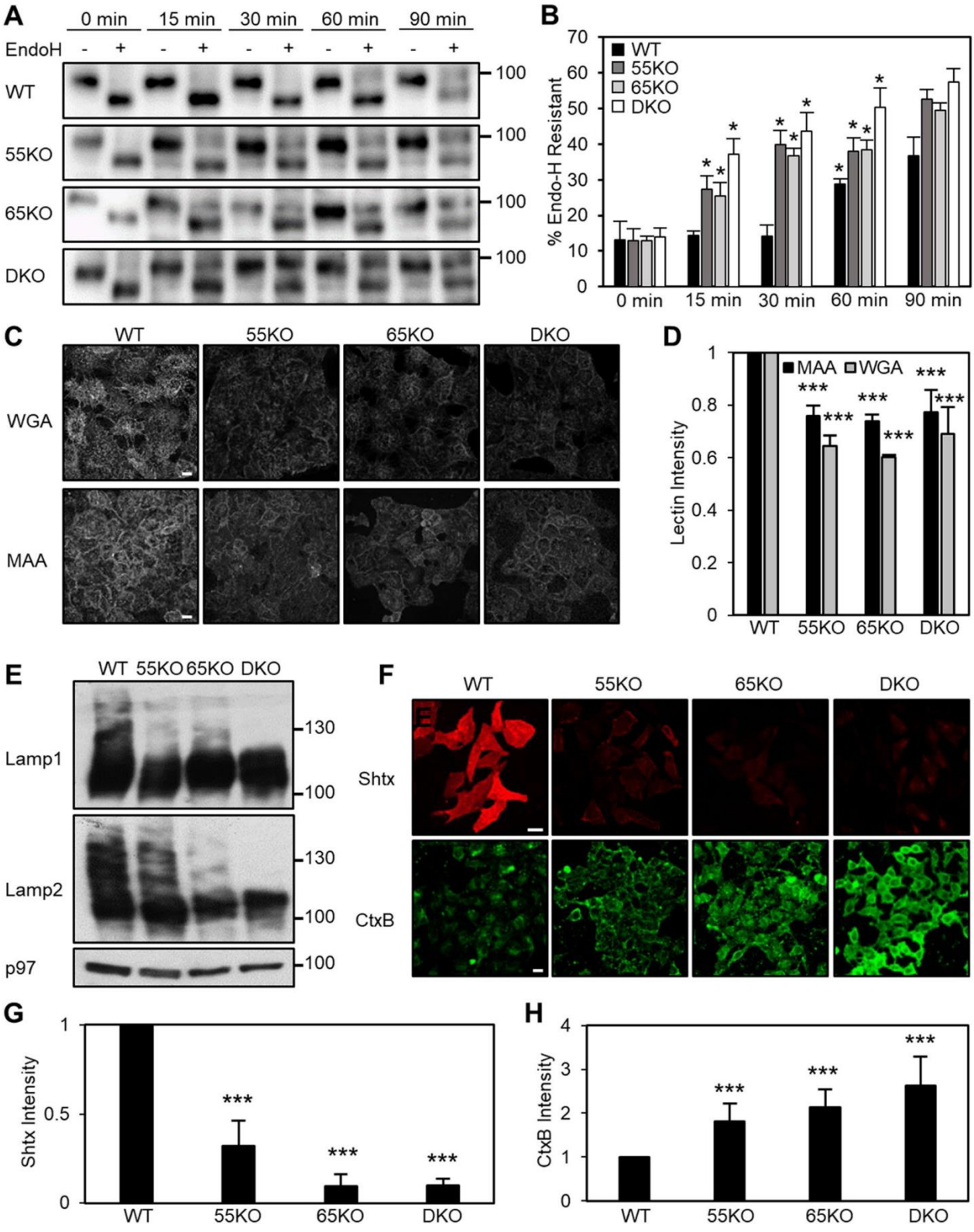

Figure 2.6. GRASP deletion accelerates protein trafficking but causes glycosylation defects. (A) GRASP deletion accelerates VSV-G trafficking. HeLa wild-type and GRASP knockout cells were infected

with VSV-G-ts045-GFP adenovirus and incubated at 40.5°C for 16 h followed by cyclohexamide treatment for 1 h. Cells were then shifted to 32°C to permit trafficking of VSV-G from the ER to the plasma membrane through the Golgi. Cells were collected at the indicated time points, treated with endoglycosydase H (Endo-H), and analyzed by Western blot for GFP. Note that GRASP deletion increased VSV-G Endo-H resistance by the 15-min time point. **(B)** Quantification of the percentage of Endo-H resistant (upper band) VSV-G from A. **(C)** GRASP deletion reduces the amount of sialic acid modifications on the cell surface. Wild-type and indicated GRASP knockout HeLa cells were stained with WGA or MAA lectin without permeabilization. Note the reduced WGA and MAA intensity on GRASP knockout cells. **(D)** Flow cytometric analysis of WT and GRASP knockout HeLa cells stained with WGA and MAA. The fluorescence intensity of 10,000 cells was determined by flow cytometry across three biological replicates. Error bars represent SEM. A Student's t test was used to determine statistical significance. **(E)** GRASP deletion reduces glycosylation of Lamp1 and Lamp2 glycoproteins. HeLa wild-type and GRASP knockout cells were analyzed by Western blots for Lamp1 and Lamp2; note their increased migration shift on the gel when GRASPs are deleted. **(F)** GRASP deletion impacts glycolipids at the cell surface. Wild-type and indicated GRASP knockout HeLa cells were stained with Shiga toxin B (Shtx) or cholera toxin B (CtxB) without permeabilization. Note the reduced ShTx intensity but increased CtxB intensity in GRASP knockout cells. **(G)** Quantitation of cell-surface ShTx intensity from cells in F. **(H)** Quantification of cell-surface cholera toxin from cells in F. For G and H, the mean intensity of 200 cells from each condition was quantified in maximum projections across three biological replicates. Error bars represent SEM. A Student's t test was performed to determine statistical significance. *$p < 0.05$; ***$p < 0.001$.

To determine whether GRASP deletion affects glycosylation of lipids, we stained cell surface with fluorescence-labeled Shiga Toxin B, which binds globotriaosylceramide (Gb3)[198], and Cholera Toxin B, which binds monosialotetrahexosylganglioside (GM1)[199]. Both Gb3 and GM1 gangliosides are glycolipids synthesized in the Golgi and then transported to the cell surface. Shiga Toxin cell surface stain was significantly reduced in GRASP55 knockout cells and completely abolished in both GRASP65 knockout and GRASP55/65 double knockout cells compared to a relative strong stain of wild type HeLa cells. Conversely, GRASP single- or double-knockout cells displayed higher levels of Cholera Toxin stain compared to wild-type HeLa cells (Figure 2.6F-H). Importantly, the effect of GRAP depletion on Gb3 and GM1 levels at the cell surface of double-knockout cells was rescued after adding back both GRASP proteins (Supplemental Figure 2.S8). Taken together, these results indicate that GRASP knockout enhances protein trafficking, but impairs accurate glycosylation of both proteins and lipids.

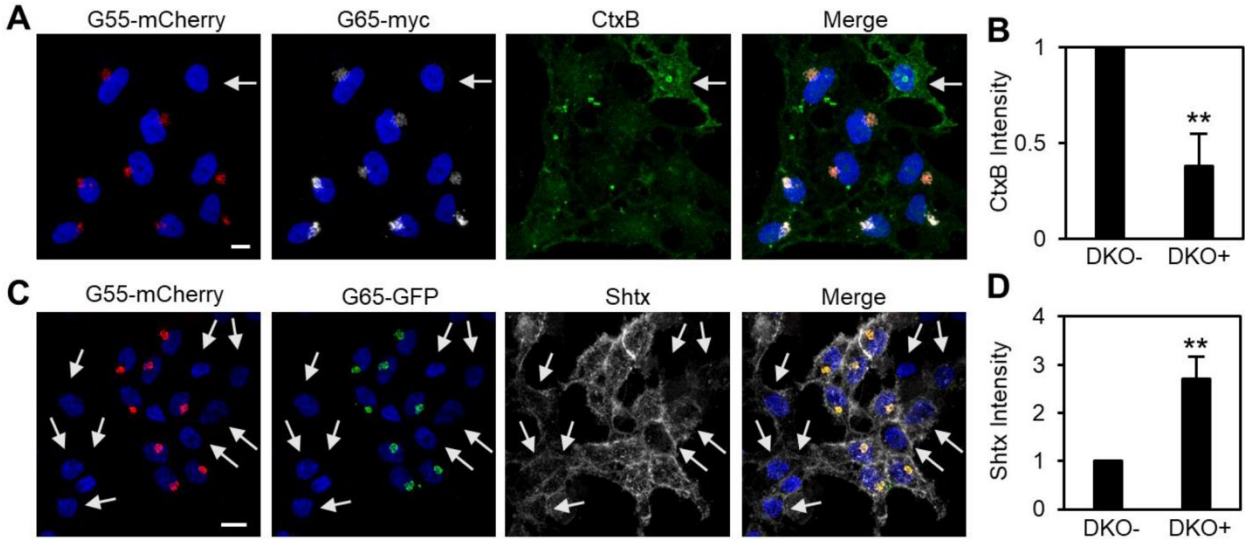

Figure 2.S8. Adding back GRASP proteins rescues GM1 and Gb3 cell-surface levels in GRASP double knockout cells. GRASP double-knockout HeLa cells were co-transfected with the indicated GRASP plasmids and stained with either cholera toxin B (**A**; CtxB) or shiga toxin B (**C**; Shtx). Arrows indicate untransfected cells. Scale bars are 10μm. **(B)** Quantitation of cell-surface CtxB intensity from non-expressing (DKO-) or GRASP expressing (DKO+) from A. **(D)** Quantitation of cell-surface Shtx intensity from nonexpressing (DKO-) or GRASP expressing (DKO+) from C. Greater than 100 cells from 3 independent experiments were quantified. Errors bars represent SEM. **, $p < 0.01$.

Discussion

In this study, we have provided new evidence that GRASP55/65 play essential roles in Golgi structure formation, in particular stacking. Knockout of a single GRASP protein reduces the number of cisternae in the stack, while double depletion of both GRASP proteins results in disorganization of the entire Golgi stack. These results are consistent with our previous results that inhibition of GRASP65 by micro-injection of GRASP65 antibodies[12] or by depletion of GRASP proteins by RNAi[13, 107], both disrupted the Golgi structure[13, 64]. These results demonstrate that GRASP55/65 function as Golgi stacking factors.

A second function for the GRASP proteins in Golgi structure formation is to link the Golgi stacks together to form a ribbon[15, 90]. In this study, however, knocking out a single GRASP protein in either HeLa or HEK293 cells did not cause significant Golgi fragmentation. Recently a GRASP65 knockout mouse has been reported, with only limited defects in the structure and function of the Golgi[105]. One major concern of this knockout mouse is the potential for only partial deletion of the gene, leaving a possibility that an N-terminal 115 amino acid fragment of GRASP65 may still be translated; this fragment is sufficient for oligomerization[106-108], a key property essential for Golgi stacking[12, 95]. The lack of an obvious phenotype in Golgi stacking in the GRASP65 knockout mouse may also be due to the complementation by GRASP55[11, 109]. Therefore, a complete knockout of both GRASPs is needed to further evaluate their functions. In this study, we designed multiple sgRNAs targeting to exon 1 of GRASP55 and exon 2 of GRASP65, which are directly downstream of the first ATG for translation initiation. Treatment of cells with these sgRNAs resulted in either insertions or deletions that caused a frame shift of the gene with an immediate

stop codon, as confirmed by DNA sequencing of individual clones (Table 2.2). This ensures that no functional, truncated proteins are generated in the cell lines. Analysis of these cells with light and electron microscopy demonstrated that double-deletion of both GRASPs completely disrupted Golgi stack formation and ribbon linking. Based on these results and previous literature, we conclude that stacking is the primary function of GRASP proteins.

GRASP depletion also accelerates protein trafficking and impairs accurate glycosylation of proteins and lipids on the cell surface. These results are consistent with our previous study with GRASP depletion by RNAi[64]. A plausible explanation for this finding is that when Golgi cisternae are fully stacked, vesicles can only form and fuse at the peripheral area of the cisternae; once the cisternae are unstacked, more membrane area becomes accessible, thereby increasing the rate of vesicle budding and cargo transport through the Golgi[195, 200]. In support of this, an *in vitro* budding assay has consistently demonstrated that unstacking increased the rate of COPI vesicle formation from Golgi membranes[200]. GRASP proteins have also been implicated in cell cycle control[71]. In this study, we did not observe significant change in cells growth or apoptosis, similar to GRASP knockdown[64], although more careful characterization of cell growth in these cell lines is needed in the future.

An interesting observation we have made in this study is that when one GRASP protein was deleted, the level of the other GRASP protein often increased. For example, when GRASP65 was deleted, GRASP55 protein level increased by 1.6-fold (Figure 2.2). These results reveal an autonomous regulatory mechanism in maintaining the Golgi integrity and function. That is, not only GRASP55

and GRASP65 play complimentary roles in Golgi stack formation and function, the total amount of GRASP proteins in the cell might be also regulated and therefore the total force to hold Golgi cisternae into stacks remains consistent. The nature of this mechanism, including the regulation of GRASP mRNA and protein synthesis and regulation by cellular metabolic activities, as well as GRASP targeting and degradation, will be interesting future topics of this study.

In conclusion, we have generated GRASP55 and GRASP65 single- and double-knockout HeLa and HEK293 cells. Characterization of these cell lines demonstrated that GRASP55 or GRASP65 single-knockout partially impaired Golgi cisternal stacking; whereas double-knockout of both GRASP proteins disassembled the entire Golgi structure. Furthermore, disassembly of the Golgi structure accelerated protein trafficking, but also impaired accurate glycosylation of cell surface proteins and lipids. These cell lines provide useful tools to study the mechanism and biological significance of Golgi structure formation, and could potentially be used to study the pathology of diseases in which the Golgi is defective, such as Alzheimer's disease[201, 202], congenital disorders of glycosylation[203], Foot-and-Mouth Disease[204], Reoxygenation Injury[205] and cancer[206].

Materials and Methods

Reagents, plasmids, and antibodies

All reagents were purchased from Sigma-Aldrich, Invitrogen, Roche, Calbiochem and Fisher unless otherwise stated. Antibodies used in this study include monoclonal antibodies against LAMP1 (H4A3, Developmental Studies Hybridoma Bank, (DSHB)), LAMP2 (H4B4, DSHB), Integrin β1 (P5D2, DSHB), integrin α-5 (BIIG2, DSHB) Shiga Toxin B (A42L, Thermo-Fisher) and β-actin (Sigma); polyclonal antibodies against GRASP55 (ProteinTech), GRASP65 (UT465, Joachim Seemann, UT Southwestern), GM130 (N73, Joachim Seemann, UT Southwestern), Golgin-45 (ProteinTech), TGN46 (Bio-Rad), GFP (Santa Cruz). Vesicular Stomatitis Virus G protein (VSV-G)-GFP adenovirus was a gift from David Sheff and Heike Fölsch. pUC19 plasmid was a gift from Daniel Klionsky. pSpCas9(BB)-2A-GFP(PX458), pSpCas9(BB)-2A-Puro (PX459) plasmids are from Addgene. Other materials used in this study: TRITC - Wheat germ agglutinin (WGA) (EY laboratories), TRITC-Maackia amurensis Lectin (MAA) (EY laboratories), FITC-Cholera Toxin B subunit (C1655, Sigma), Shiga Toxin Type 1 Subunit B (NR-860, BEI Resources) and Puromycin (Thermo-Fisher).

CRISPR-Cas9 knockout of GRASP genes

Guide RNA sequences targeting the GRASP55 and GRASP65 genetic loci were designed using the MIT Zhang Lab sgRNA Design Tool (crispr.mit.edu). Duplexed sgRNA oligos purchased from Invitrogen were digested and ligated into pSpCas9(BB)-2A-GFP(PX458) and pSpCas9(BB)-2A-Puro(PX459) to generate GRASP55/65 GFP or Puro plasmids, respectively. CRISPR knock-out cells were generated by transfection with GRASP55/65 GFP or Puro plasmids followed by

enrichment of GFP-expressing cells by FACS sorting or by selection with 1 μg/ml puromycin, respectively. Individual clones were generated by plating cells at low density and isolating individual colonies. GRASP knockout was confirmed by Western blotting, immunofluorescence, and DNA sequencing. For sequencing of GRASP55 and GRASP65, genomic loci were amplified by Polymerase chain reaction (PCR) using the following primers:

GRASP55 (5'-CGCGGATCCTGGTGTGTGTTGAGTTCGCT-3', 3'-CCCAAGCTTCTCCAGCCCGTCCTCCTA-5').

GRASP65 (5'-CGCGGATCCTCTAGAGCAGCATTCCCACAG-3', 3'-CCCAAGCTTGATGGGCCAAGGTAGTGGATG-5').

PCR products were cloned into pUC19 and the DNA sequence of 10-20 clones from each cell line was determined by Sanger Sequencing at the University of Michigan DNA Sequencing Core using M13Rev standard sequencing primer. The sequencing results are aligned with NCBI Reference Sequences of GRASP55 (NM_015530.4) and GRASP65 (NC_000003.12).

Immunofluorescence microscopy

Immunofluorescence was performed as described previously[95, 207]. Briefly, HeLa and HEK293 cells were fixed in 2% paraformaldehyde (PFA) in Phosphate-buffered saline (PBS) for 15 min followed by quenching with 50 mM NH_4Cl in PBS for 10 min and permeabilization with 0.1% Triton-X-100 in PBS for 10 min. Permeabilized cells were blocked with 2% Bovine Serum Albumin (BSA) in PBS for 1 hour followed by incubation with primary antibodies for 1.5 hours, washed with PBS, and incubated with secondary antibodies for 45 min at room temperature. DNA was stained with Hoechst (1 μg/ml) and coverslips were mounted with Moviol. Wide-field

fluorescence microscopy was performed on a Zeiss Observer Z1 using a 63x/1.4 oil objective at a Z-step of 0.5 µm. Standard confocal microscopy was performed on a Leica SP5 using a 63x/1.4 oil objective at 400 Hz scan rate in a 512x512 scan field with a Z-step of 0.5 µm. Airyscan confocal images were collected using an LSM 880 confocal system outfitted with an Airyscan detector (Carl Zeiss, Jena, Germany) to optimize resolution of fixed cell preparations. Briefly, multitrack acquisition was performed with 405, 488, and 633 nm wavelengths using a Plan-Apochromat 63x/1.4 oil objective. Images were scanned with a pixel scaling of 37 nm in XY with a Z-step of 144 nm. Resulting emission was centered on a 32-element GaAsP-based spatial detector, and channels were reassigned to a central GaAsP element to effectively reduce imaging volumes from 1.25 Airy units to 0.2 Airy units. This reassignment step was performed via the ZEN software (Carl Zeiss) using a recommended Wiener filter parameter for weighing noise in given images. Final images were assessed against confocal (non-Airyscan) images to ensure artifact-free improvements in resolution and signal-to-noise.

Electron microscopy (EM)

EM was performed as previously described[207]. Briefly, cells were plated in 6-well dishes. After 24 hours of culture, cells were fixed with 2.5% glutaraldehyde and then processed for Epon embedding. Sections of 60 nm were mounted onto Formvar-coated nickel grids and double contrasted with 2% uranyl acetate for 5 minutes and 3% lead citrate for 5 minutes. Grids were imaged using a Philips CM100 Biotwin and JEOL JEM-1400 transmission electron microscope. Golgi stacks and Golgi clusters were identified using morphological criteria and quantitated using standard stereological techniques. For HeLa wild type and GRASP knockout cells, the profiles had to contain a nuclear profile with an intact nuclear envelope. A cisterna was defined as a membrane-

bound structure in the Golgi cluster whose length is at least 4× its width, normally 20–30 nm in width and longer than 150 nm[20], and a stack is the set of flattened, disk-shaped cisternae resembling a stack of plates. Multiple unstacked cisternae and vesicles were counted as disorganized membrane clusters, whereas stacked structures with two or more cisternae were counted as distinguishable Golgi stacks and only stacked structures with well aligned, smooth, normal length cisternae were counted as well-organized Golgi stacks.

Lectin staining

Lectin staining was performed as previously described[203]. In short, cells were grown on coverslips to 70% confluency then incubated with ice-cold PBS for 15 min followed by fixation with 1% PFA for 15 min and quenching with 50 mM NH_4Cl for 10 min. Cells were then washed three times with PBS and blocked in 1% BSA in PBS for 30 min at room temperature. After blocking, cells were incubated with fluorophore-conjugated lectins for 30 min at room temperature followed by three 10 min PBS washes and mounted onto glass slides. The following lectins (and working concentrations) were used: TRITC-WGA (2 μg/ml), TRITC-MAA (20 μg/ml).

Fluorescence activated cell sorting (FACS)

Flow cytometry analysis for lectin staining was performed as previously described[208]. In short, cells were grown to 70% confluency then incubated with ice-cold PBS for 15 min followed by treatment with 20 mM EDTA for 5 min. Cells were collected after treatment with 20 mM EDTA for 5 min and re-suspended in 0.1% BSA. After blocking on ice for 30 min in 0.1% BSA/PBS, cells were incubated with fluorophore- conjugated lectins in 0.1% BSA with indicated

concentration for 30 min while shaking on ice followed by washing with ice cold PBS. Cells are then fixed with 1% PFA for 15 min and quenched with 50 mM NH_4Cl for 10 min before submitted for flow cytometry. Cells were analyzed using the LSRFortessa (BD Biosciences) flow cytometer. Cells were gated for correct cell size vs. complexity and fluoresce intensity. Analysis was done using FCS Express 6 software.

VSVG trafficking assay

VSVG trafficking assay was performed as previously described[64]. Briefly, cells were plated in 3.5 cm dishes and cultured overnight. Subsequently, the media was removed and serum-free media was added that contained VSV-G-ts045-GFP adenovirus. Following a 2 hour incubation with the virus, the viral containing media was removed and cells were grown in full media at 40.5°C for 16 hours. Cells were then treated with 50 µg/ml cyclohexamide for 1 hour prior to shifting the temperature to 32°C. Cells were harvested at the indicated time points and an Endo-H assay was performed.

Shiga toxin and cholera toxin binding assay

Shiga Toxin and Cholera Toxin Assay were performed as previously described[209]. In short, for Shiga toxin binding assay, cells were plated onto coverslips and cultured overnight. Cells were then washed three times with cold PBS and incubated with 4 µg/ml purified Shiga toxin 1B subunit in cold media for 30 min on ice. After three times wash with ice-cold PBS, cells were fixed with 4% PFA, quenched with 50 mM NH_4Cl, followed by subsequent incubation with an anti-shiga toxin B primary antibody for 1.5 hours and secondary antibody for 1.5 hours at room temperature.

DNA was stained with Hoechst. Coverslips were mounted with Moviol. Images were taken on a Leica SP5 confocal microscope.

For Cholera toxin binding, cells were plated onto coverslips and cultured overnight. Then cells were washed three times with ice-cold PBS and incubated with 4 µg/ml FIFC-conjugate Cholera toxin B subunit in cold media for 30 min on ice. Cells were then washed three times with ice-cold PBS and fixed with 4% PFA, quenched with 50 mM NH_4Cl, and DNA was then stained with Hoechst. Images were taken on a Leica SP5 confocal microscope.

Acknowledgement

We thank Kamlesh Bisht and JK Nandakumar for technical support on CRISPR technique, Joachim Seemann for antibodies, and David Sheff and Heike Fölsch for VSV-G ts045-GFP adenovirus. We thank other members of the Wang lab for suggestions, reagents and technical support. This work was supported in part by the National Institutes of Health Grant GM112786.

Abbreviations

BSA, Bovine Serum Albumin; CRISPR, Clustered Regularly Interspaced Short Palindromic Repeats; EndoH, endoglycosidase; EM, electron microscope; FACS, fluorescence activated cell sorting; GRASP55, Golgi reassembly stacking protein of 55 kDa; GRASP65, Golgi reassembly stacking protein of 65 kDa; MAA, Maackia amurensis lectin; PBS, Phosphate-buffered saline; PCR, Polymerase chain reaction; sgRNA, single-guide RNA; TGN, trans-Golgi network; VSV-G, vesicular stomatitis virus G protein; WGA, Wheat germ agglutinin.

Chapter III. GRASP55 collaborates with the PI3K UVRAG complex to facilitate autophagosome-lysosome fusion

Abstract

It has been indicated that the Golgi apparatus contributes to autophagy, but how it is involved in autophagosome formation and maturation is not well understood. Here we show that, upon amino acid starvation, *trans*-Golgi derived membrane fragments colocalize with autophagosomes. Depletion of the Golgi stacking protein GRASP55, but not GRASP65, increases both LC3-II and p62 levels. Further studies show that upon amino acid starvation, GRASP55 facilitates autophagosome-lysosome fusion through two actions, one is by physically tethering autophagosomes and lysosomes through the interactions with LC3 on autophagosomes and LAMP2 on late endosomes/lysosomes, and the other is by interacting with Beclin 1 to facilitate the assembly and membrane association of the phosphoinositide 3-kinase (PI3K) complex II. These findings indicate that GRASP55 plays an important role in autophagosome maturation during amino acid starvation.

Introduction

Autophagy is an important cellular process in response to nutrient starvation[123-125]. It is induced by different signal pathways; amino acid depletion inactivates mammalian target of rapamycin (mTOR), whereas glucose depletion activates AMP kinase (AMPK)[123], both of which subsequently activate Unc-51 like autophagy activating kinase (ULK1/2), Atg13, Atg101 and focal adhesion kinase (FAK)-family interacting protein of 200 kDa (FIP200)[123]. These autophagy regulators activate class III phosphoinositide 3-kinase (PI3K) complex I, which involves Vps34, Beclin 1, Atg14L, p150 and AMBRA1[123]. PI3P enriched pre-autophagosomal structure (PAS) then recruits the Atg5-Atg12-Atg16L protein complex and microtubule-associated protein 1 light chain 3 (LC3) to initiate two ubiquitin-like reactions that help PAS to elongate and recruit membranes to form autophagosomes[132, 133]. Upon fusion of the double membrane, fully formed autophagosomes fuse with lysosomes to generate autolysosomes for degradation of the sequestrated materials[123]. Rab7 GTPase and its effectors[134], including the SNAP (Soluble NSF (N-ethylmaleimide-sensitive factor) Attachment Protein Receptor (SNARE) complex consisting of Syntaxin 17, SNAP29, and VAMP7/8[135], Tectonin beta-propeller repeat-containing protein 1 (TECPR1)[136], the HOPS complex[137], and the PI3K complex II formed by Beclin 1, Vps34, Vps15, UVRAG and Bif-1[138, 139], are involved in autophagosome-lysosome fusion.

Several membrane organelles have been indicated as the membrane source for autophagosomes. It has been shown that the endoplasmic reticulum (ER)[116, 178, 210, 211], mitochondria[212] and plasma membrane[156] could provide lipid and some key proteins for autophagosome formation. The Golgi apparatus may also have a role in autophagosome formation. Atg9, a transmembrane protein

cycling between the *trans*-Golgi network (TGN) and endosomes, relocates to autophagosomes upon amino acid starvation or rapamycin treatment in mammalian cells, which implicates that Golgi may deliver membranes to autophagosomes[66]. Furthermore, adaptor protein complex 1 (AP1)-mediated clathrin vesicles deliver membranes from the TGN to autophagosomes[67]. In addition, Beclin 1 and the PI3K complex are concentrated on the TGN[69], and Beclin 1-associated autophagy-related key regulator (Barkor) is required for the relocalization of the PI3K complex from the TGN to autophagosomes[70]. All these results indicate that the Golgi contributes to autophagy.

The Golgi apparatus, an essential organelle for protein and lipid modifications, trafficking, and sorting, exists as stacks of flattened cisternal membranes in most eukaryotic cells. Formation of this stacked structure depends on two Golgi reassembly stacking proteins, GRASP55 and GRASP65, which are localized to the *medial-trans* and *cis* cisternae, respectively. These peripheral membrane proteins form *trans*-oligomers from adjacent cisternae to hold Golgi cisternae together into stacks[12, 13]. During mitosis, GRASP proteins are phosphorylated, which inhibits their oligomerization, resulting in Golgi cisternal unstacking; while in telophase, dephosphorylation allows GRASPs to reoligomerize and Golgi cisternae to restack[104].

How the Golgi responds to nutrient deprivation and how it contributes to autophagy remain mostly elusive. In this study, we investigated the role of the Golgi in autophagy and made an unexpected finding that GRASP55 contributes to autophagosome maturation upon amino acid starvation by

physically tethering autophagosomes and lysosomes and by facilitating the assembly of the class II PI3K complex.

Results

Amino acid starvation induces Golgi derived vesicles to colocalize with autophagosomes

To determine how the Golgi responds to amino acid starvation, HeLa cells were treated with Earle's Balanced Salt Solution (EBSS) and Bafilomycin A1 (BafA1) for 1-8 h as indicated (Fig. 3.1A), and stained for LC3, GM130 and TGN46 to reveal the autophagosomes, *cis*-Golgi, and *trans*-Golgi, respectively. Consistent with previous reports[213], this treatment results in autophagosome accumulation (Fig. 3.1A-D). Interestingly, the Golgi, especially the *trans* Golgi, generated vesicular structures that colocalized with autophagosomes (Fig. 3.1A, C). These results demonstrate that amino acid starvation triggers mild Golgi fragmentation. We then determined the effect of EBSS treatment on the level of major Golgi structural proteins. While most proteins decreased their levels or did not change, GRASP55 significantly increased its protein level upon starvation (Fig. 3.1D-E), indicating that GRASP55 might play a role in amino acid starvation-induced autophagy. Similarly, EBSS alone or together with other lysosome inhibitors, NH_4Cl or Chloroquine (CQ), or with the mTOR inhibitor rapamycin, also induced the *trans*-Golgi to form and release vesicular structures that colocalize with autophagosomes. The same treatments also increased LC3 and GRASP55 protein levels (Fig. 3.S1, S2). Since long-term amino acid starvation results in cell death, we used 4 h treatment in our following experiments.

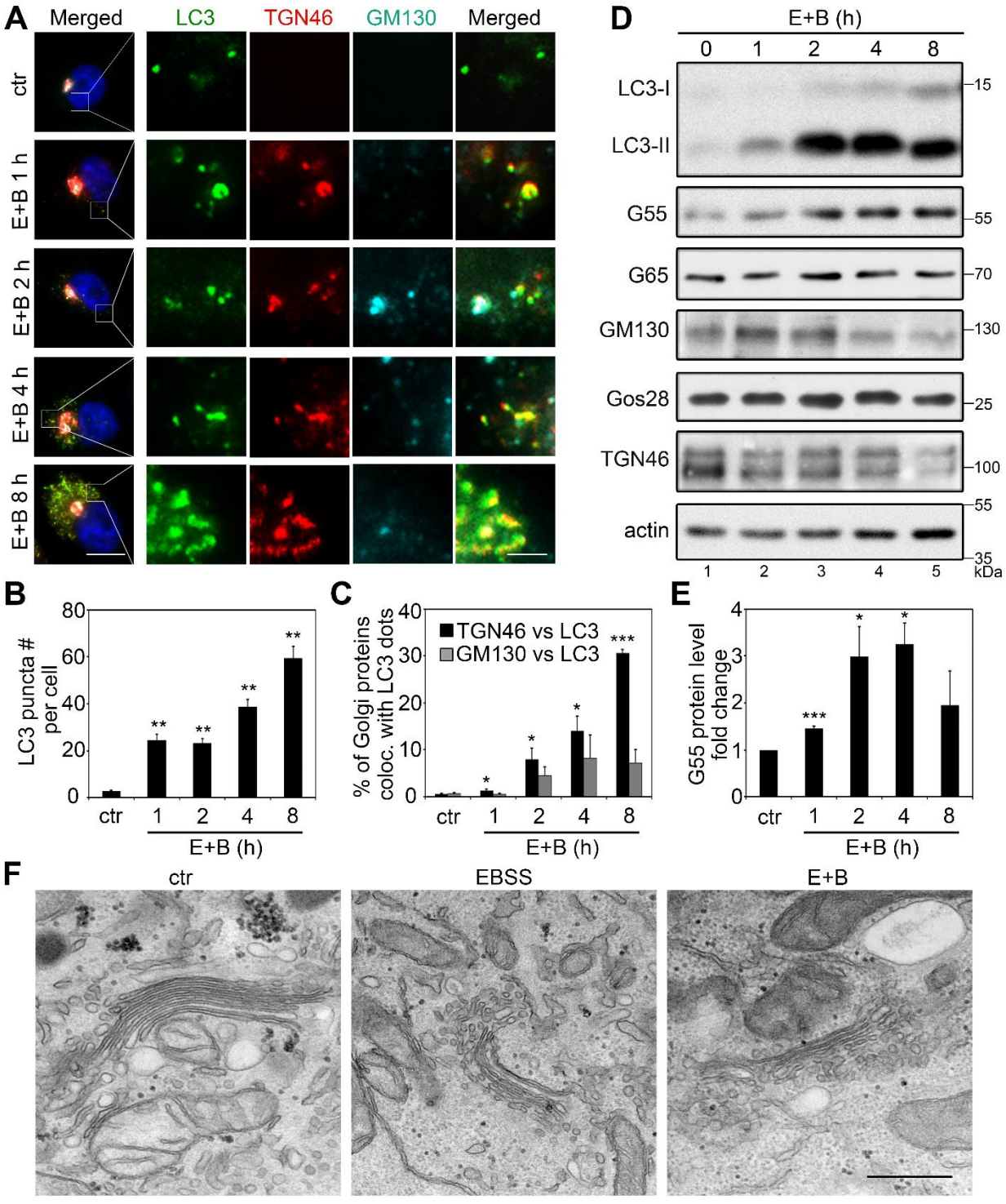

Figure 3.1. Amino acid starvation induces Golgi derived vesicles to colocalize with autophagosomes. **(A)** Golgi derived fragments colocalize with autophagosomes upon amino acid starvation. HeLa cells were incubated with growth medium (ctr) or with EBSS and 400 nM BafA1 (E+B) for the indicated times, stained for LC3, TGN46, GM130, and DNA. The four columns on the right are at higher magnifications of the area

indicated in the first column on the left. Scale bar, 10 μm on the left, 2 μm on the right. **(B)** Quantification of (A) for the average number of LC3 puncta per cell from three independent experiments. Values are shown as mean ± SD from three independent experiments; statistical significance of the results was assessed by Student's t-test. *, $p<0.05$; **, $p<0.01$; ***, $p<0.001$. **(C)** Quantification of (A) for the percentage of TGN46 and GM130 signals that colocalized with LC3. **(D)** Western blots of LC3 and major Golgi proteins in HeLa cells treated as in (A). **(E)** Quantification of (D) for the GRASP55 protein level. **(F)** Electron microscopy pictures of HeLa cells treated with growth medium (ctr), EBSS, or EBSS with 400 nM BafA1 (E+B) for 4 h. Scale bar is 500 nm.

To further investigate how amino acid starvation affects Golgi morphology, we performed electron microscopy (EM). Compared to growth medium (control condition), EBSS treatment or EBSS with BafA1 significantly reduced the cisternal length and caused fenestration of the Golgi cisternae in particular in the *medial-trans* cisternae (Fig. 3.1F, Fig. 3.S3). Notably, many autophagosomes were observed in the close proximity of the Golgi stacks (Fig. 3.1F, Fig. 3.S3), consistent with a role of the Golgi in contributing to autophagy.

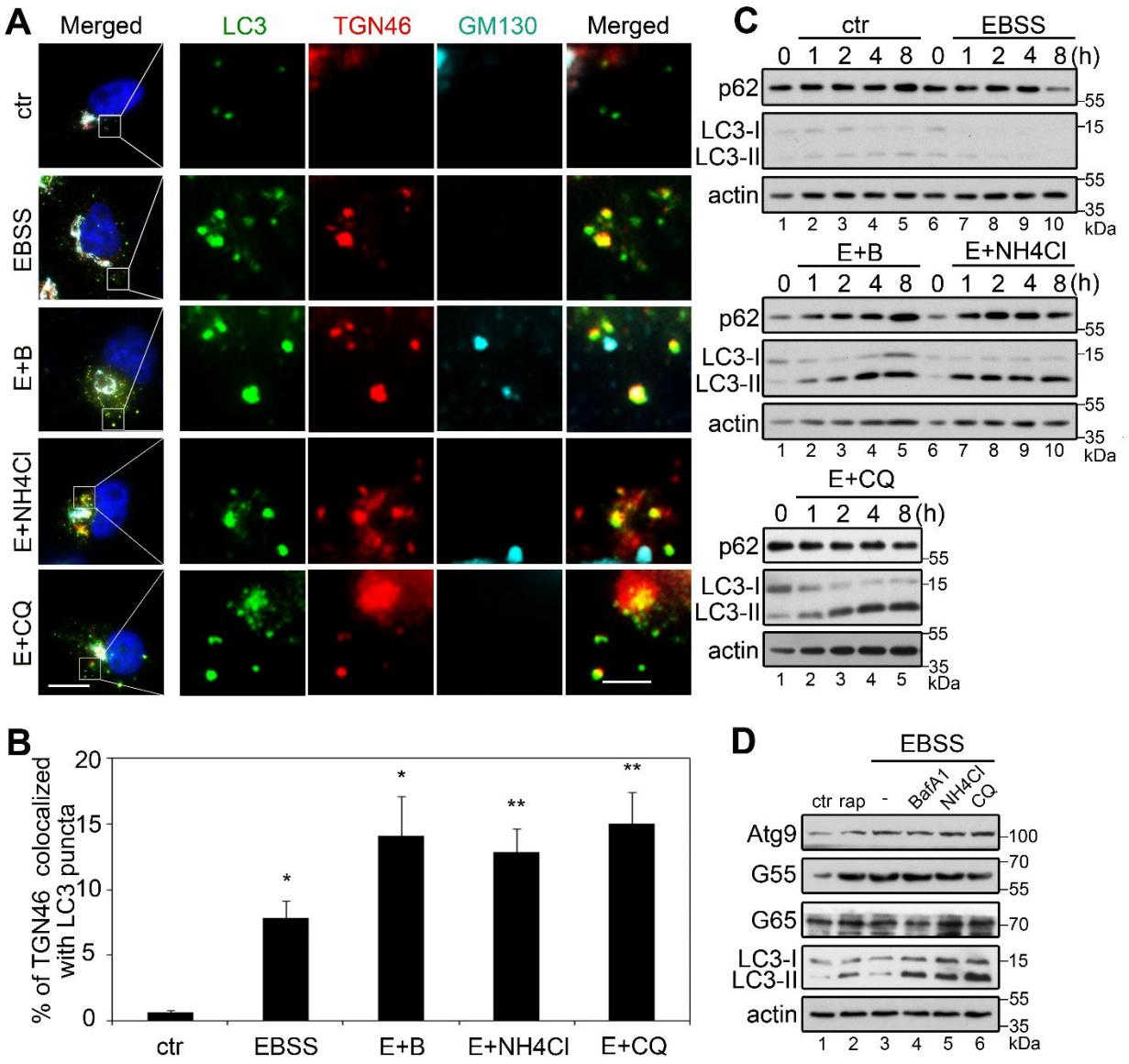

Figure 3.S1. Amino acid starvation with different lysosome inhibitors induces Golgi derived vesicles to colocalize with autophagosomes. (A) HeLa cells were incubated with growth medium (ctr), EBSS, or EBSS with 400 nM BafA1 (E+B), 20 mM NH_4Cl (E+NH_4Cl) or 50 μM CQ (E+CQ) for 4 h, stained for LC3, TGN46, GM130, and DNA. The four columns on the right are high magnifications of the indicated area in the column on the left. Scale bars, 10 μm on the left; 2 μm on the right. **(B)** Quantification of (A) for the percentage of TGN46 signal that colocalized with LC3. **(C)** Western blots of p62, LC3 and actin in cells from (A). **(D)** GRASP55 protein level increases upon autophagy induction. Western blots of GRASP55 (G55), LC3 and actin in HeLa cells treated with growth medium (ctr), 5 μM rapamycin (rap), EBSS, or EBSS and 400 nM BafA1, 20 mM NH_4Cl or 50 μM CQ for 4 h.

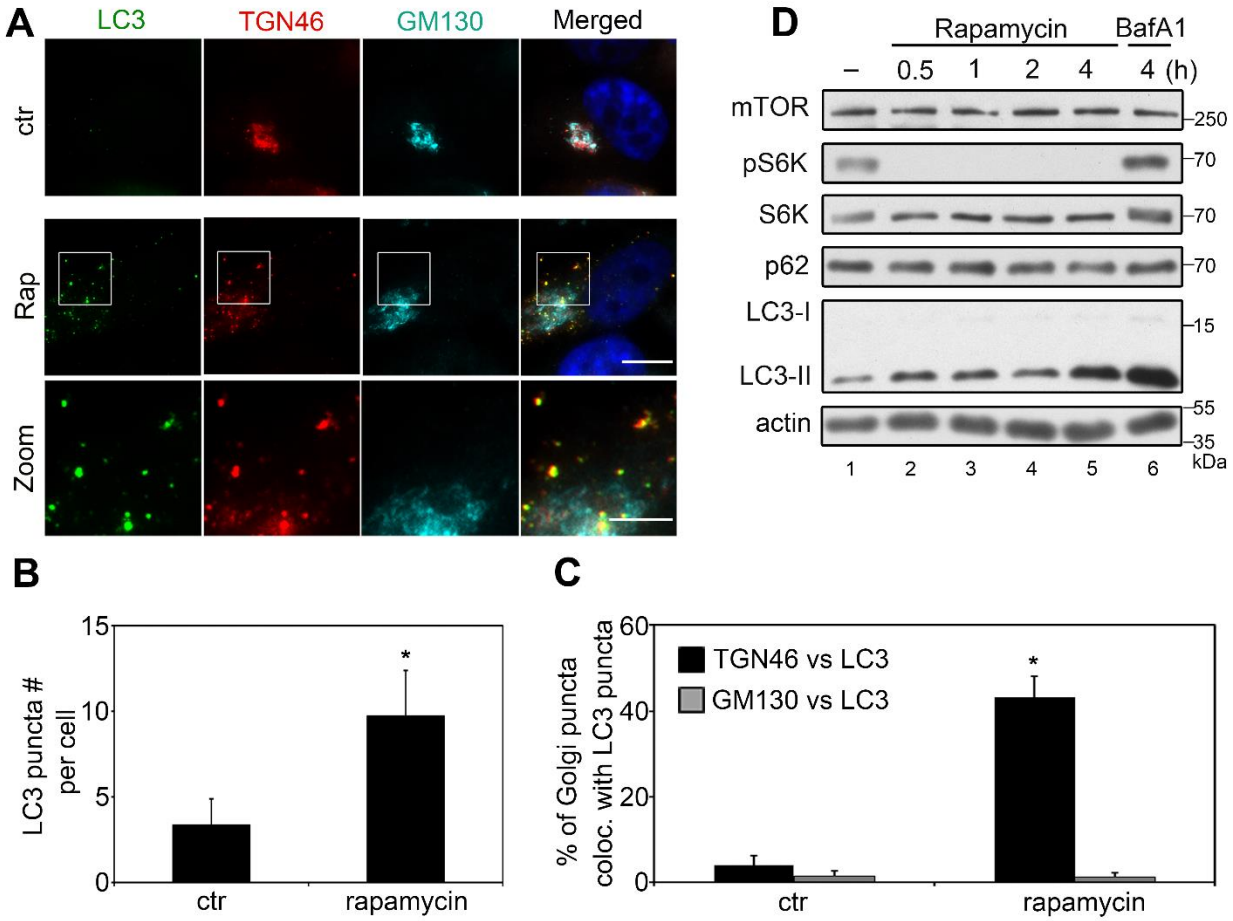

Figure 3.S2. Inhibition of mTOR induces Golgi derived vesicles to colocalize with autophagosomes. **(A)** HeLa cells were incubated with growth medium (ctr) with or without 5 μM rapamycin (Rap) for 4 h, stained for LC3, TGN46, GM130, and DNA. The bottom row is a high magnification of the squared area in the upper row (Rap). Scale bar: upper, 10 μm; lower, 5 μm. **(B)** Quantification of (A) for the average number of LC3 puncta per cell. **(C)** Quantitation of (A) for the percentage of TGN46 or GM130 positive puncta that colocalized with LC3 puncta. **(D)** Western blots of mTOR, pS6K, S6K, p62, LC3 and actin in HeLa cells treated with growth medium (-), growth medium with 5 μM rapamycin (Rap) for indicated times, or growth medium with 400 nM BafA1 for 4 h.

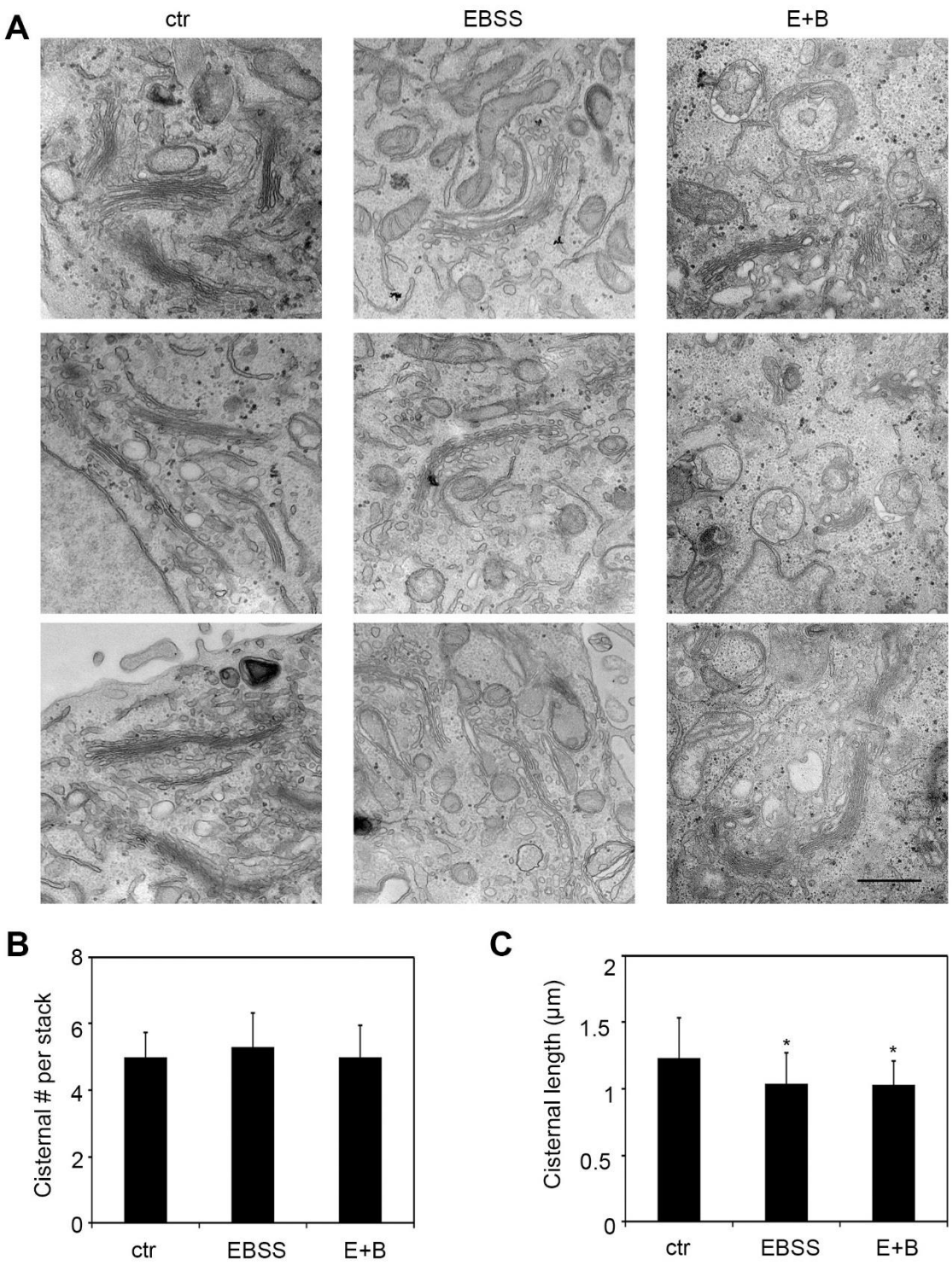

Figure 3.S3. The Golgi is partially fragmented upon amino acid starvation. (A) Electron microscopy pictures of HeLa cells treated with growth medium (ctr), EBSS, or EBSS and BafA1 (E+B) for 4 h. Scale bar is 500 nm. **(B-C)** Quantification of cisternal number per stack and cisternal length in (A) from 3

independent experiments, at least 20 cells across three biological replicates were quantified. Error bars represent SD.

GRASP55 depletion inhibits autophagosome maturation

As the protein level of GRASP55 was increased by amino acid starvation (Fig. 3.1D-E, S1D), we investigated its role in autophagy. Knockdown of GRASP55, but not GRASP65, significantly increased the number of autophagosomes under both control and amino acid starvation conditions (Fig. 3.2A-B). GRASP55 depletion also increased both LC3 and p62 protein levels (Fig. 3.2C). These results show that GRASP55 is required for autophagosome maturation rather than formation, indicating that GRASP55 may be involved in autophagosome-lysosome fusion.

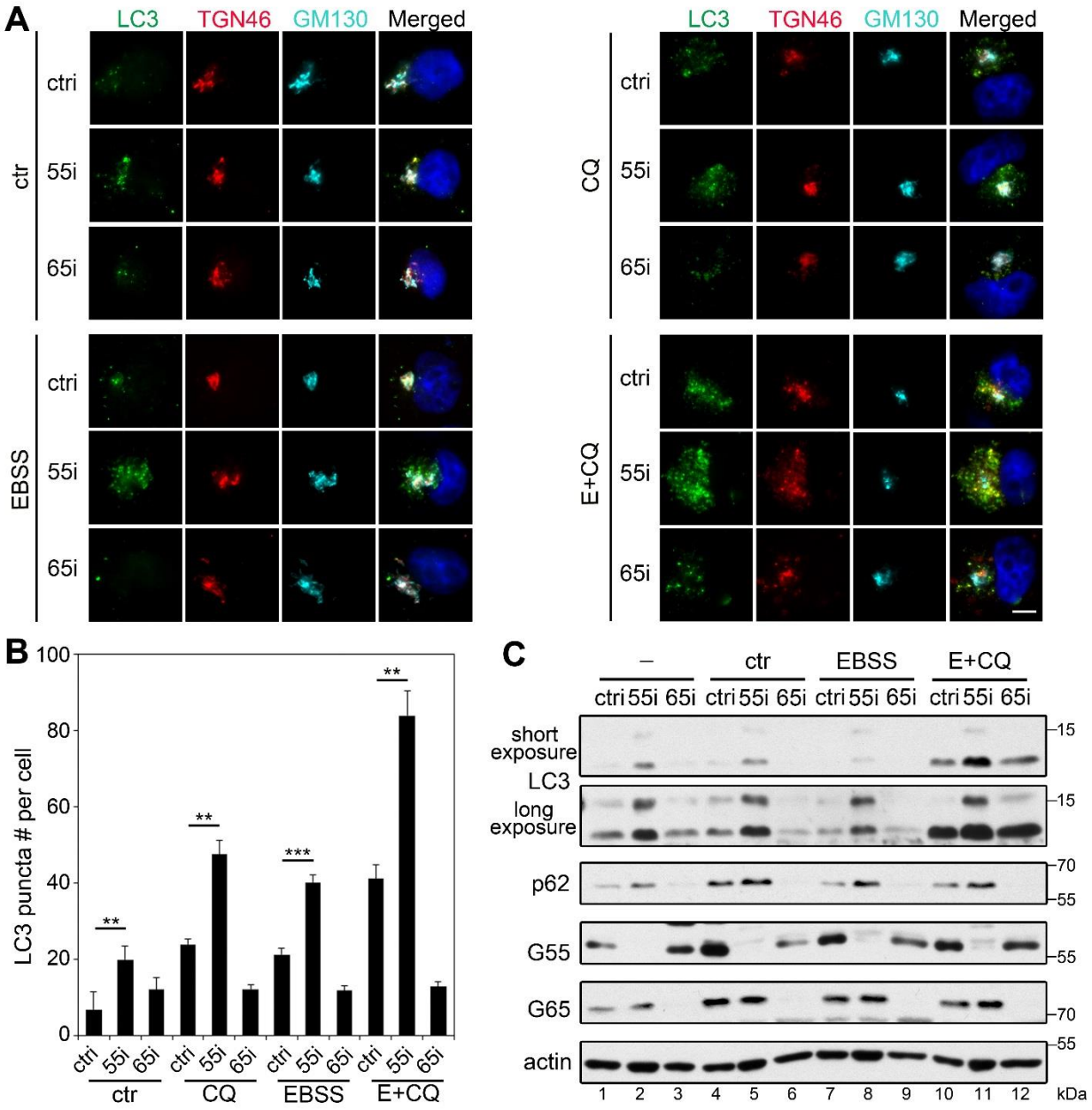

Figure 3.2. GRASP55 depletion results in autophagosome accumulation. (A) GRASP55 depletion increases the number of autophagosomes. HeLa cells were transfected with control (ctri), GRASP55 (55i) or GRASP65 (65i) RNAi as indicated for 72 h, treated with growth medium (ctr), EBSS, chloroquine (CQ) or EBSS with 50 μM CQ (E+CQ) for 4 h, and stained for LC3, TGN46, GM130, and DNA. Scale bar is 10 μm. **(B)** Quantification of (A) for the average number of LC3 puncta per cell. **(C)** Western blots of indicated proteins in HeLa cells treated with growth medium (ctr), EBSS, or EBSS with 50 μM CQ for 4 h. None treated cells (–) were used as a control. Two different exposure of LC3 were shown.

To further clarify the role of GRASP55 in autophagosome maturation, we determined the effect of GRASP55 depletion on autophagic flux in HeLa cells that express the RFP-GFP-LC3 reporter [LC3 tagged by both the red (RFP) and green (GFP) fluorescent proteins][214]. This dual tagged LC3 construct emits both red and green fluorescence lights upon excitation at neutral pH as in autophagosomes. Upon autophagosome-lysosome fusion, GFP is quenched by the acidic pH in the autolysosomes, and thus only red fluorescence is seen. This reporter allows us to distinguish autolysosomes from autophagosomes[214]. Under control condition, depletion of GRASP55, but not GRASP65, not only increased the number of RFP-GFP-LC3 puncta, but also increased the percentage of LC3 positive puncta in yellow (Fig. 3.3A). Similar results were obtained after amino acid starvation (Fig. 3.3B), whereas addition of BafA1, which neutralizes lysosome pH and inhibits autophagosome-lysosome fusion[215, 216], increased the number of the dual-color autophagosomes in all experimental conditions (Fig. 3.3). These results support our hypothesis that GRASP55 facilitates autophagosome-lysosome fusion upon amino acid starvation.

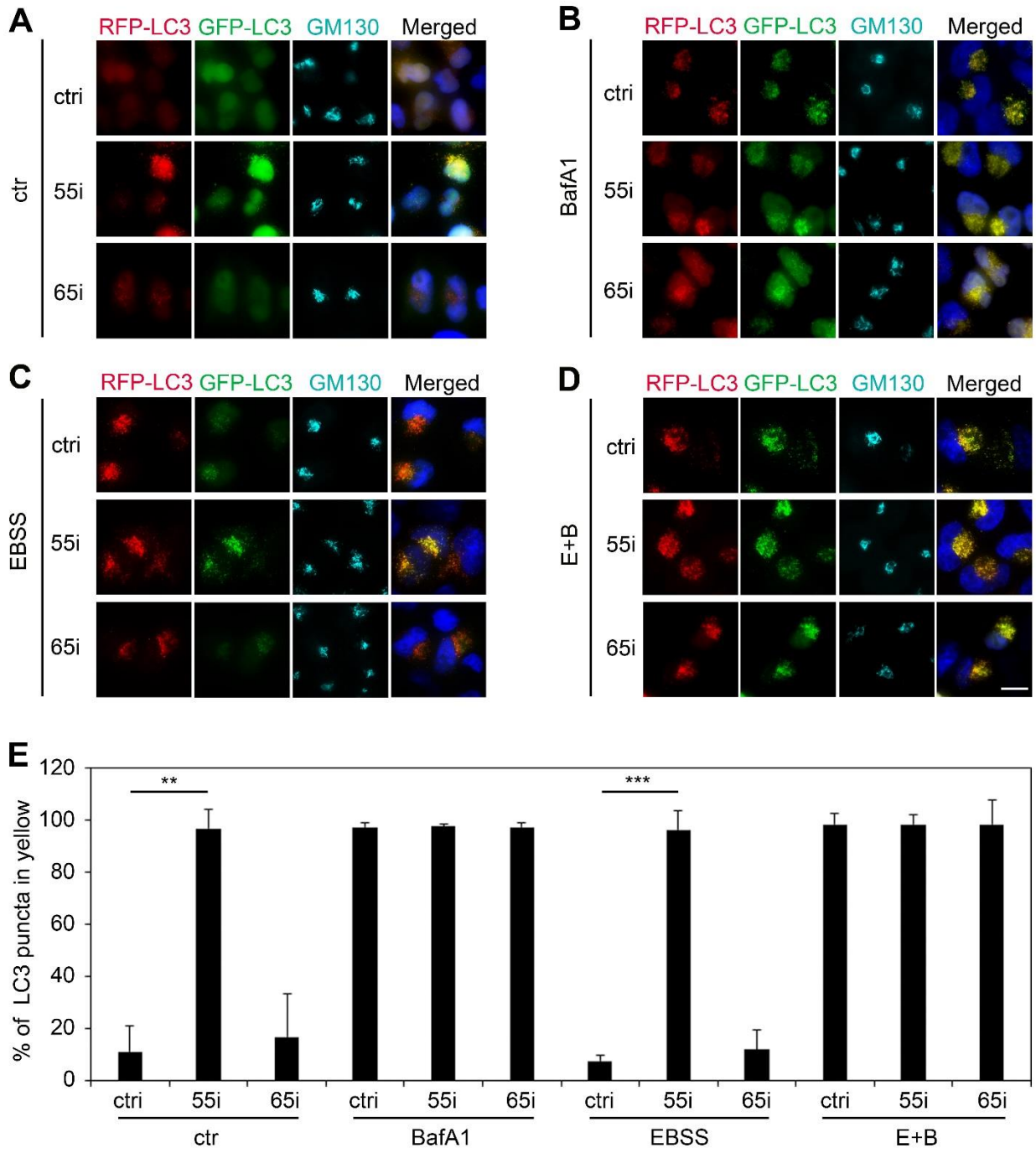

Figure 3.3. GRASP55 depletion results in autophagosome maturation defect. (A-D) GRASP55 depletion inhibits autophagosome maturation. RFP-GFP-LC3 expressing HeLa cells were transfected with non-specific (ctri), GRASP55 (55i) or GRASP65 RNAi (65i) for 72 h, treated with growth medium (control) (D), EBSS (E), or EBSS and 400 nM BafA1 (E+B) (F) for 4 h, and stained for GM130 and DNA. Scale bar is 20 μm. **(E)** Quantification of (A-D) for the percentage of LC3 puncta that were positive for both GFP and RFP (yellow).

GRASP55 is targeted to autophagosomes and lysosomes upon amino acid starvation

To further investigate how GRASP55 facilitates autophagosome maturation, we determined its subcellular localization under starvation conditions. Upon amino acid starvation, GRASP55 forms puncta outside of the Golgi region, which colocalized well with autophagosomes indicated by GFP-LC3 (Fig. 3.4A-B) or endogenous LC3 (Fig. 3.4C-D). In addition, GRASP55 in puncta also colocalized with LAMP2 (late endosomes and lysosomes), but not with EEA1 (early endosomes) or LAMP1 (late endosomes) (Fig. 3.4C-D). To determine whether GRASP55 is located at the surface or is engulfed into autophagosomes, we performed a protease K (PK) protection assay. In this experiment, we used LC3 as a marker. The membrane bound form of LC3, LC3-II, is localized both in the lumen and at the surface of autophagosomes, and thus, was partially protected from protease digestion. While its soluble form, LC3-I, as well as the cytoplasmic protein, actin, were both degraded. Like LC3-I, GRASP55 was also completely degraded, suggesting that GRASP55 localizes to the surface of the autophagosomes upon amino acid starvation (Fig. 3.4E). These results indicate that GRASP55 functions at the surface of autophagosomes rather than a substrate for autophagy mediated degradation.

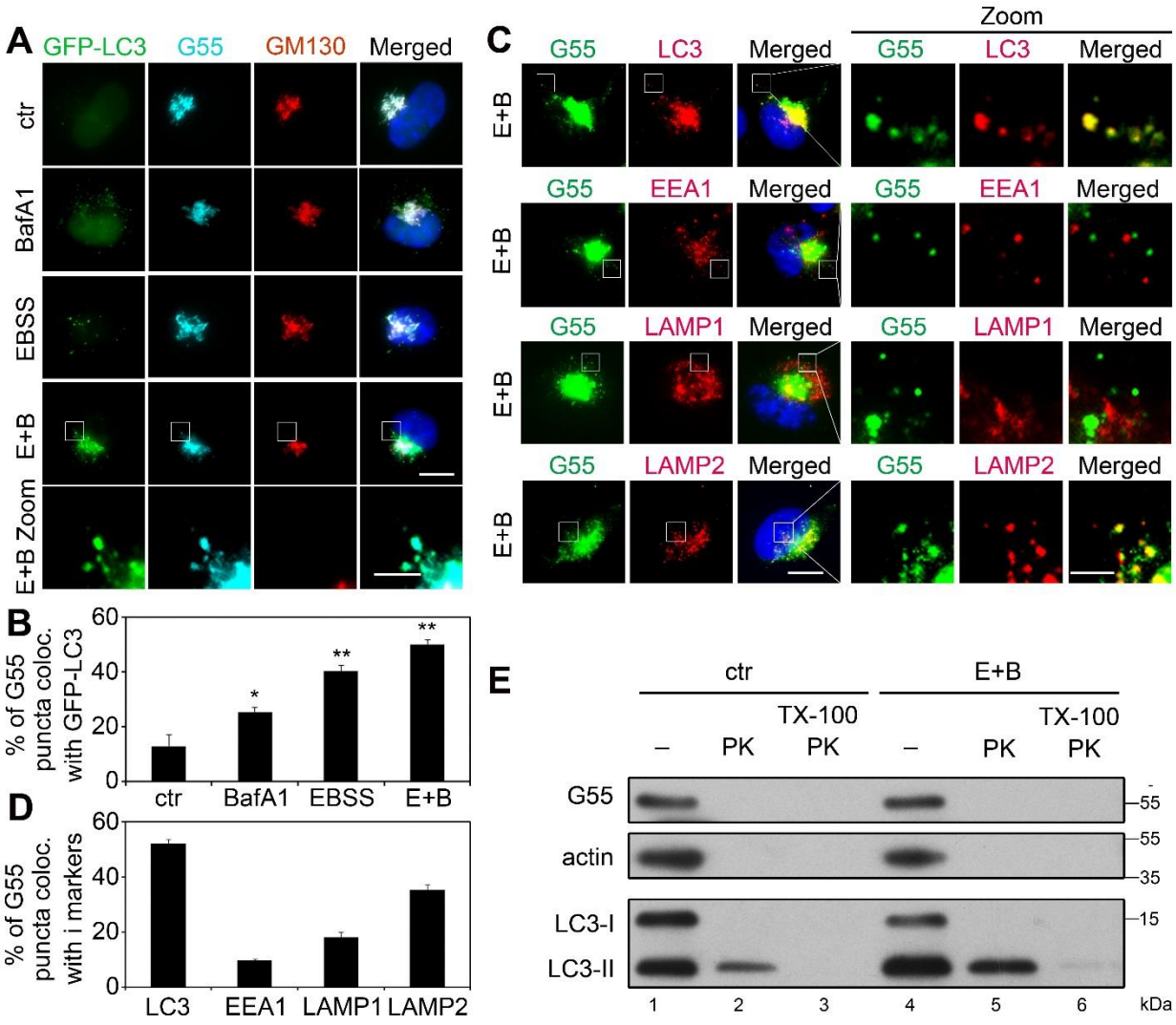

Figure 3.4. GRASP55 is localized to autophagosomes and lysosomes upon starvation. (A) GRASP55 colocalizes with GFP-LC3 upon starvation. GFP-LC3 HeLa cells were treated with growth medium (ctr), EBSS or EBSS and 400 nM BafA1 (E+B) for 4 h, stained for GRASP55 (G55), GM130, and DNA. The bottom row shows higher magnifications of the indicated area in the above row. Scale bar, 10 μm in the upper three rows and 3 μm in the bottom row, respectively. **(B)** Quantification of (A) for the percentage of GRASP55 puncta that colocalized with GFP-LC3. (**C**) GRASP55 colocalizes with LC3 and LAMP2 but not EEA1 or LAMP1 upon starvation. HeLa cells were treated with EBSS and 400 nM BafA1 (E+B) for 4 h, stained for GRASP55 (G55), LC3, EEA1, LAMP1, or LAMP2 and DNA as indicated. The three rows on the right are higher magnifications of the boxed area in the three rows on the left. Scale bars, 10 μm in the left rows and 3 μm in the right rows, respectively. **(D)** Quantification of (C) for the percentage of GRASP55 puncta that colocalized with LC3, EEA1, LAMP1 or LAMP2. **(E)** Western blot of the proteinase K protection assay. HeLa cells were treated with growth medium (ctr) or EBSS and 400 nM BafA1 (E+B) for 4 h, then the collected PNS were equally divided into three tubes, one left untreated, one was incubated with 2.5 μg/ml protease K only, and one was treated with both protease K and 1% TritonX-100 (TX-100) for 10 min, and all the samples were analyzed by Western blotting.

GRASP55 binds LC3 and LAMP2 to facilitate autophagosome-lysosome fusion

Since GRASP55 forms oligomers and functions as a membrane tether in Golgi stacking[13], we determined the possibility that it may function in a similar way to link autophagosomes and lysosomes and to facilitate their fusion. In support of this hypothesis, knockout of GRASP55 by CRISPR/Cas9[27] significantly reduced LC3-LAMP2 colocalization (Fig. 3.5A-B). To determine how GRASP55 is targeted to autophagosomes, we tested the possibility that GRASP55 might interact with LC3, as they colocalized upon amino acid starvation (Fig. 3.5A-D). Indeed, GRASP55, but not GFP, coimmunoprecipitated with LC3 under amino acid starvation (Fig. 3.5C). Given that GRASP55 is required for autophagosome-lysosome fusion (Fig. 3.2) and that GRASP55 puncta colocalize with LAMP2 (Fig. 3.5C-D), we also determined and confirmed GRASP55-LAMP2 interaction using a similar approach (Fig. 3.5D). Thus, GRASP55 interacts with LC3 on autophagosomes and LAMP2 on lysosomes, and functions as a tether for autophagosome-lysosome fusion.

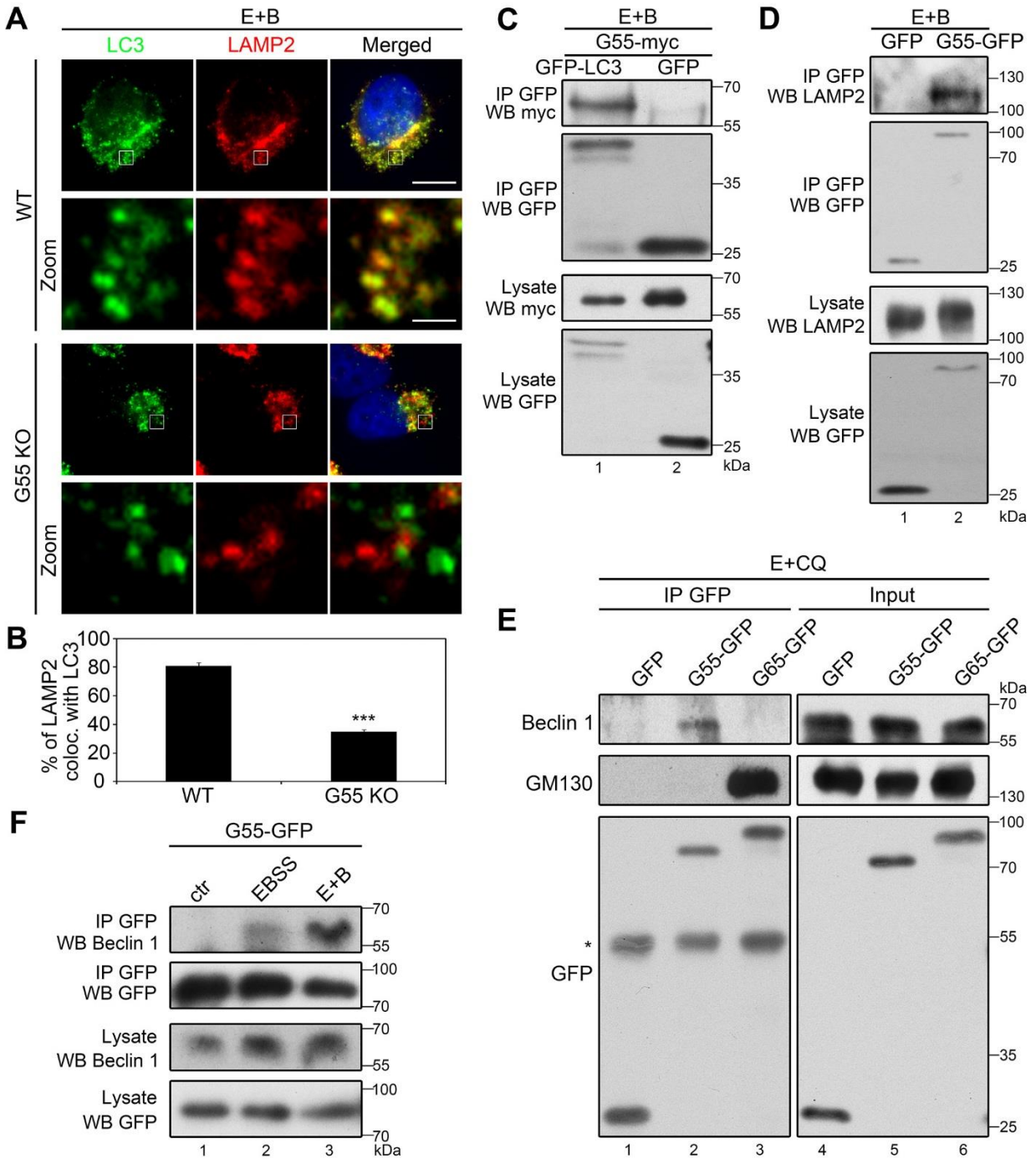

Figure 3.5. GRASP55 binds LC3 and LAMP2 to facilitate autophagosome-lysosome fusion. (A) GRASP55 knockout reduces LC3-LAMP2 colocalization. Wild type (WT) or GRASP55 knockout (G55KO) HeLa cells were treated with EBSS and 400 nM BafA1 (E+B) for 4 h, and stained for LC3, LAMP2, and DNA. The bottom row (Zoom) shows a higher magnification of the boxed area in the upper row. Scale bars, 10 μm in the upper row and 2 μm in the lower row, respectively. **(B)** Quantification of (A) for the percentage of LAMP2 puncta that colocalized with LC3 in wild type or GRASP55 knockout cells. **(C)** GRASP55 binds LC3. GFP-LC3 or GFP expressing HeLa cells were transfected with GRASP55-myc for 16 h, treated with

EBSS and 400 nM BafA1 (E+B) for 4 h, and immunoprecipitated with a GFP antibody followed by Western blotting. **(D)** GRASP55 binds LAMP2. GFP or GRASP55-GFP (G55-GFP) expressing HeLa cells were treated with EBSS and 400 nM BafA1 (E+B) for 4 h, and immunoprecipitated with a GFP antibody followed by Western blotting. **(E)** GRASP55 binds Beclin 1. GFP, G55-GFP or GRASP65-GFP (G65-GFP) expressing HeLa cells were treated with EBSS and 50 μM CQ for 4 h and immunoprecipitated with a GFP antibody followed by Western blotting for Beclin 1, GM130 and GFP. *, IgG heavy chain. **(F)** Amino acid starvation enhances GRASP55-Beclin 1 interaction. GRASP55-GFP transfected HeLa cells were treated with growth medium (ctr), EBSS, or EBSS and 400 nM BafA1 (E+B) for 4 h and immunoprecipitated with a GFP antibody followed by Western blotting for Beclin 1 and GFP.

GRASP55 binds PI3K complex II

Autophagosome-lysosome fusion involves multiple proteins, including Beclin 1[138]. Therefore, we determined the interaction between GRASP55 and Beclin 1 by coimmunoprecipitation. GRASP55 coprecipitated with Beclin 1 after amino acid starvation, while GRASP65 copurified with GM130, a known binding protein for GRASP65 (Fig. 3.5E). In comparison with control condition, amino acid starvation and BafA1 treatment significantly enhanced GRASP55 and Beclin 1 interaction (Fig. 3.5F).

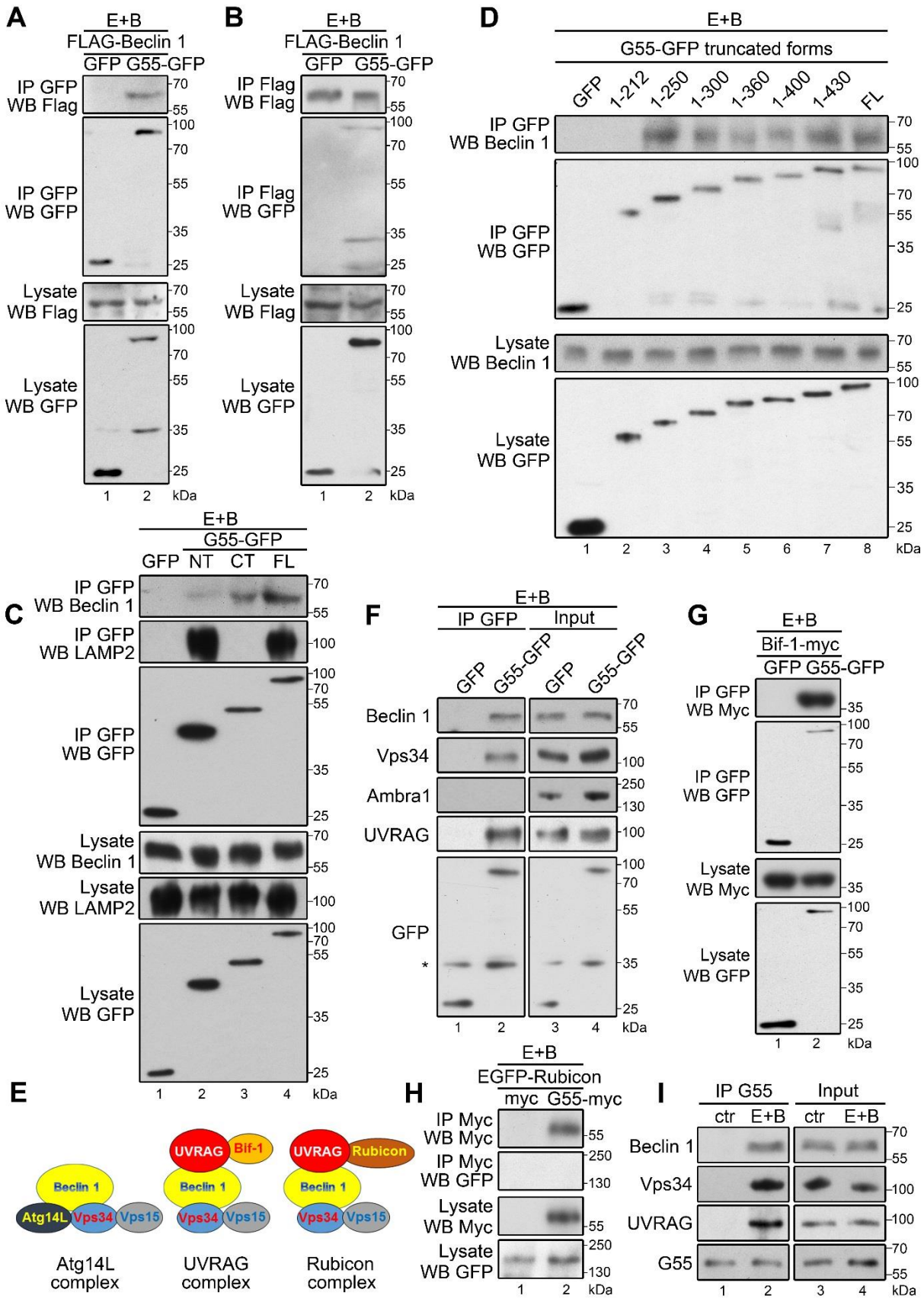
A
E+B
FLAG-Beclin 1
GFP G55-GFP
IP GFP WB Flag
IP GFP WB GFP
Lysate WB Flag
Lysate WB GFP
kDa
B
E+B
FLAG-Beclin 1
GFP G55-GFP
IP Flag WB Flag
IP Flag WB GFP
Lysate WB Flag
Lysate WB GFP
kDa
D
E+B
G55-GFP truncated forms
GFP 1-212 1-250 1-300 1-360 1-400 1-430 FL
IP GFP WB Beclin 1
IP GFP WB GFP
Lysate WB Beclin 1
Lysate WB GFP
kDa
C
E+B
G55-GFP
GFP NT CT FL
IP GFP WB Beclin 1
IP GFP WB LAMP2
IP GFP WB GFP
Lysate WB Beclin 1
Lysate WB LAMP2
Lysate WB GFP
kDa
F
E+B
IP GFP
Input
GFP G55-GFP GFP G55-GFP
Beclin 1
Vps34
Ambra1
UVRAG
GFP
*
kDa
G
E+B
Bif-1-myc
GFP G55-GFP
IP GFP WB Myc
IP GFP WB GFP
Lysate WB Myc
Lysate WB GFP
kDa
E
Beclin 1
Atg14L
Vps34
Vps15
Atg14L complex
UVRAG
Bif-1
Beclin 1
Vps34
Vps15
UVRAG complex
UVRAG
Rubicon
Beclin 1
Vps34
Vps15
Rubicon complex
H
E+B
EGFP-Rubicon
myc G55-myc
IP Myc WB Myc
IP Myc WB GFP
Lysate WB Myc
Lysate WB GFP
kDa
I
IP G55
Input
ctr E+B ctr E+B
Beclin 1
Vps34
UVRAG
G55
kDa

Figure 3.6. GRASP55 interacts with Beclin 1 and the PI3K UVRAG complex. (A-B) GRASP55 binds Beclin 1 under amino acid starvation condition. HeLa cells were transfected with GRASP55-GFP and Flag-Beclin 1 for 16 h, then treated with EBSS and 400 nM BafA1 (E+B) for 4 h and immunoprecipitated with a GFP antibody (A) or Flag antibody (B) followed by Western blotting. **(C-D)** C-terminus of GRASP55 binds Beclin 1. HeLa cells were transfected with GFP, or GFP-tagged the N-terminus (aa1-212, NT), C-terminus (aa213-452, CT), or full length (FL) GRASP55, or indicated truncation mutants for 16 h, treated with EBSS and 400 nM BafA1 (E+B) for 4 h and immunoprecipitated with a GFP antibody followed by Western blotting for GFP and Beclin 1. **(E)** Diagram showing the components in the three distinct PI3K complexes. **(F-H)** GRASP55 binds PI3K UVRAG complex. HeLa cells were transfected with indicated proteins, treated with EBSS and 400 nM BafA1 (E+B) for 4 h, and analyzed by immunoprecipitation and Western blotting. **(I)** Endogenously expressed GRASP55 interacts with the PI3K UVRAG complex. NRK cells were treated with growth medium (ctr) or EBSS and 400 nM BafA1 (E+B) for 4 h and immunoprecipitated with a GRASP55 antibody followed by Western blotting for Beclin 1, Vps34, UVRAG and GRASP55.

Beclin 1 is a major component of the phosphoinositide 3-kinase (PI3K) complex, and class II PI3K complex is known to mediate autophagosome-lysosome fusion by enriching phosphoinositide 3 (PI3P) at the interface[217]. As GRASP55 functions as a linker for autophagosome-lysosome fusion and also binds Beclin 1, this inspired us to further investigate the relationship between GRASP55 and Beclin 1 in autophagosome maturation. We first confirmed GRASP55-Beclin 1 interaction by reciprocal immunoprecipitations (Fig. 3.6A-B). We then mapped the domain structure of GRASP55 that interacts with Beclin 1 using our available GRASP55 truncation mutants; we found that the C-terminus of GRASP55 interacts with Beclin 1, likely through the aa 212-250 region (Fig. 3.6C-D). This is consistent with the domain structure and function of GRASP55 in Golgi stacking; while its N-terminal GRASP domain forms dimers and *trans*-oligomers, its C-terminal Serine/Proline Rich (SPR) domain is heavily phosphorylated during mitosis and regulates the oligomerization property of the N-terminal GRASP domain[13, 104]. In addition, the C-terminal SPR domain of GRASP65 is also known to interact with other proteins such as the actin elongation factor Mena[15].

There are three different PI3K complexes that play distinct roles in autophagy[217]. The Atg14L-Ambra1 complex generates PI3P on phagophore to recruit certain Atg components to expand the phagophore[218]; theUVRAG-Bif-1 generates PI3P at the interface between autophagosome and lysosome to facilitate autophagosome and lysosome fusion[138]; whereas the UVRAG-Rubicon complex[218] inhibits the role of PI3K complex II in autophagosome maturation (Fig 3.6E). In addition to Beclin 1, GRASP55 also coimmunoprecipitated with Vps34 (Fig. 3.6F), the core protein of all three PI3K complexes, indicating that GRASP55 interacts with the PI3K complexes rather than Beclin 1 alone. To distinguish which PI3K complex interacts with GRASP55, we performed coimmunoprecipitation of GRASP55 with different components of the PI3K complexes. A positive interaction was detected between GRASP55 and UVRAG, but not Ambra1 (Fig. 3.6F), indicating that GRASP55 interacts with UVRAG complex, but not with Atg14L complex. Further experiments showed that GRASP55 interacted with Bif-1, a component of UVRAG complex, but not Rubicon complex (Fig. 3.6G-H). Moreover, the interactions between GRASP55, Beclin 1, Vps34 and UVRAG were confirmed by coimmunoprecipitation of endogenous proteins (Fig. 3.6I). These results demonstrate that GRASP55 interacts with UVRAG complex, but not with Atg14L or Rubicon complex. Since UVRAG complex functions in autophagosome-lysosome fusion[138], these results support the function of GRASP55 in autophagosome maturation.

GRASP55 facilitates UVRAG complex assembly and membrane association

Since GRASP55 interacts with Beclin 1, UVRAG, Bif-1 and Vps34, four of the five components of UVARG complex, it is of our interest to investigate whether GRASP55 regulates its assembly. To do this we assessed the interactions between Beclin 1, UVRAG, Bif-1 and Vps34 in wild type and GRASP55 knockout cells. While GRASP55 knockout had no effect on Beclin 1 and Vps34 interaction, it significantly reduced the interaction of Beclin 1 with UVRAG and Bif-1 (Fig. 3.7A). In addition, GRASP55 knockout also reduced the protein level of UVRAG and Bif-1, suggesting a role of GRASP55 in stabilizing UVRAG complex. These results indicate that GRASP55 facilitates PI3K UVRAG complex assembly.

It has been previously shown that Beclin 1 is concentrated on the Golgi under control conditions[69, 70], which was confirmed in our study by fluorescence microscopy (Fig. 3.7B). Upon amino acid starvation, Beclin 1 was redistributed to puncta structures (autophagosomes) (Fig. 3.7B), which fits the idea that Beclin 1 shuttles between the Golgi and autophagosomes[69]. In GRASP55 knockout cells, Beclin 1 displayed a defused cytosolic pattern, suggesting that GRASP55 deletion reduced Beclin 1 membrane association (Fig. 3.7C). To verify this observation, we performed subcellular fractionation of wild type and GRASP55 knockout HeLa cells cultured under control and amino acid starvation conditions. We separated membranes from cytosol by ultracentrifugation of the postnuclear supernatant (PNS) and analyzed Beclin 1 level in each fraction by Western blot. Under growth condition, a large fraction of Beclin 1 was found in the membrane-bound fraction, while GRASP55 knockout significantly reduced the amount of Beclin 1 in the membrane fraction. Under amino acid starvation, more Beclin 1 is associated with membranes, while GRASP55 deletion reduced this amount (Fig. 3.7D-E). To confirm the

specificity, we exogenously expressed GRASP55 in GRASP55 knockout cells, which increased Beclin 1 membrane association under control condition (Fig. 3.7F-G). These results demonstrate that GRASP55 facilitates Beclin 1 membrane association.

It has been previously shown that GAPR1 interacts with Beclin 1 on the Golgi to inhibit autophagy[69], while our results suggested that GRASP55 binds Beclin 1 under starvation conditions to facilitate PI3K complex II formation and autophagosome maturation. To determine how GRASP55 and GAPR1 interplay to regulate Beclin 1 function, we determined the interactions between GRASP55, GAPR1, and Beclin1 under different conditions. Interestingly, our results showed that Beclin 1 preferentially binds GAPR1 under growth condition, while it interacts more with GRASP55 under starvation condition (Fig. 3.7H-I). These results indicate that both GRASP55 and GAPR1 are important regulators for Beclin 1, and a balance between these two proteins controls Beclin 1 localization and function at the Golgi or autophagosomes.

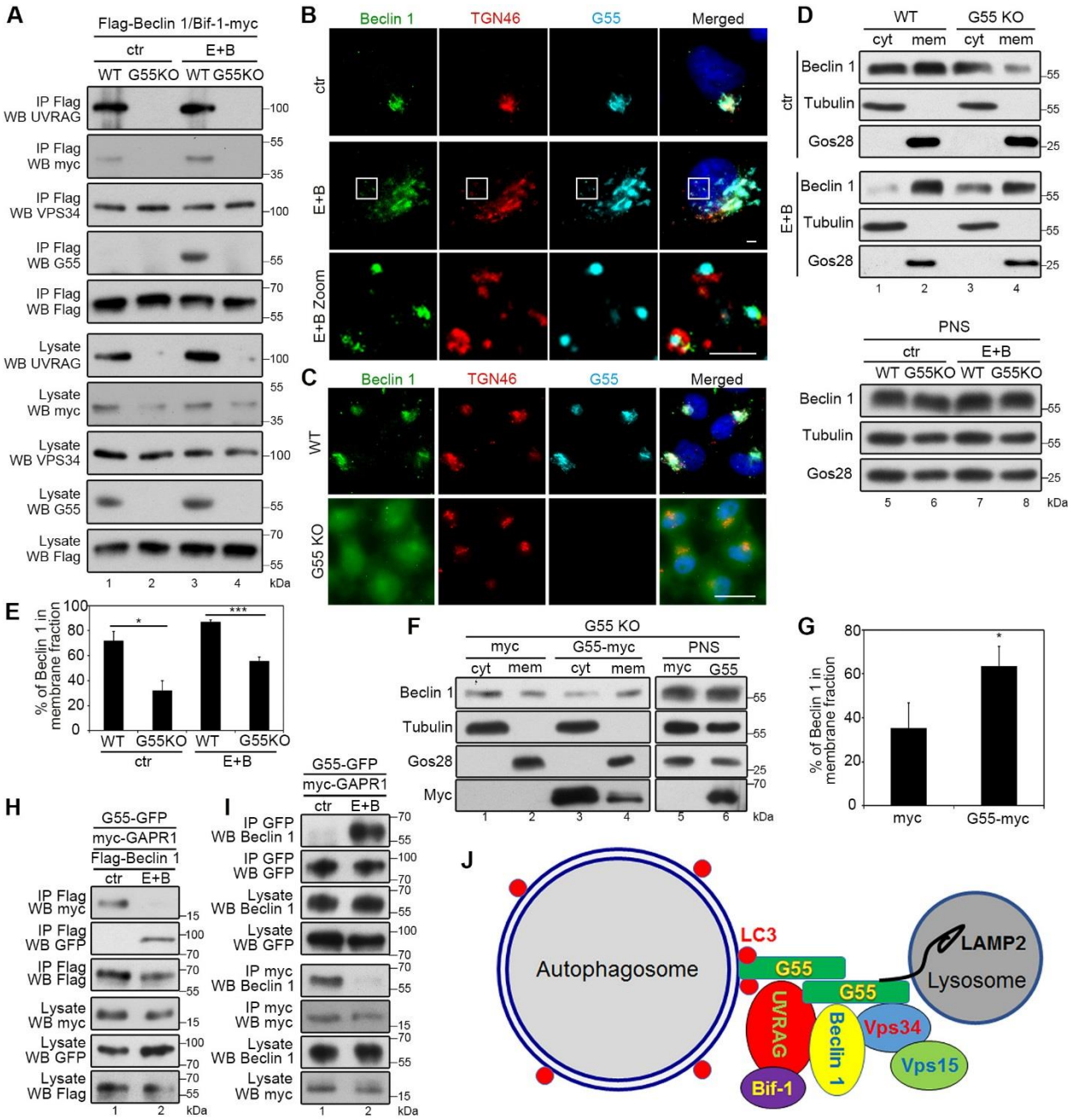

Figure 3.7. GRASP55 facilitates the assembly and membrane association of the PI3K UVRAG complex. (A) GRASP55 helps the assembly of the PI3K complex II. Wild type or GRASP55 knockout (G55KO) HeLa cells were transfected with Flag-Beclin 1 and Bif-1-myc for 16 h, treated with growth medium (ctr) or EBSS and 400 nM BafA1 (E+B) for 4 h and immunoprecipitated with a Flag antibody followed by Western blotting for UVRAG, Vps34, GRASP55, myc and Flag. **(B)** Beclin 1 partially relocates to autophagosomes upon amino acid starvation. HeLa cells were treated with growth medium (ctr) or EBSS and 400 nM BafA1 (E+B) for 4 h, stained for Beclin 1, TGN46, and DNA. Scale bar, 2 μm. **(C)** GRASP55 knockout reduces Beclin 1 membrane association. Wild type or GRASP55 knockout (G55 KO) cells were stained for Beclin 1, TGN46, and DNA. Scale bar, 20 μm. **(D)** GRASP55 enhances Beclin 1

membrane association. Wild type or GRASP55 knockout (G55 KO) HeLa cells treated with growth medium (ctr) or EBSS and 400 nM BafA1 (E+B) for 4 h, collected to generate PNS, which was separated into cytosol (cyt) and membranes (mem) by ultracentrifugation. All samples were analyzed by Western blotting for Beclin 1, tubulin and Gos28. **(E)** Quantitation of (D) for the percentage of Beclin 1 in the membrane fraction. **(F)** The reduced membrane association of Beclin 1 in GRASP55 knockout HeLa cells can be rescued by GRASP55 expression. GRASP55 knockout (G55 KO) HeLa cells were transfected with myc or GRASP55-myc (G55-myc) and analyzed as in (D). **(G)** Quantification of (F) for the percentage of Beclin 1 in membrane fractions. **(H-I)** GRASP55 competes with GAPR1 for Beclin 1 interaction. (H) HeLa cells were transfected with GRASP55-GFP, myc-GAPR1 and Flag-Beclin 1 for 16 h, treated with growth medium (ctr) or EBSS and 400 nM BafA1 (E+B) for 4 h, immunoprecipitated with a Flag antibody, and blotted for myc, GFP and Flag. (I) HeLa cells were transfected with GRASP55-GFP and myc-GAPR1 for 16 h, treated with growth medium (ctr) or EBSS and 400 nM BafA1 (E+B) for 4 h, immunoprecipitated with a GFP or myc antibody, and blotted for GFP, myc and Beclin 1. **(J)** Working model. Upon amino acid starvation, *trans*-Golgi derived vesicles translocate to autophagosomes, whereas GRASP55 binds LC3 and LAMP2 to mediate autophagosome-lysosome fusion. Additionally, it helps assembly of the class II PI3K complex at the interface of autophagosome and lysosome to facilitate autophagosome maturation.

Discussion

In this study, we have made an unexpected finding that the Golgi stacking protein GRASP55 contributes to autophagosome maturation by linking autophagosomes and late endosomes/lysosomes through the interaction with LC3 and LAMP2 and by facilitating PI3K complex II assembly (Fig. 3.7J). This is the first study that links autophagosome/lysosome membrane tethering and PI3K complex assembly together.

Upon amino acid starvation, the Golgi undergoes partial fragmentation in the order from *trans* to *cis*, and the derived Golgi fragments colocalize with autophagosomes (Fig. 3.1), consistent with the previous publications that Golgi plays a role in autophagosome formation[66, 67]. In a parallel study, we found that glucose starvation does not affect Golgi morphology as seen in amino acid starvation, but also causes GRASP55 retargeting to autophagosome-lysosome interface[230], suggesting that GRASP55 play an essential role in autophagosome maturation under different autophagy-inducing conditions. It has been shown that amino acid depletion directly inactivates mTOR, whereas glucose starvation activates c-Jun amino-terminal kinase (JNK), IκB kinase (IKK) and indirectly inhibits mTOR through AMPK[123]; the different signal pathways involved might have different downstream effectors on Golgi which modulate it differently. Another possible reason is that amino acid starvation directs Transcription factor EB (TFEB) translocation to nucleus to initiate transcription of a large amount of autophagy and lysosome related proteins[151] and the increased protein synthesis triggers increased Golgi transport to autophagosomes, which is comparably milder in glucose starvation. How the Golgi becomes fragmented upon amino acid starvation is not clear, but it is possible that losing GRASP55 in the Golgi by relocating to

autophagosomes (Fig. 3.4A-D) may count in part for the reason. Amino acid starvation only affects the subcellular localization of GRASP55, but not GRASP65, consistent with our previous results that GRASP55 knockout has a relatively more dramatic effect on the Golgi morphology than GRASP65 deletion[27]. However, given that GRASP55 level increases (Fig. 3.1D-E) and that only a relatively small proportion of GRASP55 is targeted to autophagosomes upon amino acid starvation (Fig. 3.4A-D), the amount of GRASP55 in the Golgi should not be significantly reduced. Thus, the exact mechanism leading to Golgi fragmentation induced by amino acid starvation remains unknown.

GRASP55 and GRASP65 were originally discovered as close homologues in mammalian cells with similar molecular features and functions in Golgi stacking[195]. Furthermore, unlike GRASP65, GRASP55 is targeted to autophagosomes upon amino acid starvation. Both GRASPs have been shown to be involved in Golgi stacking, ribbon linking, cell cycle progression, and unconventional secretion[18, 72, 195, 219], GRASP65 is also involved in spindle dynamics during mitosis[16] and apoptosis[17]; while GRASP55 also facilitates autophagy[19]. Consistent with the role of GRASP55 in autophagy, we found that depletion of GRASP55, but not GRASP65, resulted in autophagosome accumulation (Fig. 3.2A-C). These results indicate that these two GRASP proteins may have gained different functions during evolution in addition to their roles in Golgi structure formation.

Our study revealed a novel role for GRASP55 as a membrane tether in autophagy. Under both glucose starvation[230] or amino acid starvation (Fig 3.5), GRASP55 interacts with both LC3 on autophagosomes and LAMP2 on lysosomes, supporting that GRASP55 may function as a

membrane tether to facilitate autophagosome-lysosome fusion. GRASP55 depletion significantly reduced LC3-LAMP2 colocalization (Fig. 3.5A-B) and autophagic flux as indicated by the increased levels of the autophagy substrates LC3 and p62 (Fig. 3.2C). Previously, it has been shown that the HOPS tethering complex[137] is also involved in autophagosome-lysosome tethering. While the relationship between GRASP55 and the HOPS complex is a major future effort of our study, the significant reduction of LC3-LAMP2 colocalization in GRASP55 knockout cells indicates an important role for GRASP55 in autophagosome-lysosome tethering (Fig. 3.5A-B).

In addition to direct linking autophagosomes and lysosomes, GRASP55 also facilitates PI3K UVRAG complex assembly. First, under amino acid starvation condition, GRASP55 interacts with multiple components of PI3K complex II, including Beclin 1, VPS34, UVRAG, and Bif-1, but not with Ambra1, a protein specific for Atg14L complex, or Rubicon, a component in Rubicon complex (Fig. 3.7E-I). Second, GRASP55 facilitates Beclin 1's membrane association. Under growth condition, Beclin 1 is concentrated on the Golgi; upon amino acid starvation, it colocalizes with GRASP55 on autophagsomes (Fig. 3.7B). Depletion of GRASP55 significantly reduced Beclin 1 membrane association under both control and amino acid starvation conditions, which was rescued by exogenously expressed GRASP55 (Fig. 3.7D-G). In addition, GRASP55 depletion resulted in a reduced level of UVRAG and Bif-1, indicating that GRASP55 may stabilize UVRAG and Bif-1, although the mechanism is unknown so far. Given the important role of PI3K UVRAG complex in autophagosome-lysosome fusion, these results confirm that GRASP55 plays a critical role in autophagosome maturation.

The alternative interaction of Beclin 1 with GAPR-1 and GRASP55 is striking, as Beclin 1 almost conclusively interacts with GAPR-1 under growth condition and with GRASP55 after amino acid starvation. Given that both GRASP55 and Beclin 1 largely remains on the Golgi even after amino acid starvation (Fig. 3.67B), the mechanism that regulates Beclin 1 interaction with GAPR-1 and GRASP55 remains as a mystery. GAPR1 is known as a lipid raft-associated protein on the Golgi[68]. Through binding to Beclin 1, it works as a negative regulator by inhibiting Beclin 1 redistribution to non-Golgi vesicles that contribute to autophagosome formation[69]. Opposite to GAPR1, Beclin 1 preferably interacts with GRASP55 upon amino acid starvation, presumably the pool that is targeted to autophagosomes (Fig. 3.7B and H-I), indicating that GRASP55 functions as a positive regulator for Beclin 1 autophagosome localization and function in autophagosome maturation. In conclusion, our study uncovered a novel role for the Golgi stacking protein GRASP55 in autophagosome maturation.

Materials and Methods

Cell Lines

HeLa and normal rat kidney (NRK) cells were cultured in Dubelcco's modified Eagle's medium (DMEM) supplemented with 10% super calf serum (Gemini) and 100 units/ml penicillin-streptomycin at 37°C with 5% CO2. HeLa cells stably expressing GFP, GRASP55-GFP, or GRASP65-GFP were previously generated by Dr. Yi Xiang[13]. GRASP55 knockout HeLa cells were established previously[27], mRFP-GFP-LC3 expressing HeLa cells[220] were kindly provided by Dr. David Rubinsztein (University of Cambridge). GFP-LC3 HeLa cells were generated by transfection of GFP-LC3 plasmid into HeLa cells followed by fluorescence activated cell sorting (FACS) and 1 μg/ml puromycin selection of GFP-LC3 stable expressed HeLa cells.

Reagents, plasmids, and antibodies

All reagents were purchased from Sigma-Aldrich, Roche, Calbiochem and Fisher unless otherwise stated. Constructs for GFP-tagged full length GRASP65 and GRASP55 were previously described[13]. GRASP55 was constructed in pcDNA3.1/myc-His (-) A vector as GRASP55-myc. GFP-LC3 was purchased from Addgene deposited by Dr. Jayanta Debnath (University of California, San Francisco)[221] and was used to generate the GFP-LC3 expressing HeLa cells. pBICEP-CMV2 3xFLAG-Beclin 1 and GAPR-1-myc were kindly provided by Dr. Beth Levine (UT Southwestern)[69]. Myc-Bif-1 was kindly provided by Dr. Yoshinori Takahashi (Penn State University)[222]. pEGFP-Rubicon was purchased from Addgene deposited by Dr. Tamotsu Yoshimori (Osaka University)[223].

Antibodies used in this study include monoclonal antibodies against LAMP1 [H4A3, Developmental Studies Hybridoma Bank, (DSHB)], LAMP2 (H4B4, DSHB), GFP (ProteinTech), GM130 (Transduction lab), Tubulin (DSHB), Gos28 (Transduction lab), Vps34 (Santa Cruz), Ambra1 (Santa Cruz), UVRAG (Santa Cruz), Flag (M2, Sigma) and β-actin (Sigma); polyclonal antibodies against GRASP55 (ProteinTech), GRASP65 (UT465, Joachim Seemann, UT Southwestern), GM130 (N73, Joachim Seemann), TGN46 (Bio-Rad), GFP (Santa Cruz), LC3 (MBL), p62 (Sigma), Beclin 1 (ProteinTech and Santa Cruz), Atg9 (Genetex) and EEA1 (Santa Cruz). Myc antibody was kindly provided by Dr. David Sheff.

Cell Transfection

Polyethylenimine (PEI) was used for transient transfection of plasmids according to manufacturer's instructions (Polysciences, Inc.). Cells were used 16 h after transfection. For knockdown experiments, HeLa cells or mRFP-GFP-LC3 expressing cells were transfected with Lipofectamine RNAiMAX according to manufacturer's instructions (Invitrogen) and cells were used 72 h after transfection. Control non-specific RNAi was purchased from Ambion. Human GRASP55 and GRASP65 targeting sequences were previously described[13, 64].

Immunofluorescence microscopy

Immunofluorescence microscopy was performed as described previously[27, 207]. Briefly, HeLa cells were fixed in 3% paraformaldehyde (PFA) in Phosphate-buffered saline (PBS) for 15 min followed by quenching with 50 mM NH_4Cl in PBS for 10 min and permeabilized with 0.3% Triton-X-100 in PBS for 10 min. Permeabilized cells were blocked with 0.2% gelatin and 0.04% NaN_3 in PBS

(PGA) for 10 min followed by incubation with primary antibodies for 1 h at room temperature, washed with PBS, and incubated with secondary antibodies for 1 h at room temperature. Cells were stained for DNA with Hoechst (1 µg/ml) and coverslips were mounted with Moviol. Wide-field fluorescence microscopy was performed on a Zeiss Observer Z1 using a 63x/1.4 oil objective at a Z-step of 0.5 µm; shown are max projections. Axiovision software was used for image acquisition and analysis. For quantification, ImageJ was used to count the number of LC3 puncta and for the colocalization analysis following the user's manual.

Electron microscopy (EM)

EM was performed as previously described[207]. Briefly, cells were plated in 6-well dishes. After 24 hours of culture, cells were fixed with 2.5% glutaraldehyde and then processed for Epon embedding. Sections of 60 nm were mounted onto Formvar-coated nickel grids and double contrasted with 2% uranyl acetate for 5 minutes and 3% lead citrate for 5 minutes. Grids were imaged using a Philips CM100 Biotwin transmission EM. EM images were taken from the perinuclear region of the cell where Golgi membranes were normally concentrated. Golgi stacks and Golgi clusters were identified using morphological criteria and quantified using standard stereological techniques. They had to contain a nuclear profile with an intact nuclear envelope. A cisterna was defined as a membrane-bound structure in the Golgi cluster whose length is at least 4x its width, normally 20–30 nm in width and longer than 150 nm and a stack is the set of flattened, disk-shaped cisternae resembling a stack of plates[20].

Subcellular fractionation

Subcellular fractionation was performed as previously described[224]. Briefly, cells were washed with homogenization buffer (0.25 M sucrose, 1 mM EDTA, 1 mM magnesium acetate, 10 mM HEPES-KOH, pH 7.2, and protease inhibitors) and resuspended in 800 µl of homogenization buffer by pipetting. Cells were cracked with a ball bearing homogenizer as monitored under a microscope by trypan blue exclusion to a breakage of 75–80%. The homogenate was centrifuged for 10 min at 1000 x g, 4 °C. The post-nuclear supernatant (PNS) was isolated and subjected to ultracentrifugation in a TLA55 rotor at 120,000 x g for 1 h. The supernatant (cytosol) was collected, and the membranes in the pellet were resuspended in homogenization buffer. Equal volume fractions of the PNS, cytosol, and membrane fractions were analyzed by Western blotting.

Modulation of Autophagy

To induce autophagy and check Golgi phenotype under amino acid starvation condition, HeLa or NRK cells cultured in control medium were extensively washed with PBS and then treated with control medium (DMEM medium, 10% super calf serum and 100 units/ml penicillin-streptomycin), EBSS (prepared following Sigma E6132 recipe) EBSS supplemented with either 400 nM BafA1, 50 µM CQ, or 20 mM NH_4Cl, or control medium with 5 µM rapamycin for the indicated times.

Immunoprecipitation

To determine the interaction between GRASP55 and other proteins, HeLa cells transfected with indicated plasmids, or GFP, GRASP55-GFP, and GRASP65-GFP stable HeLa cells, were lysed in

20 mM Tris-HCl, pH 8.0, 150 mM NaCl, 0.5% NP40 and EDTA-free protease inhibitors (Roche). Protein A or Protein G beads were pre-incubated with indicated antibodies for 2 h at 4ºC. Lysate was cleared by centrifugation, and incubated with the pretreated beads overnight at 4ºC, subsequently washed and analyzed by Western blotting.

Protease K protection assay

Protease K protection assay was performed as previously described[225]. Briefly, HeLa cells were split onto 10 cm dishes and cultured in control medium. On the second day, one dish was treated with control medium and the other with EBSS and 400 nM BafA1 for 4 h. Cells were then collected and resuspended in HBS buffer (20 mM HEPES pH 7.4, 220 mM mannitol, 70 mM sucrose, 1 mM EDTA, protease inhibitor), homogenized with a ball-baring homogenizer and centrifuged to generate post-nuclear supernatant (PNS). Each PNS was equally divided into three tubes, one left untreated, one was incubated with 2.5 μg/ml Protease K (from 10 mg/ml stock), and the other was treated with both protease K and 1% Triton X-100 (from 20% stock) for 10 min on ice. Protease K was then inhibited by adding 1 mM PMSF (from 100 mM stock in isopropanol) and incubated on ice for 10 min. Proteins in each sample were precipitated by methanol/chloroform. The pellets were dissolved in sample buffer (50 mM Tris-HCl, pH 6.8, and 2% SDS) and analyzed by Western blotting.

Quantification and Statistical Analysis

All data represent the mean ± SD (standard deviation) of at least three independent experiments. At least 20 cells were counted for colocalization analysis or 300 cells for puncta number

measurement. A statistical analysis was conducted with two-tailed Student's t-test. Differences in means were considered statistically significant at $p < 0.05$. Significance levels are: *, $p<0.05$; **, $p<0.01$; ***, $p<0.001$. Analyses were performed using imageJ. Figures were assembled with Photoshop CS5.

Acknowledgement

We thank Dr. David Rubinsztein (University of Cambridge) for the mRFP-GFP-LC3 cell line; Dr. Beth Levine (UT Southwestern) for pBICEP-CMV2 3xFLAG-Beclin 1 and GAPR-1-myc constructs; Dr. Yoshinori Takahashi (Penn State University) for myc-Bif-1 construct; Joachim Seemann for GRASP65 and GM130 antibodies; Dr. John Schiefelbein (University of Michigan) for mannitol; and members of the Wang lab for helpful and constructive discussions and comments on the project. This work was supported in part by the National Institutes of Health (Grant GM112786), MCubed and the Fast Forward Protein Folding Disease Initiative of the University of Michigan to Y. Wang.

Abbreviations

AMPK, AMP kinase; AP1, adaptor protein complex 1; BafA1, Bafilomycin A1; Barkor, Beclin 1-associated autophagy-related key regulator; CQ, Chloroquine; EBSS, Earle's Balanced Salt Solution; EM, Electron microscopy; ER, endoplasmic reticulum; FACS, fluorescence activated cell sorting; FAK, focal adhesion kinase; FIP200, FAK-family interacting protein of 200 kDa; GFP, green fluorescent protein; GRASP55, Golgi Reassembly Stacking Protein of 55 kDa; GRASP65, Golgi Reassembly Stacking Protein of 65 kDa; IKK, IκB kinase; JNK, c-Jun amino-terminal kinase; LAMP1, lysosomal-associated membrane protein 1; LAMP2, Lysosomal-associated membrane protein 2; LC3, microtubule-associated protein light chain 3; mTOR, mammalian target of rapamycin; PAS, pre-autophagosomal structure; PBS, Phosphate-buffered saline; PEI, Polyethylenimine; PFA, paraformaldehyde; PI3K, phosphoinositide 3-kinase; PK, protease K; PNS, postnuclear supernatant; RFP, red fluorescent protein; TECPR1, Tectonin beta-propeller repeat-containing protein 1; TFEB, Transcription factor EB; SD, standard deviation; SNARE, SNAP (Soluble NSF(N-ethylmaleimide-sensitive factor) Attachment Protein Receptor; TGN, trans-Golgi network; ULK1/2, Unc-51 like autophagy activating kinase; UVRAG, UV radiation resistance-associated gene protein; VAMP7/8, vesicle associated membrane protein 7/8.

Chapter IV. Conclusion

The Golgi apparatus resides at the center of secretory pathway and its important functions in protein and lipid modifications, trafficking and sorting have been well documented. In conventional trafficking, Golgi receives almost the entire output of ER, where proteins and lipids undergo multiple modifications including glycosylation[2, 3], phosphorylation[4] and proteolytic cleavage[5]. Then these maturated cargo proteins and lipids are sorted and transported at TGN to plasma membrane, endosome, lysosomes and secretory granules to maintain cell homeostasis[6, 7]. In most eukaryotic cells, Golgi Apparatus is composed of stacks of tightly aligned flattened cisternae, which are laterally linked into ribbon like structure in the perinuclear region[8]. GRASP65 and GRASP55, which are localized to the *cis*- and *medial-trans*-cisternae respectively[10, 11], have been shown to play an essential role in Golgi structure formation. They form dimers and trans-oligomers to hold adjacent cisternae together to form a stack and link individual stack together through bridging proteins to form Golgi ribbons[12-15]. However, recently a GRASP65 knockout mouse has been reported, with only limited defects in the structure and function of the Golgi[105], which raise the concern if GRASP proteins play a role in Golgi stack formation or ribbon linking, if Golgi structure has a role in protein glycosylation or trafficking. Meanwhile, GRASP proteins have also been shown to be involved in spindle dynamics[16], apoptosis[17], unconventional secretion[18] and autophagy[19]. Although GRASP proteins, especially GRASP55 has been shown to be involved in autophagy and autophagy dependent unconventional secretion, the exact mechanism of how GRASP55 regulates autophagy progress is still a mystery. To resolve these

mysteries, my research focused mainly on these two questions: 1) How do GRASP proteins regulate Golgi structure and Golgi function, especially glycosylation or trafficking? 2) How does GRASP55 play a role in autophagy?

GRASP proteins' role in Golgi stacking and Golgi function

GRASP65 and GRASP55 are localized to the *cis*- and *medial*-/*trans*- cisternae, respectively. In interphase, they form homo-dimers and trans-oligomers from adjacent cisternae to hold Golgi cisternae together to form a stack[12, 13]. GRASP proteins are also implicated in Golgi ribbon formation by linking individual Golgi stacks, likely through bridging proteins[14, 15]. GRASP proteins interact with other Golgi structural proteins to regulate the morphology of the Golgi. For instance, GRASP65 interacts with GM130, while GRASP55 forms a complex with Golgin-45. Both GM130 and Golgin-45 are coiled-coil golgins involved in membrane tethering and Golgi structure formation[102, 193]. Thus, GRASPs and their interacting proteins are essential for Golgi structure formation[194-196].

In Chapter II, I have provided new evidence that GRASP55/65 play essential roles in Golgi structure formation, particularly in stacking. Consistent with our former papers using micro-injection of antibody[12] or siRNA[13, 107] against GRASP proteins, knockout of GRASP proteins also impairs Golgi cisternae stacking by reducing Golgi cisternae number per stack. These results demonstrate that GRASP55/65 function as Golgi stacking factors.

GRASP proteins also have essential roles in Golgi ribbon linking[15, 90]. In Chapter II, to our surprise, knocking out a single GRASP protein in either HeLa or HEK293 cells did not cause significant Golgi fragmentation. Recently, a homozygous GRASP65 knockout mice is generated, which had limited defects on Golgi structure and function[105]. One major concern of their study is that, their targeting vector knockout GRASP65 between exon 3 and 4 which still generates a shortened

mRNA and a 115 N-terminus amino acid peptide with the whole PDZ1 domain. As PDZ1 domain itself could oligomerize and form oligomers to stack Golgi cisternae, but lack of SPR domain to bind to Mena to link the Golgi cisternae, it makes sense that these homozygous GRASP65 knockout mice have a stacked but unlinked Golgi cisternae[106-108]. In Chapter II, we designed sgRNAs targeting exon 1 of GRASP55 and exon 2 of GRASP65, respectively. And the sequencing results of individual knockout clones which we picked indicate that all of the alleles generated by CRISPR have a frameshift mutation which leads to an early stop codon. And all of the peptides generated by these alleles are around 10 amino acids long which could not function as a PDZ1 domain. This ensures that no functional, truncated proteins are generated in the cell lines. Analysis of these cells with light and electron microscopy demonstrated that double-deletion of both GRASPs completely disrupted Golgi stack formation and ribbon linking. Based on these results and previous literature, we conclude that GRASP proteins are necessary for both Golgi stacking and ribbon linking.

However, we also have found out an interesting phenotype in knockout cell lines which we didn't see in our former papers. Single knockout of one GRASP protein would increase another GRASP protein's level and some other Golgins which function together with GRASP proteins in maintaining Golgi stack integrity. This phenotype indicates a compensation model that GRASP55 and GRASP65 not only play a complimentary role but also a compensational role in Golgi cisternal stacking. Taking account of the evolutional nature of GRASP55, which GRASP65 evolves from GRASP55, it is reasonable that they could compensate each other's role in Golgi stacking. However, the mechanism for the compensation of the other GRASP protein under GRASP

knockout condition remained unclear. Further biomedical experiments could be done to check GRASP mRNA level and protein half-life to clarify the underlying mechanism.

Moreover, in Chapter II, I also studied GRASP proteins' role in protein trafficking and glycosylation. I find that GRASP depletion accelerates protein trafficking and impairs accurate glycosylation of proteins and lipids on the cell surface. These results are consistent with our previous study with GRASP depletion by RNAi[64]. Our hypothesis based on these findings is that when Golgi cisternae are fully stacked, vesicles can only form and fuse at the peripheral area of the cisternae; once the cisternae are unstacked, more membrane area becomes accessible, thereby increasing the rate of vesicle budding and cargo transport through the Golgi[195, 200]. In support of this, an in vitro budding assay has consistently demonstrated that unstacking increased the rate of COPI vesicle formation from Golgi membranes[200]. Meanwhile, the proper stacked Golgi slows down trafficking but allows enough time for cargos to be modified by glycosylation enzymes in an order to achieve accurate glycosylation; while knockout of GRASP proteins mass up Golgi structure and results in glycosylation defect.

In conclusion, in Chapter II, we generate GRASP55 and GRASP65 single and double knockout HeLa and HEK cells. Take advantage of these cell lines, we confirm that GRASP55 or GRASP65 single knockout partially impairs Golgi cisternae formation whereas double knockout of two GRASP proteins totally disassemble the Golgi structure. And the partially or totally dispersed Golgi accelerates protein trafficking at the expense of inaccurate protein glycosylation and sorting. Golgi fragmentation phenotype is common in various disease and stress conditions and the

fragmented Golgi is involved in mediating multiple signal pathways in responding to these different conditions[201-206]. Generation of GRASP knockout cell lines could provide us a powerful tool to investigate the underlying mechanism of Golgi defect in these diseases and figure out the proper treatment.

GRASP55 mediates autophagosome-lysosome fusion

In Chapter III, I studied how Golgi responds to nutrition starvation and how GRASP55 plays a role in autophagy. Autophagy, as an important conserved process to maintain cellular homeostasis, has been studied for more than 50 years. However, the membrane source of autophagosome and different organelles' role in different process of autophagosome formation are still elusive. Different from yeast, in which PAS is assembled *de novo*[226], mammalian autophagosomes membrane come from different cellular organelles. Some studies have shown that autophagosomes are initiated at ER-mitochondria contact site and form a special isolation membrane structure called omegasome[154] and DFCP1, as a PI3P binding protein, translocates from ER and Golgi to omegasome which colocalize with LC3 and Atg5[210]. Meanwhile, it has been shown that Atg5 and LC3 are sequentially localized to outer membrane of mitochondria transiently, which suggests that a subdomain or an independent compartment of mitochondria is involved in autophagosome formation[227]. Plasma membrane, as another membrane source of autophagosome has also been studied that Atg16L1 localized at the plasma membrane via Atg16L1-AP2-clathrin interactions and important for the periods of increased autophagy[228]. Recently, Golgi has been shown to play an important role in autophagosome formation. It has been shown that the newly formed autophagosome colocalized on TGN and the formation of autophagosomes requires AP1 mediated

clathrin vesicles[67]. Atg9, which cycles between TGN and endosome, translocates to autophagosomes upon starvation in mammalian cells, but is restricted to TGN after ULK1 knockdown, suggesting that TGN is the PAS for autophagosome formation[229]. Consistent with these former studies, I have found that, under amino acid starvation, Golgi undergoes fragmentation in an order from the *trans* to *cis* cisternae, and these Golgi derived clusters colocalize with autophagosomes. EM pictures of starved HeLa cells show that Golgi cisternae per stack are not changed, but the cisternae length is significantly reduced; moreover, Golgi is close to forming autophagosomes and provides membrane vesicles for autophagosome elongation. Above all, we provide new evidence that Golgi contributes to autophagosome formation.

While basal autophagy is important for cellular homeostasis, autophagy could also be induced by multiple cellular stress or nutrient starvation. However, different autophagy induction methods have different effect on Golgi morphology. For instance, amino acid starvation induces Golgi derived clusters formation and colocalize with autophagosomes shown in this and other studies[67] while glucose starvation has no apparent effect on Golgi[230]. One possible explanation is that amino acid depletion directly inactivates mTOR, whereas glucose starvation activates c-Jun amino-terminal kinase (JNK), IκB kinase (IKK) and indirectly inhibits mTOR through AMPK[231]; the different signal pathway involved might have different downstream effectors on Golgi which modulate it differently. Another possible reason is that amino acid starvation directs TFEB translocation to nucleus to initiate transcription of large amount of autophagy and lysosome related proteins[151] and the increased amount of protein synthesis triggers Golgi vesicle transportation to autophagosomes directly, which is comparably difficult to find out in mild autophagy induction method such as glucose starvation. To figure out the exact mechanism of these different effects on

Golgi induced by different nutrient starvation methods will be interesting future topic of Chapter III.

GRASP55 and GRASP65 are two homologous peripheral membrane proteins, which are localized to the *cis*- and *medial-trans* cisternae, respectively. However, GRASP55 and GRASP65 seem to have different roles in autophagy. GRASP55 depletion increased accumulation of autophagosomes by impairing autophagosome-lysosome fusion; on the other hand, GRASP65 depletion largely reduced autophagosome number per cell upon starvation. Moreover, GRASP65 got phosphorylated upon amino acid starvation but not GRASP55 (data not shown). Our former GRASP-CRISPR knockout paper had also shown that knockout of GRASP55 showed more dramatic fragmentation phenotype of Golgi compared to GRASP65[27]. In addition, GRASP65 has been shown to be involved in enzyme distribution[90], cell cycle progression[16], and apoptosis[17]; while GRASP55 mediates unconventional secretion[18, 92]. Taken together, it will not be our surprise to hypothesis that GRASP65 has a completely different role in autophagy compared to GRASP55 which we are interested to figure it out.

In Chapter III, I have revealed a novel role for GRASP55 as a membrane tether in autophagy. Similar to glucose starvation[230], upon amino acid starvation, GRASP55 binds to both LC3 and LAMP2, while depletion of GRASP55 significantly reduce LC3-LAMP2 colocalization which indicates GRASP55's tethering role in autophagosome-lysosome fusion. Other than GRASP55, Rab7 GTPase and its effector[166, 232], the HOPS tethering complex[137], and the STX17-SNAP29-VAMP7/8 SNARE complex[135], have also been shown to mediate autophagosome-lysosome fusion;

this triggered us to hypothesis that GRASP55, through binding to LC3 and LAMP2, pulls autophagosomes and lysosomes to close proximity, while Rab7, HOPS and the SNARE complexes promote the membrane fusion process. One of the future directions of Chapter III is to understand how GRASP55 interacts with these other players to coordinate this process.

Beclin 1 has been shown to have a membrane association domain, evolutionarily conserved domain (ECD), which controls autophagosome size and number in yeast[219, 233]. In this study, we have found that GRASP55 is also involved in Beclin 1 membrane association. In growth condition, Beclin 1 largely localizes on Golgi; it leaves Golgi upon starvation, which shows the same pattern as GRASP55. Moreover, depletion of GRASP55 significantly reduces Beclin 1 membrane association which could be rescued by over-expression of GRASP55, further confirming GRASP55's role in Beclin 1 membrane association. How GRASP55 interacts with Beclin 1, if GRASP55 could bind to ECD domain of Beclin 1 still remain unclear and is an interesting future direction. Beclin 1 and Vps34 are core proteins of three distinct PI3K complexes, in which Atg14L-Ambra1 complex works in phagophore elongation, UVRAG-Bif1 complex works in autophagosome-lysosome fusion, while UVRAG-Rubicon complex inhibits it[217]. In Chapter III, I have found that GRASP55 specifically interacts with PI3K complex II and plays a necessary role in complex assembly and stability. How this specificity is achieved, how GRASP55 mediates PI3K complex assembly and stability, if any other Golgi protein or autophagy protein is also involved in this process are all interesting questions that we'd like to answer in future studies.

Another main finding of Chapter III is the alternative interaction of Beclin 1 with GAPR-1 and GRASP55, as Beclin 1 almost conclusively interacts with GAPR-1 under growth condition and with GRASP55 upon amino acid starvation. Given that both GRASP55 and Beclin 1 largely remains on the Golgi even after amino acid starvation, the mechanism that regulates Beclin 1 interaction with GAPR-1 and GRASP55 remains as a mystery. GAPR1 is known as a lipid raft-associated protein on the Golgi[68]. Through binding to Beclin 1, it works as a negative regulator by inhibiting Beclin 1 redistribution to non-Golgi vesicles that contribute to autophagosome formation[69]. Opposite to GAPR1, Beclin 1 preferably interacts with GRASP55 upon amino acid starvation, presumably through the pool that is targeted to autophagosomes, indicating that GRASP55 functions as a positive regulator for Beclin 1 autophagosome localization and function in autophagosome maturation.

These findings help us to establish the model of autophagosome-lysosome fusion with GRASP55 as an important player (Figure 4.1). PE-conjugated LC3 and two SNARE proteins, STX17 and SNAP29 are localized on autophagosomes; while Rab7, LAMP2 and VAMP8 are localized on lysosomes[140]. At the beginning of fusion, GRASP55 interacts with LC3 and LAMP2[230], and works as a linker to keep autophagosome and lysosome in close proximity; meanwhile PI3K UVRAG complex is recruited to the interface between autophagosome and lysosome (Chapter III). Then UVRAG binds to VPS16, a subunit of HOPS which stimulates Rab7 GTPase activity[184]. HOPS subunits VPS39 and VPS41 also interact with Rab7 effectors PLEKHM1 and RILP, respectively[234]. Upon recruitment to the interface between autophagosome and lysosome, HOPS interacts with STX17 and help position and align SNAREs to promote its assembly[172, 235]. Another tethering factor, EPG5 is recruited to the interface by interaction with Rab7, VAMP8 and LC3[236]. EPG5[168],

as well as another tethering factor, ATG14L[237], binds to assembled STX17-SNAP29 complex to facilitate and stabilize the assembly of STX17-SNAP29-VAMP8 *trans*-SNARE complex.

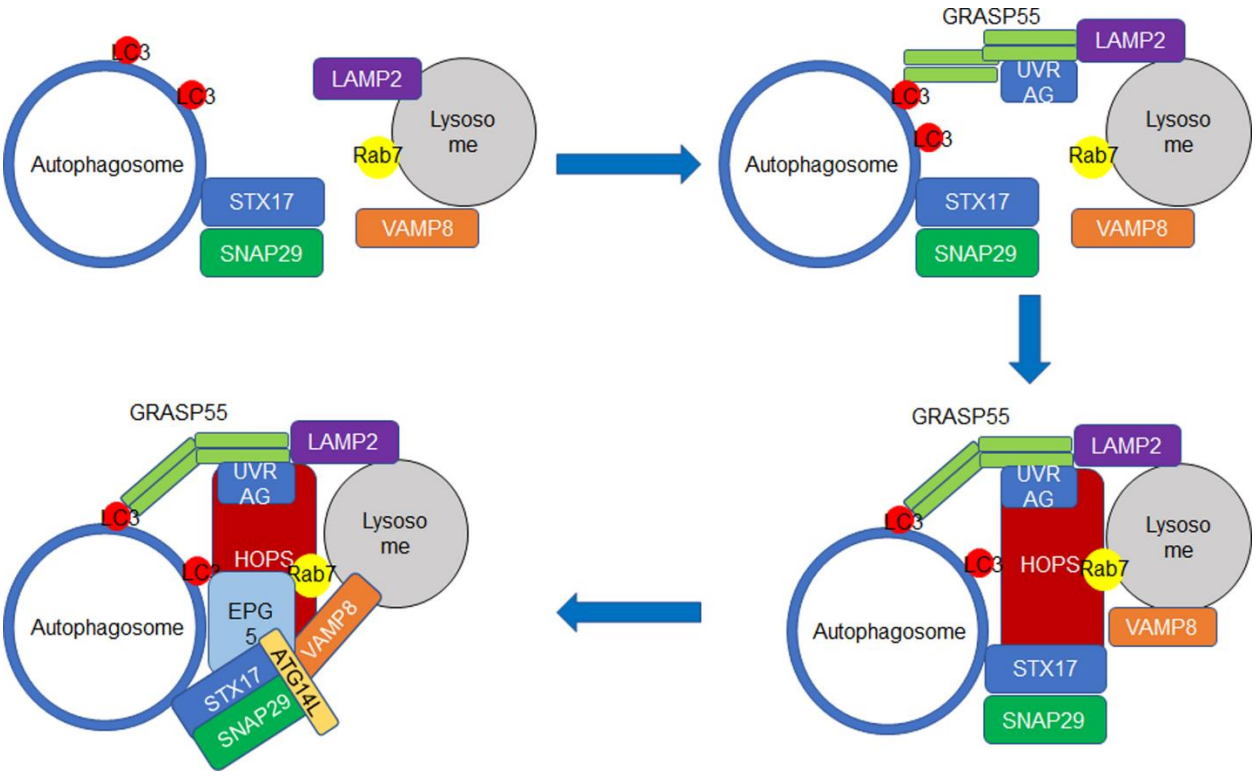

Figure 4.1 Autophagosome-lysosome fusion model. At the end of autophagy process, GRASP55 interacts with LC3 and LAMP2, and works as a linker to keep autophagosome and lysosome in close proximity; meanwhile PI3K UVRAG complex is recruited to the interface between autophagosome and lysosome. Then UVRAG binds to HOPS, which also interacts with Rab7 effectors PLEKHM1 and RILP. Upon recruitment, HOPS interacts with STX17 to promote SNARE assembly. Another tethering factor, EPG5 is recruited to the interface by interaction with Rab7, VAMP8 and LC3. EPG5 and another tethering factor, ATG14L, bind to assembled STX17-SNAP29 complex to facilitate and stabilize the assembly of STX17-SNAP29-VAMP8 trans-SNARE complex.

In conclusion, in Chapter III, we have found that, upon amino acid starvation, Golgi derived membrane clusters colocalize with autophagosomes and contribute to autophagosome elongation

and formation, when GRASP55 is recruited to autophagosomes and subsequently interacts with LC3 and LAMP2. Meanwhile, it helps assembly of PI3K complex II at the interface of autophagosome and lysosome to facilitate autophagosome maturation. This study proposes a novel target for modulating autophagy and would be beneficial for treatment of autophagy related diseases.

References

1. Farquhar MG, Palade GE. The Golgi apparatus: 100 years of progress and controversy. Trends in cell biology 1998; 8:2-10.
2. Kornfeld R, Kornfeld S. Assembly of asparagine-linked oligosaccharides. Ann Rev Biochem 1985; 54:631-64.
3. Zhang X, Wang Y. Glycosylation Quality Control by the Golgi Structure. J Mol Biol 2016; 428:3183-93.
4. Wang Y, Taguchi T, Warren G. Purification of Rat Liver Golgi Stacks. In: Celis J, ed. Cell Biology: A Laboratory Handbook, 3rd Edition. San Diego: Elsevier Science (USA), 2006:33-9.
5. Kayed R, Head E, Thompson JL, McIntire TM, Milton SC, Cotman CW, et al. Common structure of soluble amyloid oligomers implies common mechanism of pathogenesis. Science 2003; 300:486-9.
6. Bravo DA, Gleason JB, Sanchez RI, Roth RA, Fuller RS. Accurate and efficient cleavage of the human insulin proreceptor by the human proprotein-processing protease furin. Characterization and kinetic parameters using the purified, secreted soluble protease expressed by a recombinant baculovirus. Journal of Biological Chemistry 1994; 269:25830-7.
7. Shorter J, Lindquist S. Hsp104 catalyzes formation and elimination of self-replicating Sup35 prion conformers. Science 2004; 304:1793-7.

8. Ladinsky MS, Mastronarde DN, McIntosh JR, Howell KE, Staehelin LA. Golgi structure in three dimensions: functional insights from the normal rat kidney cell. J Cell Biol 1999; 144:1135-49.
9. Rambourg A, Clermont Y, Ovtracht L, Kepes F. Three-dimensional structure of tubular networks, presumably Golgi in nature, in various yeast strains: a comparative study. Anat Rec 1995; 243:283-93.
10. Barr FA, Puype M, Vandekerckhove J, Warren G. GRASP65, a protein involved in the stacking of Golgi cisternae. Cell 1997; 91:253-62.
11. Shorter J, Watson R, Giannakou ME, Clarke M, Warren G, Barr FA. GRASP55, a second mammalian GRASP protein involved in the stacking of Golgi cisternae in a cell-free system. The EMBO journal 1999; 18:4949-60.
12. Wang Y, Seemann J, Pypaert M, Shorter J, Warren G. A direct role for GRASP65 as a mitotically regulated Golgi stacking factor. The EMBO journal 2003; 22:3279-90.
13. Xiang Y, Wang Y. GRASP55 and GRASP65 play complementary and essential roles in Golgi cisternal stacking. J Cell Biol 2010; 188:237-51.
14. Feinstein TN, Linstedt AD. GRASP55 Regulates Golgi Ribbon Formation. Molecular biology of the cell 2008; 19:2696-707.
15. Tang D, Zhang X, Huang S, Yuan H, Li J, Wang Y. Mena-GRASP65 interaction couples actin polymerization to Golgi ribbon linking. Molecular biology of the cell 2016; 27:137-52.
16. Sutterlin C, Polishchuk R, Pecot M, Malhotra V. The Golgi-associated protein GRASP65 regulates spindle dynamics and is essential for cell division. Molecular biology of the cell 2005; 16:3211-22.

17. Cheng JP, Betin VM, Weir H, Shelmani GM, Moss DK, Lane JD. Caspase cleavage of the Golgi stacking factor GRASP65 is required for Fas/CD95-mediated apoptosis. Cell Death Dis 2010; 1:e82.

18. Gee HY, Noh SH, Tang BL, Kim KH, Lee MG. Rescue of DeltaF508-CFTR Trafficking via a GRASP-Dependent Unconventional Secretion Pathway. Cell 2011; 146:746-60.

19. Dupont N, Jiang S, Pilli M, Ornatowski W, Bhattacharya D, Deretic V. Autophagy-based unconventional secretory pathway for extracellular delivery of IL-1beta. The EMBO journal 2011; 30:4701-11.

20. Lucocq JM, Berger EG, Warren G. Mitotic Golgi fragments in HeLa cells and their role in the reassembly pathway. J Cell Biol 1989; 109:463-74.

21. Shorter J, Warren G. Golgi architecture and inheritance. Annu Rev Cell Dev Biol 2002; 18:379-420.

22. Rabouille C, Hui N, Hunte F, Kieckbusch R, Berger EG, Warren G, et al. Mapping the distribution of Golgi enzymes involved in the construction of complex oligosaccharides. Journal of cell science 1995; 108:1617-27.

23. Möbius W, Donselaar EV, Ohno‐Iwashita Y, Shimada Y, Heijnen HFG, Slot JW, et al. Recycling Compartments and the Internal Vesicles of Multivesicular Bodies Harbor Most of the Cholesterol Found in the Endocytic Pathway. Traffic 2003; 4:222-31.

24. Mironov AA, Pavelka M. The Golgi apparatus : state of the art 110 years after Camillo Golgi's discovery. Wien: Springer, 2010.

25. Losev E, Reinke CA, Jellen J, Strongin DE, Bevis BJ, Glick BS. Golgi maturation visualized in living yeast. Nature 2006; 441:1002-6.

26. Langhans M, Hawes C, Hillmer S, Hummel E, Robinson DG. Golgi Regeneration after Brefeldin A Treatment in BY-2 Cells Entails Stack Enlargement and Cisternal Growth followed by Division. Plant Physiology 2007; 145:527-38.
27. Bekier ME, 2nd, Wang L, Li J, Huang H, Tang D, Zhang X, et al. Knockout of the Golgi stacking proteins GRASP55 and GRASP65 impairs Golgi structure and function. Molecular biology of the cell 2017; 28:2833-42.
28. Koga D, Ushiki T. Three-dimensional ultrastructure of the Golgi apparatus in different cells: high-resolution scanning electron microscopy of osmium-macerated tissues. Archives of Histology and Cytology 2006; 69:357-74.
29. Hawes C. Cell biology of the plant Golgi apparatus. New Phytol 2005; 165:29-44.
30. Diao A, Rahman D, Pappin DJ, Lucocq J, Lowe M. The coiled-coil membrane protein golgin-84 is a novel rab effector required for Golgi ribbon formation. J Cell Biol 2003; 160:201-12.
31. Yadav S, Puri S, Linstedt AD. A primary role for Golgi positioning in directed secretion, cell polarity, and wound healing. Molecular biology of the cell 2009; 20:1728-36.
32. Sohda M, Misumi Y, Yoshimura S-i, Nakamura N, Fusano T, Sakisaka S, et al. Depletion of vesicle-tethering factor p115 causes mini-stacked Golgi fragments with delayed protein transport. Biochemical and Biophysical Research Communications 2005; 338:1268-74.
33. Sutterlin C, Colanzi A. The Golgi and the centrosome: building a functional partnership. J Cell Biol 2010; 188:621-8.
34. Egea G, Lazaro-Dieguez F, Vilella M. Actin dynamics at the Golgi complex in mammalian cells. Curr Opin Cell Biol 2006.

35. Bentley M, Liang Y, Mullen K, Xu D, Sztul E, Hay JC. SNARE Status Regulates Tether Recruitment and Function in Homotypic COPII Vesicle Fusion. Journal of Biological Chemistry 2006; 281:38825-33.

36. Staehelin LA, Kang B-H. Nanoscale Architecture of Endoplasmic Reticulum Export Sites and of Golgi Membranes as Determined by Electron Tomography. Plant Physiology 2008; 147:1454-68.

37. Hidalgo Carcedo C, Bonazzi M, Spano S, Turacchio G, Colanzi A, Luini A, et al. Mitotic Golgi partitioning is driven by the membrane-fissioning protein CtBP3/BARS. Science 2004; 305:93-6.

38. Colanzi A, Deerinck TJ, Ellisman MH, Malhotra V. A specific activation of the mitogen-activated protein kinase kinase 1 (MEK1) is required for Golgi fragmentation during mitosis. J Cell Biol 2000; 149:331-9.

39. Wei JH, Seemann J. Mitotic division of the mammalian Golgi apparatus. Semin Cell Dev Biol 2009; 20:810-6.

40. Tang D, Xiang Y, De Renzis S, Rink J, Zheng G, Zerial M, et al. The ubiquitin ligase HACE1 regulates Golgi membrane dynamics during the cell cycle. Nat Commun 2011; 2:501.

41. Huang S, Tang D, Wang Y. Monoubiquitination of syntaxin 5 regulates Golgi membrane dynamics during the cell cycle. Developmental cell 2016; 38:73-85.

42. Tang D, Mar K, Warren G, Wang Y. Molecular mechanism of mitotic Golgi disassembly and reassembly revealed by a defined reconstitution assay. J Biol Chem 2008; 283:6085-94.

43. Huang S, Wang Y. Golgi structure formation, function, and post-translational modifications in mammalian cells. F1000Res 2017; 6:2050.

44. Lodish UH. Molecular Cell Biology. W.H. Freeman, 2016.

45. Barlowe C, Schekman R. SEC12 encodes a guanine-nucleotide-exchange factor essential for transport vesicle budding from the ER. Nature 1993; 365:347.

46. Huang M, Weissman JT, Béraud-Dufour S, Luan P, Wang C, Chen W, et al. Crystal structure of Sar1-GDP at 1.7 Å resolution and the role of the NH(2) terminus in ER export. The Journal of Cell Biology 2001; 155:937-48.

47. Futai E, Hamamoto S, Orci L, Schekman R. GTP/GDP exchange by Sec12p enables COPII vesicle bud formation on synthetic liposomes. The EMBO Journal 2004; 23:4146-55.

48. Lee MCS, Miller EA, Goldberg J, Orci L, Schekman R. BI-DIRECTIONAL PROTEIN TRANSPORT BETWEEN THE ER AND GOLGI. Annual Review of Cell and Developmental Biology 2004; 20:87-123.

49. Stephens DJ, Pepperkok R. Illuminating the secretory pathway: when do we need vesicles? Journal of Cell Science 2001; 114:1053-9.

50. Alvarez C, Fujita H, Hubbard A, Sztul E. ER to golgi transport. Requirement for p115 at a pre-golgi vtc stage [In Process Citation]. J Cell Biol 1999; 147:1205-22.

51. Allan BB, Moyer BD, Balch WE. Rab1 recruitment of p115 into a cis-SNARE complex: programming budding COPII vesicles for fusion. Science 2000; 289:444-8.

52. Seemann J, Jokitalo EJ, Warren G. The role of the tethering proteins p115 and GM130 in transport through the Golgi apparatus in vivo. Molecular biology of the cell 2000; 11:635-45.

53. Hsu VW, Yang J-S. Mechanisms of COPI vesicle formation. FEBS letters 2009; 583:3758-63.

54. Lee SY, Yang JS, Hong W, Premont RT, Hsu VW. ARFGAP1 plays a central role in coupling COPI cargo sorting with vesicle formation. J Cell Biol 2005; 168:281-90.

55. Glick BS, Nakano A. Membrane traffic within the Golgi apparatus. Annu Rev Cell Dev Biol 2009; 25:113-32.

56. Bonfanti L, Mironov AA, Jr., Martinez-Menarguez JA, Martella O, Fusella A, Baldassarre M, et al. Procollagen traverses the Golgi stack without leaving the lumen of cisternae: evidence for cisternal maturation. Cell 1998; 95:993-1003.

57. Mironov AA, Beznoussenko GV, Nicoziani P, Martella O, Trucco A, Kweon H-S, et al. Small cargo proteins and large aggregates can traverse the Golgi by a common mechanism without leaving the lumen of cisternae. The Journal of Cell Biology 2001; 155:1225-38.

58. Orci L, Stamnes M, Ravazzola M, Amherdt M, Perrelet A, Sollner TH, et al. Bidirectional transport by distinct populations of COPI-coated vesicles. Cell 1997; 90:335-49.

59. Malsam J, Satoh A, Pelletier L, Warren G. Golgin tethers define subpopulations of COPI vesicles. Science 2005; 307:1095-8.

60. De Matteis MA, Luini A. Exiting the Golgi complex. Nature reviews 2008; 9:273-84.

61. Seaman MNJ. The retromer complex – endosomal protein recycling and beyond. Journal of Cell Science 2012; 125:4693-702.

62. Ohtsubo K, Marth JD. Glycosylation in cellular mechanisms of health and disease. Cell 2006; 126:855-67.

63. Varki A. Factors controlling the glycosylation potential of the Golgi apparatus. Trends in cell biology 1998; 8:34-40.

64. Xiang Y, Zhang X, Nix DB, Katoh T, Aoki K, Tiemeyer M, et al. Regulation of protein glycosylation and sorting by the Golgi matrix proteins GRASP55/65. Nat Commun 2013; 4:1659.

65. He C, Song H, Yorimitsu T, Monastyrska I, Yen WL, Legakis JE, et al. Recruitment of Atg9 to the preautophagosomal structure by Atg11 is essential for selective autophagy in budding yeast. J Cell Biol 2006; 175:925-35.

66. Young ARJ, Chan EYW, Hu XW, Köchl R, Crawshaw SG, High S, et al. Starvation and ULK1-dependent cycling of mammalian Atg9 between the TGN and endosomes. Journal of cell science 2006; 119:3888-900.

67. Guo Y, Chang C, Huang R, Liu B, Bao L, Liu W. AP1 is essential for generation of autophagosomes from the trans-Golgi network. Journal of cell science 2012; 125:1706-15.

68. Eberle HB, Serrano RL, Füllekrug J, Schlosser A, Lehmann WD, Lottspeich F, et al. Identification and characterization of a novel human plant pathogenesis-related protein that localizes to lipid-enriched microdomains in the Golgi complex. Journal of cell science 2002; 115:827-38.

69. Shoji-Kawata S, Sumpter R, Leveno M, Campbell GR, Zou Z, Kinch L, et al. Identification of a candidate therapeutic autophagy-inducing peptide. Nature 2013; 494:201-6.

70. Sun Q, Fan W, Chen K, Ding X, Chen S, Zhong Q. Identification of Barkor as a mammalian autophagy-specific factor for Beclin 1 and class III phosphatidylinositol 3-kinase. Proc Natl Acad Sci U S A 2008; 105:19211-6.

71. Sutterlin C, Hsu P, Mallabiabarrena A, Malhotra V. Fragmentation and dispersal of the pericentriolar Golgi complex is required for entry into mitosis in mammalian cells. Cell 2002; 109:359-69.

72. Duran JM, Kinseth M, Bossard C, Rose DW, Polishchuk R, Wu CC, et al. The Role of GRASP55 in Golgi Fragmentation and Entry of Cells into Mitosis. Molecular biology of the cell 2008; 19:2579-87.

73. Kodani A, Sutterlin C. The Golgi Protein GM130 Regulates Centrosome Morphology and Function. Molecular biology of the cell 2008; 19:745-53.

74. Kodani A, Kristensen I, Huang L, Sutterlin C. GM130-dependent control of Cdc42 activity at the Golgi regulates centrosome organization. Molecular biology of the cell 2009; 20:1192-200.

75. Royle SJ, Bright NA, Lagnado L. Clathrin is required for the function of the mitotic spindle. Nature 2005; 434:1152-7.

76. Miserey-Lenkei S, Couëdel-Courteille A, Del Nery E, Bardin S, Piel M, Racine V, et al. A role for the Rab6A′ GTPase in the inactivation of the Mad2-spindle checkpoint. The EMBO Journal 2006; 25:278-89.

77. Bisel B, Wang Y, Wei JH, Xiang Y, Tang D, Miron-Mendoza M, et al. ERK regulates Golgi and centrosome orientation towards the leading edge through GRASP65. J Cell Biol 2008; 182:837-43.

78. Rivero S, Cardenas J, Bornens M, Rios RM. Microtubule nucleation at the cis-side of the Golgi apparatus requires AKAP450 and GM130. The EMBO journal 2009; 28:1016-28.

79. Efimov A, Kharitonov A, Efimova N, Loncarek J, Miller PM, Andreyeva N, et al. Asymmetric CLASP-dependent nucleation of noncentrosomal microtubules at the trans-Golgi network. Developmental cell 2007; 12:917-30.

80. Hicks SW, Machamer CE. Golgi structure in stress sensing and apoptosis. Biochimica et biophysica acta 2005; 1744:406-14.

81. Lane JD, Lucocq J, Pryde J, Barr FA, Woodman PG, Allan VJ, et al. Caspase-mediated cleavage of the stacking protein GRASP65 is required for Golgi fragmentation during apoptosis. J Cell Biol 2002; 156:495-509.

82. Walker A, Ward C, Sheldrake TA, Dransfield I, Rossi AG, Pryde JG, et al. Golgi fragmentation during Fas-mediated apoptosis is associated with the rapid loss of GM130. Biochem Biophys Res Commun 2004; 316:6-11.

83. Mancini M, Machamer CE, Roy S, Nicholson DW, Thornberry NA, Casciola-Rosen LA, et al. Caspase-2 is localized at the Golgi complex and cleaves golgin-160 during apoptosis. J Cell Biol 2000; 149:603-12.

84. Lowe M, Lane JD, Woodman PG, Allan VJ. Caspase-mediated cleavage of syntaxin 5 and giantin accompanies inhibition of secretory traffic during apoptosis. Journal of cell science 2004; 117:1139-50.

85. Chiu R, Novikov L, Mukherjee S, Shields D. A caspase cleavage fragment of p115 induces fragmentation of the Golgi apparatus and apoptosis. J Cell Biol 2002; 159:637-48.

86. Sbodio JI, Hicks SW, Simon D, Machamer CE. GCP60 preferentially interacts with a caspase-generated golgin-160 fragment. J Biol Chem 2006; 281:27924-31.

87. Hicks SW, Machamer CE. The NH2-terminal Domain of Golgin-160 Contains Both Golgi and Nuclear Targeting Information. J Biol Chem 2002; 277:35833-9.

88. Behnia R, Barr FA, Flanagan JJ, Barlowe C, Munro S. The yeast orthologue of GRASP65 forms a complex with a coiled-coil protein that contributes to ER to Golgi traffic. J Cell Biol 2007; 176:255-61.

89. Kondylis V, Spoorendonk KM, Rabouille C. dGRASP localization and function in the early exocytic pathway in Drosophila S2 cells. Molecular biology of the cell 2005; 16:4061-72.

90. Puthenveedu MA, Bachert C, Puri S, Lanni F, Linstedt AD. GM130 and GRASP65-dependent lateral cisternal fusion allows uniform Golgi-enzyme distribution. Nature cell biology 2006; 8:238-48.

91. D'Angelo G, Prencipe L, Iodice L, Beznoussenko G, Savarese M, Marra P, et al. GRASP65 and GRASP55 sequentially promote the transport of C-terminal valine bearing cargoes to and through the golgi complex. J Biol Chem 2009; 284:34849-60.

92. Giuliani F, Grieve A, Rabouille C. Unconventional secretion: a stress on GRASP. Curr Opin Cell Biol 2011; 23:498-504.

93. White DT, McShea KM, Attar MA, Santy LC. GRASP and IPCEF Promote ARF-to-Rac Signaling and Cell Migration by Coordinating the Association of ARNO/cytohesin 2 with Dock180. Molecular biology of the cell 2010; 21:562-71.

94. Ramirez IB, Lowe M. Golgins and GRASPs: holding the Golgi together. Semin Cell Dev Biol 2009; 20:770-9.

95. Wang Y, Satoh A, Warren G. Mapping the functional domains of the Golgi stacking factor GRASP65. J Biol Chem 2005; 280:4921-8.

96. Preisinger C, Korner R, Wind M, Lehmann WD, Kopajtich R, Barr FA. Plk1 docking to GRASP65 phosphorylated by Cdk1 suggests a mechanism for Golgi checkpoint signalling. The EMBO journal 2005; 24:753-65.

97. Jesch SA, Lewis TS, Ahn NG, Linstedt AD. Mitotic phosphorylation of Golgi reassembly stacking protein 55 by mitogen-activated protein kinase ERK2. Molecular biology of the cell 2001; 12:1811-7.

98. Barr FA, Nakamura N, Warren G. Mapping the interaction between GRASP65 and GM130, components of a protein complex involved in the stacking of Golgi cisternae. The EMBO journal 1998; 17:3258-68.

99. Nakamura N, Rabouille C, Watson R, Nilsson T, Hui N, Slusarewicz P, et al. Characterization of a cis-Golgi matrix protein, GM130. J Cell Biol 1995; 131:1715-26.

100. Sonnichsen B, Lowe M, Levine T, Jamsa E, Dirac-Svejstrup B, Warren G. A role for giantin in docking COPI vesicles to Golgi membranes. J Cell Biol 1998; 140:1013-21.

101. Shorter J, Beard MB, Seemann J, Dirac-Svejstrup AB, Warren G. Sequential tethering of Golgins and catalysis of SNAREpin assembly by the vesicle-tethering protein p115. J Cell Biol 2002; 157:45-62.

102. Short B, Preisinger C, Korner R, Kopajtich R, Byron O, Barr FA. A GRASP55-rab2 effector complex linking Golgi structure to membrane traffic. J Cell Biol 2001; 155:877-83.

103. Tang D, Yuan H, Vielemeyer O, Perez F, Wang Y. Sequential phosphorylation of GRASP65 during mitotic Golgi disassembly. Biology open 2012; 1:1204-14.

104. Zhang X, Wang Y. GRASPs in Golgi Structure and Function. Frontiers in Cell and Developmental Biology 2015; 3:84.

105. Veenendaal T, Jarvela T, Grieve AG, van Es JH, Linstedt AD, Rabouille C. GRASP65 controls the cis Golgi integrity in vivo. Biology open 2014; 3:431-43.

106. Feng Y, Yu W, Li X, Lin S, Zhou Y, Hu J, et al. Structural insight into Golgi membrane stacking by GRASP65 and GRASP55 proteins. J Biol Chem 2013; 288:28418-27.

107. Tang D, Yuan H, Wang Y. The Role of GRASP65 in Golgi Cisternal Stacking and Cell Cycle Progression. Traffic 2010; 11:827-42.

108. Truschel ST, Sengupta D, Foote A, Heroux A, Macbeth MR, Linstedt AD. Structure of the membrane-tethering GRASP domain reveals a unique PDZ ligand interaction that mediates Golgi biogenesis. J Biol Chem 2011; 286:20125-9.

109. Lee I, Tiwari N, Dunlop MH, Graham M, Liu X, Rothman JE. Membrane adhesion dictates Golgi stacking and cisternal morphology. Proc Natl Acad Sci U S A 2014; 111:1849-54.

110. Mali P, Yang L, Esvelt KM, Aach J, Guell M, DiCarlo JE, et al. RNA-guided human genome engineering via Cas9. Science 2013; 339:823-6.

111. Cong L, Ran FA, Cox D, Lin S, Barretto R, Habib N, et al. Multiplex genome engineering using CRISPR/Cas systems. Science 2013; 339:819-23.

112. Kinseth MA, Anjard C, Fuller D, Guizzunti G, Loomis WF, Malhotra V. The Golgi-associated protein GRASP is required for unconventional protein secretion during development. Cell 2007; 130:524-34.

113. Manjithaya R, Anjard C, Loomis WF, Subramani S. Unconventional secretion of Pichia pastoris Acb1 is dependent on GRASP protein, peroxisomal functions, and autophagosome formation. J Cell Biol 2010; 188:537-46.

114. Schotman H, Karhinen L, Rabouille C. dGRASP-mediated noncanonical integrin secretion is required for Drosophila epithelial remodeling. Developmental cell 2008; 14:171-82.

115. Bruns C, McCaffery JM, Curwin AJ, Duran JM, Malhotra V. Biogenesis of a novel compartment for autophagosome-mediated unconventional protein secretion. J Cell Biol 2011; 195:979-92.

116. Curwin AJ, Brouwers N, Alonso YAM, Teis D, Turacchio G, Parashuraman S, et al. ESCRT-III drives the final stages of CUPS maturation for unconventional protein secretion. eLife 2016; 5.

117. Barr FA, Preisinger C, Kopajtich R, Korner R. Golgi matrix proteins interact with p24 cargo receptors and aid their efficient retention in the Golgi apparatus. J Cell Biol 2001; 155:885-91.

118. Kuo A, Zhong C, Lane WS, Derynck R. Transmembrane transforming growth factor-alpha tethers to the PDZ domain-containing, Golgi membrane-associated protein p59/GRASP55. The EMBO journal 2000; 19:6427-39.

119. Infante C, Ramos-Morales F, Fedriani C, Bornens M, Rios RM. GMAP-210, A cis-Golgi network-associated protein, is a minus end microtubule-binding protein. J Cell Biol 1999; 145:83-98.

120. Ablasser A, Schmid-Burgk JL, Hemmerling I, Horvath GL, Schmidt T, Latz E, et al. Cell intrinsic immunity spreads to bystander cells via the intercellular transfer of cGAMP. Nature 2013; 503:530-4.

121. Bortesi L, Fischer R. The CRISPR/Cas9 system for plant genome editing and beyond. Biotechnology Advances 2015; 33:41-52.

122. Yang H, Wang H, Jaenisch R. Generating genetically modified mice using CRISPR/Cas-mediated genome engineering. Nature Protocols 2014; 9:1956.

123. Weidberg H, Shvets E, Elazar Z. Biogenesis and cargo selectivity of autophagosomes. Annual review of biochemistry 2011; 80:125-56.

124. Yin Z, Pascual C, Klionsky DJ. Autophagy: machinery and regulation. Microb Cell 2016; 3:588-96.

125. Levine B, Kroemer G. Autophagy in the pathogenesis of disease. Cell 2008; 132:27-42.

126. Mizushima N, Komatsu M. Autophagy: Renovation of Cells and Tissues. Cell 2011; 147:728-41.

127. Kunz JB, Schwarz H, Mayer A. Determination of Four Sequential Stages during Microautophagy in Vitro. Journal of Biological Chemistry 2004; 279:9987-96.

128. Cuervo AM, Wong E. Chaperone-mediated autophagy: roles in disease and aging. Cell Res 2014; 24:92-104.

129. Shintani T, Klionsky DJ. Autophagy in Health and Disease: A Double-Edged Sword. Science (New York, NY) 2004; 306:990-5.

130. Klionsky DJ, Emr SD. Autophagy as a Regulated Pathway of Cellular Degradation. Science (New York, NY) 2000; 290:1717-21.

131. Zaffagnini G, Martens S. Mechanisms of Selective Autophagy. Journal of Molecular Biology 2016; 428:1714-24.

132. Joachim J, Jefferies HB, Razi M, Frith D, Snijders AP, Chakravarty P, et al. Activation of ULK Kinase and Autophagy by GABARAP Trafficking from the Centrosome Is Regulated by WAC and GM130. Molecular cell 2015; 60:899-913.

133. Joachim J, Razi M, Judith D, Wirth M, Calamita E, Encheva V, et al. Centriolar Satellites Control GABARAP Ubiquitination and GABARAP-Mediated Autophagy. Current biology : CB 2017.

134. McEwan David G, Popovic D, Gubas A, Terawaki S, Suzuki H, Stadel D, et al. PLEKHM1 Regulates Autophagosome-Lysosome Fusion through HOPS Complex and LC3/GABARAP Proteins. Molecular cell; 57:39-54.

135. Itakura E, Kishi-Itakura C, Mizushima N. The hairpin-type tail-anchored SNARE syntaxin 17 targets to autophagosomes for fusion with endosomes/lysosomes. Cell 2012; 151:1256-69.

136. Chen D, Fan W, Lu Y, Ding X, Chen S, Zhong Q. A mammalian autophagosome maturation mechanism mediated by TECPR1 and the Atg12-Atg5 conjugate. Molecular cell 2012; 45:629-41.

137. Jiang P, Nishimura T, Sakamaki Y, Itakura E, Hatta T, Natsume T, et al. The HOPS complex mediates autophagosome-lysosome fusion through interaction with syntaxin 17. Molecular biology of the cell 2014; 25:1327-37.

138. Liang C, Feng P, Ku B, Dotan I, Canaani D, Oh BH, et al. Autophagic and tumour suppressor activity of a novel Beclin1-binding protein UVRAG. Nature cell biology 2006; 8:688-99.

139. Takahashi Y, Coppola D, Matsushita N, Cualing HD, Sun M, Sato Y, et al. Bif-1 interacts with Beclin 1 through UVRAG and regulates autophagy and tumorigenesis. Nature cell biology 2007; 9:1142-51.

140. Kaur J, Debnath J. Autophagy at the crossroads of catabolism and anabolism. Nature Reviews Molecular Cell Biology 2015; 16:461.

141. Kim LC, Cook RS, Chen J. mTORC1 and mTORC2 in cancer and the tumor microenvironment. Oncogene 2017; 36:2191-201.

142. Ganley IG, Lam DH, Wang J, Ding X, Chen S, Jiang X. ULK1·ATG13·FIP200 Complex Mediates mTOR Signaling and Is Essential for Autophagy. The Journal of Biological Chemistry 2009; 284:12297-305.

143. Settembre C, Zoncu R, Medina DL, Vetrini F, Erdin S, Erdin S, et al. A lysosome-to-nucleus signalling mechanism senses and regulates the lysosome via mTOR and TFEB. The EMBO Journal 2012; 31:1095-108.

144. Sancak Y, Bar-Peled L, Zoncu R, Markhard AL, Nada S, Sabatini DM. Ragulator-Rag Complex Targets mTORC1 to the Lysosomal Surface and Is Necessary for Its Activation by Amino Acids. Cell; 141:290-303.

145. Han Jung M, Jeong Seung J, Park Min C, Kim G, Kwon Nam H, Kim Hoi K, et al. Leucyl-tRNA Synthetase Is an Intracellular Leucine Sensor for the mTORC1-Signaling Pathway. Cell 2012; 149:410-24.

146. Tsun Z-Y, Bar-Peled L, Chantranupong L, Zoncu R, Wang T, Kim C, et al. The Folliculin tumor suppressor is a GAP for RagC/D GTPases that signal amino acid levels to mTORC1. Molecular cell 2013; 52:10.1016/j.molcel.2013.09.016.

147. Long X, Ortiz-Vega S, Lin Y, Avruch J. Rheb Binding to Mammalian Target of Rapamycin (mTOR) Is Regulated by Amino Acid Sufficiency. Journal of Biological Chemistry 2005; 280:23433-6.

148. Meijer AJ, Lorin S, Blommaart EF, Codogno P. Regulation of autophagy by amino acids and MTOR-dependent signal transduction. Amino Acids 2015; 47:2037-63.

149. Kim J, Kundu M, Viollet B, Guan K-L. AMPK and mTOR regulate autophagy through direct phosphorylation of Ulk1. Nature cell biology 2011; 13:132-41.

150. Di Nardo A, Wertz MH, Kwiatkowski E, Tsai PT, Leech JD, Greene-Colozzi E, et al. Neuronal Tsc1/2 complex controls autophagy through AMPK-dependent regulation of ULK1. Human Molecular Genetics 2014; 23:3865-74.

151. Roczniak-Ferguson A, Petit CS, Froehlich F, Qian S, Ky J, Angarola B, et al. The Transcription Factor TFEB Links mTORC1 Signaling to Transcriptional Control of Lysosome Homeostasis. Science signaling 2012; 5:ra42-ra.

152. Moruno F, Pérez-Jiménez E, Knecht E. Regulation of Autophagy by Glucose in Mammalian Cells. Cells 2012; 1:372-95.

153. Axe EL, Walker SA, Manifava M, Chandra P, Roderick HL, Habermann A, et al. Autophagosome formation from membrane compartments enriched in phosphatidylinositol 3-phosphate and dynamically connected to the endoplasmic reticulum. The Journal of Cell Biology 2008; 182:685-701.

154. Hamasaki M, Furuta N, Matsuda A, Nezu A, Yamamoto A, Fujita N, et al. Autophagosomes form at ER–mitochondria contact sites. Nature 2013; 495:389.

155. Rowland AA, Voeltz GK. Endoplasmic reticulum–mitochondria contacts: function of the junction. Nature reviews Molecular cell biology 2012; 13:607-25.

156. Ravikumar B, Moreau K, Jahreiss L, Puri C, Rubinsztein DC. Plasma membrane contributes to the formation of pre-autophagosomal structures. Nature cell biology 2010; 12:747-57.

157. Rubinsztein David C, Shpilka T, Elazar Z. Mechanisms of Autophagosome Biogenesis. Current Biology 2012; 22:R29-R34.

158. Reggiori F, Ungermann C. Autophagosome Maturation and Fusion. Journal of Molecular Biology 2017; 429:486-96.

159. Cui Y, Zhao Q, Gao C, Ding Y, Zeng Y, Ueda T, et al. Activation of the Rab7 GTPase by the MON1-CCZ1 Complex Is Essential for PVC-to-Vacuole Trafficking and Plant Growth in Arabidopsis. The Plant Cell 2014; 26:2080-97.

160. Hegedus K, Takats S, Boda A, Jipa A, Nagy P, Varga K, et al. The Ccz1-Mon1-Rab7 module and Rab5 control distinct steps of autophagy. Molecular Biology of the Cell 2016; 27:3132-42.

161. Kinchen JM, Ravichandran KS. Identification of two evolutionarily conserved genes regulating processing of engulfed apoptotic cells. Nature 2010; 464:778.

162. Gillingham Alison K, Sinka R, Torres Isabel L, Lilley Kathryn S, Munro S. Toward a Comprehensive Map of the Effectors of Rab GTPases. Developmental Cell 2014; 31:358-73.

163. Khatter D, Raina VB, Dwivedi D, Sindhwani A, Bahl S, Sharma M. The small GTPase Arl8b regulates assembly of the mammalian HOPS complex on lysosomes. Journal of Cell Science 2015; 128:1746-61.

164. Lin X, Yang T, Wang S, Wang Z, Yun Y, Sun L, et al. RILP interacts with HOPS complex via VPS41 subunit to regulate endocytic trafficking. Scientific Reports 2014; 4:7282.

165. van der Kant R, Fish A, Janssen L, Janssen H, Krom S, Ho N, et al. Late endosomal transport and tethering are coupled processes controlled by RILP and the cholesterol sensor ORP1L. Journal of Cell Science 2013; 126:3462-74.

166. McEwan David G, Popovic D, Gubas A, Terawaki S, Suzuki H, Stadel D, et al. PLEKHM1 Regulates Autophagosome-Lysosome Fusion through HOPS Complex and LC3/GABARAP Proteins. Molecular Cell 2015; 57:39-54.

167. Nguyen TN, Padman BS, Usher J, Oorschot V, Ramm G, Lazarou M. Atg8 family LC3/GAB ARAP proteins are crucial for autophagosome-lysosome fusion but not autophagosome formation during PINK1/Parkin mitophagy and starvation. Journal of Cell Biology 2016; 215:857-74.

168. Wang Z, Miao G, Xue X, Guo X, Yuan C, Wang Z, et al. The Vici Syndrome Protein EPG5 Is a Rab7 Effector that Determines the Fusion Specificity of Autophagosomes with Late Endosomes/Lysosomes. Molecular Cell 2016; 63:781-95.

169. Chen D, Fan W, Lu Y, Ding X, Chen S, Zhong Q. A Mammalian Autophagosome Maturation Mechanism Mediated by TECPR1 and the Atg12-Atg5 Conjugate. Molecular Cell 2012; 45:629-41.

170. Tabata K, Matsunaga K, Sakane A, Sasaki T, Noda T, Yoshimori T. Rubicon and PLEKHM1 Negatively Regulate the Endocytic/Autophagic Pathway via a Novel Rab7-binding Domain. Molecular Biology of the Cell 2010; 21:4162-72.

171. Itakura E, Kishi-Itakura C, Mizushima N. The Hairpin-type Tail-Anchored SNARE Syntaxin 17 Targets to Autophagosomes for Fusion with Endosomes/Lysosomes. Cell 2012; 151:1256-69.

172. Jiang P, Nishimura T, Sakamaki Y, Itakura E, Hatta T, Natsume T, et al. The HOPS complex mediates autophagosome–lysosome fusion through interaction with syntaxin 17. Molecular Biology of the Cell 2014; 25:1327-37.

173. Takáts S, Pircs K, Nagy P, Varga Á, Kárpáti M, Hegedűs K, et al. Interaction of the HOPS complex with Syntaxin 17 mediates autophagosome clearance in Drosophila. Molecular Biology of the Cell 2014; 25:1338-54.

174. Kihara A, Kabeya Y, Ohsumi Y, Yoshimori T. Beclin–phosphatidylinositol 3-kinase complex functions at the trans-Golgi network. EMBO Reports 2001; 2:330-5.

175. Obara K, Sekito T, Ohsumi Y. Assortment of Phosphatidylinositol 3-Kinase Complexes—Atg14p Directs Association of Complex I to the Pre-autophagosomal Structure in Saccharomyces cerevisiae. Molecular Biology of the Cell 2006; 17:1527-39.

176. Suzuki K, Kirisako T, Kamada Y, Mizushima N, Noda T, Ohsumi Y. The pre-autophagosomal structure organized by concerted functions of APG genes is essential for autophagosome formation. The EMBO Journal 2001; 20:5971-81.

177. Kihara A, Noda T, Ishihara N, Ohsumi Y. Two Distinct Vps34 Phosphatidylinositol 3–Kinase Complexes Function in Autophagy and Carboxypeptidase Y Sorting inSaccharomyces cerevisiae. The Journal of Cell Biology 2001; 152:519-30.

178. Matsunaga K, Morita E, Saitoh T, Akira S, Ktistakis NT, Izumi T, et al. Autophagy requires endoplasmic reticulum targeting of the PI3-kinase complex via Atg14L. J Cell Biol 2010; 190:511-21.

179. Itakura E, Mizushima N. Characterization of autophagosome formation site by a hierarchical analysis of mammalian Atg proteins. Autophagy 2010; 6:764-76.

180. Maria Fimia G, Stoykova A, Romagnoli A, Giunta L, Di Bartolomeo S, Nardacci R, et al. Ambra1 regulates autophagy and development of the nervous system. Nature 2007; 447:1121.

181. Nazio F, Strappazzon F, Antonioli M, Bielli P, Cianfanelli V, Bordi M, et al. mTOR inhibits autophagy by controlling ULK1 ubiquitylation, self-association and function through AMBRA1 and TRAF6. Nature Cell Biology 2013; 15:406.

182. Itakura E, Kishi C, Inoue K, Mizushima N. Beclin 1 Forms Two Distinct Phosphatidylinositol 3-Kinase Complexes with Mammalian Atg14 and UVRAG. Molecular Biology of the Cell 2008; 19:5360-72.

183. Takahashi Y, Hori T, Cooper TK, Liao J, Desai N, Serfass JM, et al. Bif-1 haploinsufficiency promotes chromosomal instability and accelerates Myc-driven lymphomagenesis via suppression of mitophagy. Blood 2013; 121:1622-32.

184. Liang C, Lee J-s, Inn K-S, Gack MU, Li Q, Roberts EA, et al. Beclin1-binding UVRAG targets the class C Vps complex to coordinate autophagosome maturation and endocytic trafficking. Nature cell biology 2008; 10:776-87.

185. Matsunaga K, Saitoh T, Tabata K, Omori H, Satoh T, Kurotori N, et al. Two Beclin 1-binding proteins, Atg14L and Rubicon, reciprocally regulate autophagy at different stages. Nature Cell Biology 2009; 11:385.

186. Zhong Y, Wang QJ, Li X, Yan Y, Backer JM, Chait BT, et al. Distinct regulation of autophagic activity by Atg14L and Rubicon associated with Beclin 1- phosphatidylinositol 3-kinase complex. Nature cell biology 2009; 11:468-76.

187. Kim Y-M, Jung CH, Seo M, Kim EK, Park J-M, Bae SS, et al. mTORC1 phosphorylates UVRAG to negatively regulate autophagosome and endosome maturation. Molecular cell 2015; 57:207-18.

188. Liang C, Feng P, Ku B, Dotan I, Canaani D, Oh B-H, et al. Autophagic and tumour suppressor activity of a novel Beclin1-binding protein UVRAG. Nature Cell Biology 2006; 8:688.

189. Funderburk SF, Wang QJ, Yue Z. Beclin 1-VPS34 complex – At the Crossroads of Autophagy and Beyond. Trends in cell biology 2010; 20:355-62.

190. Münz C. Beclin-1 Targeting for Viral Immune Escape. Viruses 2011; 3:1166-78.
191. Capasso JM, Keenan TW, Abeijon C, Hirschberg CB. Mechanism of phosphorylation in the lumen of the Golgi apparatus. Translocation of adenosine 5'-triphosphate into Golgi vesicles from rat liver and mammary gland. Journal of Biological Chemistry 1989; 264:5233-40.
192. Gusarova V, Seo J, Sullivan ML, Watkins SC, Brodsky JL, Fisher EA. Golgi-associated Maturation of Very Low Density Lipoproteins Involves Conformational Changes in Apolipoprotein B, but Is Not Dependent on Apolipoprotein E. Journal of Biological Chemistry 2007; 282:19453-62.
193. Marra P, Maffucci T, Daniele T, Tullio GD, Ikehara Y, Chan EK, et al. The GM130 and GRASP65 Golgi proteins cycle through and define a subdomain of the intermediate compartment. Nature cell biology 2001; 3:1101-13.
194. Wei JH, Seemann J. Unraveling the Golgi ribbon. Traffic 2010; 11:1391-400.
195. Wang Y, Seemann J. Golgi biogenesis. Cold Spring Harb Perspect Biol 2011; 3:a005330.
196. Tang D, Wang Y. Cell cycle regulation of Golgi membrane dynamics. Trends in cell biology 2013; 23:296-304.
197. Huff J. The Airyscan detector from ZEISS: confocal imaging with improved signal-to-noise ratio and super-resolution. Nat Meth 2015; 12.
198. Gallegos KM, Conrady DG, Karve SS, Gunasekera TS, Herr AB, Weiss AA. Shiga Toxin Binding to Glycolipids and Glycans. PLoS One 2012; 7:e30368.
199. Margheri G, D'Agostino R, Trigari S, Sottini S, Del Rosso M. The β-Subunit of Cholera Toxin has a High Affinity for Ganglioside GM1 Embedded into Solid Supported Lipid Membranes with a Lipid Raft-Like Composition. Lipids 2014; 49:203-6.

200. Wang Y, Wei JH, Bisel B, Tang D, Seemann J. Golgi Cisternal Unstacking Stimulates COPI Vesicle Budding and Protein Transport. PLoS ONE 2008; 3:e1647.

201. Nakagomi S, Barsoum MJ, Bossy-Wetzel E, Sütterlin C, Malhotra V, Lipton SA. A Golgi fragmentation pathway in neurodegeneration. Neurobiology of disease 2008; 29:221-31.

202. Joshi G, Chi Y, Huang Z, Wang Y. Abeta-induced Golgi fragmentation in Alzheimer's disease enhances Abeta production. Proc Natl Acad Sci U S A 2014; 111:E1230-9.

203. Willett RA, Pokrovskaya ID, Lupashin VV. Fluorescent microscopy as a tool to elucidate dysfunction and mislocalization of Golgi glycosyltransferases in COG complex depleted mammalian cells. Methods in molecular biology (Clifton, NJ) 2013; 1022:61-72.

204. Zhou Z, Mogensen MM, Powell PP, Curry S, Wileman T. Foot-and-Mouth Disease Virus 3C Protease Induces Fragmentation of the Golgi Compartment and Blocks Intra-Golgi Transport. Journal of Virology 2013; 87:11721-9.

205. Li T, You H, Mo X, He W, Tang X, Jiang Z, et al. GOLPH3 Mediated Golgi Stress Response in Modulating N2A Cell Death upon Oxygen-Glucose Deprivation and Reoxygenation Injury. Molecular Neurobiology 2016; 53:1377-85.

206. Petrosyan A. Onco-Golgi: Is Fragmentation a Gate to Cancer Progression? Biochemistry & molecular biology journal 2015; 1:16.

207. Tang D, Xiang Y, Wang Y. Reconstitution of the cell cycle-regulated Golgi disassembly and reassembly in a cell-free system. Nat Protoc 2010; 5:758-72.

208. Bailey Blackburn J, Pokrovskaya I, Fisher P, Ungar D, Lupashin VV. COG Complex Complexities: Detailed Characterization of a Complete Set of HEK293T Cells Lacking Individual COG Subunits. Frontiers in Cell and Developmental Biology 2016; 4:23.

209. Selyunin AS, Mukhopadhyay S. A Conserved Structural Motif Mediates Retrograde Trafficking of Shiga Toxin Types 1 and 2. Traffic 2015; 16:1270-87.

210. Cruz-Garcia D, Curwin AJ, Popoff JF, Bruns C, Duran JM, Malhotra V. Remodeling of secretory compartments creates CUPS during nutrient starvation. J Cell Biol 2014; 207:695-703.

211. Malhotra V. Unconventional protein secretion: an evolving mechanism. The EMBO journal 2013; 32:1660-4.

212. Gomes LC, Di Benedetto G, Scorrano L. During autophagy mitochondria elongate, are spared from degradation and sustain cell viability. Nature cell biology 2011; 13:589-98.

213. Pilli M, Arko-Mensah J, Ponpuak M, Roberts E, Master S, Mandell MA, et al. TBK-1 promotes autophagy-mediated antimicrobial defense by controlling autophagosome maturation. Immunity 2012; 37:223-34.

214. Vicinanza M, Korolchuk VI, Ashkenazi A, Puri C, Menzies FM, Clarke JH, et al. PI(5)P regulates autophagosome biogenesis. Molecular cell 2015; 57:219-34.

215. Mauvezin C, Neufeld TP. Bafilomycin A1 disrupts autophagic flux by inhibiting both V-ATPase-dependent acidification and Ca-P60A/SERCA-dependent autophagosome-lysosome fusion. Autophagy 2015; 11:1437-8.

216. Marino ML, Pellegrini P, Di Lernia G, Djavaheri-Mergny M, Brnjic S, Zhang X, et al. Autophagy is a protective mechanism for human melanoma cells under acidic stress. J Biol Chem 2012; 287:30664-76.

217. Funderburk SF, Wang QJ, Yue Z. The Beclin 1-VPS34 complex--at the crossroads of autophagy and beyond. Trends in cell biology 2010; 20:355-62.

218. Zhong Y, Wang QJ, Li X, Yan Y, Backer JM, Chait BT, et al. Distinct regulation of autophagic activity by Atg14L and Rubicon associated with Beclin 1-phosphatidylinositol-3-kinase complex. Nature cell biology 2009; 11:468-76.
219. Rabouille C, Linstedt AD. GRASP: A Multitasking Tether. Front Cell Dev Biol 2016; 4:1.
220. Moreau K, Ravikumar B, Renna M, Puri C, Rubinsztein DC. Autophagosome precursor maturation requires homotypic fusion. Cell 2011; 146:303-17.
221. Fung C, Lock R, Gao S, Salas E, Debnath J. Induction of autophagy during extracellular matrix detachment promotes cell survival. Molecular biology of the cell 2008; 19:797-806.
222. Takahashi Y, Tsotakos N, Liu Y, Young MM, Serfass J, Tang Z, et al. The Bif-1-Dynamin 2 membrane fission machinery regulates Atg9-containing vesicle generation at the Rab11-positive reservoirs. Oncotarget 2016; 7:20855-68.
223. Matsunaga K, Saitoh T, Tabata K, Omori H, Satoh T, Kurotori N, et al. Two Beclin 1-binding proteins, Atg14L and Rubicon, reciprocally regulate autophagy at different stages. Nature cell biology 2009; 11:385-96.
224. Xiang Y, Seemann J, Bisel B, Punthambaker S, Wang Y. Active ADP-ribosylation factor-1 (ARF1) is required for mitotic Golgi fragmentation. J Biol Chem 2007; 282:21829-37.
225. Nguyen TN, Padman BS, Usher J, Oorschot V, Ramm G, Lazarou M. Atg8 family LC3/GABARAP proteins are crucial for autophagosome-lysosome fusion but not autophagosome formation during PINK1/Parkin mitophagy and starvation. J Cell Biol 2016; 215:857-74.
226. Kim J, Huang W-P, Stromhaug PE, Klionsky DJ. Convergence of Multiple Autophagy and Cytoplasm to Vacuole Targeting Components to a Perivacuolar Membrane Compartment

Prior to de Novo Vesicle Formation. The Journal of biological chemistry 2002; 277:763-73.

227. Rabouille C, Malhotra V, Nickel W. Diversity in unconventional protein secretion. Journal of cell science 2012; 125:5251-5.

228. Cabral M, Anjard C, Malhotra V, Loomis WF, Kuspa A. Unconventional secretion of AcbA in Dictyostelium discoideum through a vesicular intermediate. Eukaryot Cell 2010; 9:1009-17.

229. Zhu L, Jorgensen JR, Li M, Chuang YS, Emr SD. ESCRTs function directly on the lysosome membrane to downregulate ubiquitinated lysosomal membrane proteins. eLife 2017; 6.

230. Zhang X, Wang L, Lak B, Li J, Jokitalo E, Wang Y. GRASP55 Senses Glucose Deprivation through O-GlcNAcylation to Promote Autophagosome-Lysosome Fusion. Developmental Cell 2018; 45:245-61.e6.

231. Zhao J, Li B, Huang X, Morelli X, Shi N. Structural Basis for the Interaction between Golgi Reassembly-stacking Protein GRASP55 and Golgin45. J Biol Chem 2017; 292:2956-65.

232. Lee JG, Takahama S, Zhang G, Tomarev SI, Ye Y. Unconventional secretion of misfolded proteins promotes adaptation to proteasome dysfunction in mammalian cells. Nature cell biology 2016; 18:765-76.

233. Wei JH, Seemann J. Golgi ribbon disassembly during mitosis, differentiation and disease progression. Curr Opin Cell Biol 2017; 47:43-51.

234. Wijdeven RH, Janssen H, Nahidiazar L, Janssen L, Jalink K, Berlin I, et al. Cholesterol and ORP1L-mediated ER contact sites control autophagosome transport and fusion with the endocytic pathway. Nature Communications 2016; 7:11808.

235. Baker RW, Jeffrey PD, Zick M, Phillips BP, Wickner WT, Hughson FM. A direct role for the Sec1-Munc18-family protein Vps33 as a template for SNARE assembly. Science (New York, NY) 2015; 349:1111-4.

236. Tian Y, Li Z, Hu W, Ren H, Tian E, Zhao Y, et al. C. elegans Screen Identifies Autophagy Genes Specific to Multicellular Organisms. Cell 2010; 141:1042-55.

237. Diao J, Liu R, Rong Y, Zhao M, Zhang J, Lai Y, et al. ATG14 promotes membrane tethering and fusion of autophagosomes to endolysosomes. Nature 2015; 520:563-6.